12-1-2010

Cerebral Amyloid Angiopathy and Transition Metals in Alzheimer's Disease

Matthew Schrag
Loma Linda University

LOMA LINDA UNIVERSITY
School of Medicine
in conjunction with the
Faculty of Graduate Studies

Cerebral Amyloid Angiopathy and Transition Metals in Alzheimer's Disease

by

Matthew Schrag

A Dissertation submitted in partial satisfaction of
the requirements for the degree of
Doctor of Philosophy in Biochemistry

December 2010

Each person whose signature appears below certifies that this dissertation in his/her opinion is adequate, in scope and quality, as a dissertation for the degree Doctor of Philosophy.

_____, Chairperson
Wolff M. Kirsch, Professor of Neurological Surgery and Professor of Biochemistry

_____
Othman Ghribi, Professor of Pharmacology, Pathology and Therapeutics, University of North Dakota

_____
Daila S. Gridley, Professor of Radiation Medicine and Microbiology and Molecular Genetics

_____
Harry V. Vinters, Professor of Pathology and Laboratory Medicine, University of California Los Angeles

_____
Nathan Wall, Assistant Professor of Biochemistry

ACKNOWLEDGEMENTS

I am extraordinarily grateful to Dr. Wolff Kirsch whose support and guidance have shaped this work and greatly impacted me as a scientist. Dr. Kirsch has touched my life in an indelible way and I treasure him as a mentor and friend. To my dear friend Dr. Othman Ghribi who introduced me to research I am grateful for his patient training and encouragement to pursue science as a career. Dr. Harry V. Vinters trained me to write like a scientist, generously helping me to revise draft after draft of my manuscripts. I also thank Drs. Nathan Wall and Daila Gridley who have guided this body of work as members of my research committee.

I am honored to have met and worked with so many brilliant thinkers and scientists. I know fully that this work was not possible without contributions of many, many people and will not forget the people who have helped me along the way.

I thank my wife Sarah for her love and encouragement – she is my inspiration and the love of my life. And I thank my family for enduring support during this long process. Finally and most importantly, I want to acknowledge the role of Divine guidance in these studies. That God has chosen to give us some insight into His creation is a privilege which humbles me.

I truly hope that this effort is more than just an exercise for a degree or a job, I hope that in time we will be able to treat this devastating disease and improve the lives of people with Alzheimer's disease and their families.

CONTENTS

Approval Page iii

Acknowledgements iv

Table of Contents v

List of Figures viii

List of Tables x

List of Abbreviations xi

Abstract xiii

Chapter

1. Introduction 1

    The Clinical Problem 1
    The Research Problem 3
    Previous Work 6
    Hypothesis and Aims of Current Studies 9
    References 12

2. The effect of formalin fixation on the levels of brain transition metals in archived samples 16

    Abstract 16
    Introduction 17
    Materials and Methods 19
    Results 20
    Discussion 23
    References 28

3. Mapping iron, zinc and copper in the Alzheimer's disease brain: a quantitative meta-analysis 30

    Abstract 30
    Introduction 31
    Materials and Methods 32

        Literature search 32
        Exclusion criteria 34

Data analysis 34

Results 35
Discussion 42
Annotated References 46
General References 50

4. The effect of cerebral amyloid angiopathy on iron, copper and zinc in Alzheimer's disease 59

Abstract 59
Introduction 60
Material and Methods 61

Tissue selection 61
Atomic absorption spectrometry 62
Histology 63
Electrophoresis 65

Results 67
Discussion 82
References 88

5. Correlation of hypointensities in susceptibility weighted magnetic resonance images to tissue histology in dementia patients with cerebral amyloid angiopathy 93

Abstract 93
Introduction 94
Material and Methods 97

Patient characteristics 97
Tissue preparation 98
Imaging parameters 100
Dissection and histology 100

Results 103

Radiologic-histopathologic correlation 103
CAA-related vascular damage 109
Evidence of peri-hematoma inflammation 111
Formation of secondary ischemia and white matter lesions 112

Discussion 119
References 126

6. Continuing study: Is dynactin involved in dysfunctional axonal transport of copper in Alzheimer's disease? 130

Introduction 130
Preliminary findings 131
Future direction 134
References 138

7. Discussion and conclusion 140

TABLES

Tables Page

1. Effect of short-term fixation on transition metal concentrations in the amygdala reported in the literature 25

2. Effect of Alzheimer's disease on brain iron levels 55

3. Effect of Alzheimer's disease on brain zinc levels 57

4. Effect of Alzheimer's disease on brain copper levels 59

5. Wet to dry weights used in calculations 60

6. Patient demographics and neuropathologic findings 70

7. Temporal lobe metal concentrations 71

8. Patient demographics and locations of microbleeds on MR 101

FIGURES

Figures Page

1. Effect of long-term formalin archival on transition metal levels in paired Alzheimer's disease brain samples 21

2. Meta-data of studies reporting the effect of Alzheimer's disease on neocortical iron, zinc and copper concentrations.....39

3. Laboratory of origin is the source of heterogeneity.....41

4. Iron is deposited on arterioles in cerebral amyloid angiopathic brain 73

5. Heme degradation enzymes are induced in cerebral amyloid angiopathic brain. 76

6. Increased non-synaptic zinc levels in grey matter in Alzheimer's disease 79

7. Copper is concentrated in vascular elements in CAA 82

8. Correlation of hypointensities and tissue pathology.....106

9. MR hypointensities without grossly visible pathology.....108

10. The blooming effect induced by hemosiderin-iron.....110

11. Vascular damage associated with CAA and hemorrhage 124

12. The local tissue reaction.....126

13. Perivascular hemosiderin deposition may contribute to subsequent ischemic changes. 128

14. Synaptic copper reduced and axonal copper accumulation in AD without evidence of CAA.....134

15. Dynactin may be involved in copper trafficking 137

ABBREVIATIONS

%RSD	Percent relative standard deviation
AA	Atomic absorption
AD	Alzheimer's disease
BCS	Bathocuproine sulfate
BLVDR A/B	Biliverdin reductase A and B
BMB	Brain microbleed
BDIPY	Boron-dipyrromethene
CAA	Cerebral amyloid angiopathy
CS1, CS3	CopperSensor 1, CopperSensor3
GRE-T2*	Gradient echo T2*
HO-1	Heme oxygenase 1
ICP-MS	Inductively coupled plasma mass spectrometry
INAA	Instrumental neutron activation analysis
MCI	Mild cognitive impairment
MR	Magnetic resonance
NMDA	N-methyl d-aspartate
PD	Parkinson's disease
PIXE	Particle induced x-ray emission
SWI	Susceptibility weighted imaging
U of K	University of Kentucky

ABSTRACT OF THE DISSERTATION

Cerebral Amyloid Angiopathy and Transition Metals in Alzheimer's Disease

by

Matthew Schrag

Doctor of Philosophy, Graduate Program in Biochemistry
Loma Linda University, December 2010
Dr. Wolff M. Kirsch, Chairperson

Alterations in brain metals homeostasis and particularly brain iron overload have been postulated to play a role in Alzheimer's disease, contributing to oxidative stress and neuronal injury; however, the source of this iron is not clear and may be due to metabolic derangement(s), failed iron clearance mechanisms or exogenous deposition such as through bleeding. This series of studies was designed to evaluate the extent of metals dyshomeostasis in the Alzheimer's disease brain and specifically whether microvascular bleeding is a major contributor to Alzheimer's disease-related iron overload. Cerebral amyloid angiopathy (CAA) is a vascular manifestation of Alzheimer's disease present to some degree in up to 95% of Alzheimer's disease patients. This vasculopathy results in vascular inflammation and fragility which produces clinically detectable bleeding (by susceptibility weighted MR imaging) in many Alzheimer's disease patients. We analyzed brain iron levels by gold-standard atomic absorption spectrometry in brain tissue from patients with severe CAA, in those with Alzheimer's disease without significant vascular involvement and in aged control tissue. We also observed iron, zinc and copper in these tissues histologically by novel techniques to qualitatively assess their association with vascular and perivascular abnormalities. Increased iron in the subset of Alzheimer's disease patients with CAA is accompanied by increased levels of heme

degradation enzymes, heme oxygenase and biliverdin reductase. Finally, because the mechanism(s) underlying vascular fragility in CAA is unknown, we evaluated the role of terminal complement on cerebrovascular elements in the setting of CAA. This may provide mechanistic clues to how the structural stability of arterioles is undermined in this microangiopathy. If iron overload is a feature of CAA rather than a more general feature of Alzheimer's disease, it is possible that chelation therapies will be more effective for the subset of Alzheimer's patients with severe vasculopathy. This information combined with an effective clinical test for CAA has the potential to refine therapeutic strategies.

CHAPTER ONE

INTRODUCTION

The Clinical Problem of Alzheimer's Disease

Alzheimer's disease (AD) was described more than 100 years ago by a 43 year old neuropathologist named Dr. Alois Alzheimer who recognized the two key neuropathological markers of this neurodegenerative disease. He described extracellular plaques of a material we now know to be aggregates of a protein peptide called beta-amyloid. He also described an intraneuronal pathology he termed "tangles" which appeared as intense silver-staining of the axons of certain neurons (Zilka and Novak 2006). This pathology is now understood to result from the hyperphosphorylation of a cytoskeleton-associated protein called tau which is normally responsible for stabilizing the microtubules associated with normal neuronal axons. Upon hyperphosphorylation, this molecule can no longer function normally and aggregates within neurons, becoming visible as a neurofibrillary tangle. This is associated with destabilization of the axon and the loss of synaptic connections. These pathologies present in the context of severe neuronal loss through apoptosis and cortical atrophy leading to the clinical manifestations of the disease.

Patients affected by Alzheimer's disease typically present with mild memory impairments in or after the seventh decade of life although about 5% of cases are

hereditary (usually with autosomal dominant inheritance) and cause clinical dementia as early as the fourth or fifth decade of life (and occasionally even earlier). The earliest phase of the disease falls in a clinical category termed mild cognitive impairment (MCI) which also affects many individuals with normal age-related memory loss. Patients given the diagnosis of MCI may progress to outright dementia (at a typical rate of 17% per year) or remain cognitively stable (Landau 2010). About two-thirds of those who progress to dementia will ultimately be diagnosed as having Alzheimer's disease. This disease affects approximately 14% of adults in the United States over the age of 65 and up to 40% of octogenarians. The disease initially presents with isolated memory loss, but the cognitive impairment worsens with time to include word-finding difficulty (or anomia), visual-spacial dysfunction and ultimately loss of executive function (Samanta 2006). AD is currently believed to be the seventh most common cause of death in the United States (Alzheimer's Association 2010). The most common mechanism of death in patients affected by Alzheimer's disease is pneumonia precipitated by aspiration because of the loss of gag reflexes and cognitive protection of the airway (Kahlia 2003). Average survival after diagnosis is reported to range from 3.1 to 7.6 years (Molsa 1995, Aguerro-Torres 1999, Helmer 2001, Wolfson 2001, Brookmeyer 2002, Ganguli 2005, Helzner 2008).

A number of therapeutic options are available, but none has been shown to reverse or even slow cognitive dysfunction. Acetylcholinesterase inhibitors have been developed based on the observation that the nucleus basalis of Meynert is severely affected by Alzheimer's pathology, leading to a reduction in acetylcholine levels (Cuello 2010). These drugs are reasonably well-tolerated and produce a brief improvement in

non-cognitive symptoms of Alzheimer's disease such as performance of activities of daily living. N-methyl d-aspartate (NMDA)-receptor antagonists have been used based on evidence of glutamate-mediated neurotoxicity in AD brain. This therapy is of comparable effectiveness with acetylcholinesterase inhibitors (Areosa 2005). In many cases, the most significant medical therapy is treatment for depression. Depression is a major risk factor for AD, more than doubling the risk in an individual over age 60 (Devandan 1996). In fact, it may be reasonable to see depression in some cases as an early sign of cognitive dysfunction. As with other therapies for AD, anti-depressants have not been shown to alter cognitive function as measured by standard tests, but have shown efficacy for improvements in behavioral disturbances, performance of activities of daily living and reducing caretaker distress (Lyketsos 2003).

The Research Problem

AD as a research priority is of obvious importance -- this is a disease process that ranks among the most prolific killers in the United States. A clear understanding of the etiology and molecular mechanism(s) underlying AD, after over one-hundred years of intense study, remains elusive. At present a conclusive diagnosis can only be obtained at autopsy or through brain biopsy, which means the vast majority of dementia patients are not diagnosed until death (Alzheimer's Association 2010). These features of the disease have complicated research efforts. An enormous number of hypotheses have been presented to explain the etiology and progression of this disorder over the last half-century. A number have fallen by the wayside, like the now-rejected hypothesis that toxicity from aluminum exposure leads to the disease.

Currently, the leading hypothesis in the field of Alzheimer's disease research is the amyloid hypothesis which in its simplest form argues that beta-amyloid deposition is the initiating event in the progression of Alzheimer's neurodegeneration and that the other features of the disease descend from this initial abnormality (Hardy and Higgins 1992). This basic mechanism is nearly indisputably accurate for a number of variants of Alzheimer's disease, including the presenilin mutations, mutations in the APP gene and trisomy 21 (Down's syndrome) which all result in overproduction of beta-amyloid peptide. The mechanism is also supported by evidence that beta-amyloid applied to cultures of neurons or tissue cultures of brain results in hyperphosphorylation of tau and apoptotic death of neurons – both key additional features of Alzheimer's disease (Forloni 1993, Schrag 2008). Other data seems to contradict this hypothesis including evidence that plaques and tangles are not consistently distributed together in AD brain and vaccination against the beta-amyloid peptide, while successfully clearing plaques from the brain, was not able to consistently reverse or slow the progression of cognitive decline (Holmes 2008).

The tau hypothesis argues that abnormal phosphorylation of tau is the central pathology of Alzheimer's disease and is based on the observation that decline in cognitive function correlates far more with the extent of tau pathology than it does with beta-amyloid pathology. It is not clear whether hyperphosphorylation is due to overactivity of specific kinases (such as GSK3-beta) or deficient levels or function of key phosphatases (like tau protein phosphatase), but hyperphosphorylation results in destabilization of microtubules and loss of typical neuronal morphology (Honson and Kuret 2008).

Other hypotheses have suggested chronic hypoperfusion, abnormal microglial activation or other inflammatory mechanisms, altered calcium homeostasis, oxidative stress mechanisms etc to explain the pathologic changes associate with AD.

Increasing attention has been paid to the role of redox active transition metals as potential early players in AD pathogenesis. Free iron, in particular, with its ability to participate in Fenton chemistry, is thought to occupy a central role in initiating oxidative injury culminating in neuron loss (Castellani 2004). Additionally iron, zinc and copper are concentrated within beta-amyloid plaques, a pathological hallmark of AD (Lovell 1998). These observations have prompted intense study of central nervous system iron chelators in animal models with some degree of success, although preliminary clinical trials have had mixed results (Crapper-McLaughlin 1992, Squitti 2002, Lannfeldt 2006).

The notion that iron accumulates in the brain as an early feature of AD has both therapeutic and diagnostic implications. If true, recent advances in MRI techniques, including iron-sensitive gradient echo-T2* (GRE-T2*) and susceptibility weighted imaging sequences (SWI), should be able to detect the increased tissue iron (Haacke 2005). This methodology may provide a clinically useful biomarker of AD and a mechanism for monitoring the efficacy of iron-modulating therapies. More immediately, the technique enables in vivo evaluation of the iron-accumulation hypothesis in human beings and a correlation of iron accumulation to the clinical progression of dementia.

Previous Work

A post-mortem analysis of brain tissue from various lobar regions was performed by atomic absorption spectrometry (Magaki 2007). Samples were obtained from

cognitively normal elderly brain, early Alzheimer's disease, and severe Alzheimer's disease brain from both frontal lobe and hippocampus. Copper, and non-heme, loosely bound and total iron were measured. Total and non-heme iron levels were not significantly altered in the AD cases, while loosely bound iron (isolated from mitochondria) was increased and copper was decreased. These findings were at odds with the widely held belief that iron is markedly increased in AD – various review articles report AD brain iron to be increased by two to five fold (Avramovich-Tirosh 2008, Bush and Tanzi 2008, Molina-Holgado 2007, Huang 2004).

Our group also designed and executed a longitudinal, prospective clinical trial to evaluate radiologically the correlation of two distinct markers of brain iron with the progression of dementia using SWI (Kirsch 2009). Regional parenchymal iron concentration may be semi-quantitatively estimated in vivo using this technique because iron produces a loss of signal intensity. Additionally, punctate sources of high-iron concentration produced characteristic small, round hypointensities in some images. These hypointensities were thought to represent brain microbleeds, and in the setting of dementia are distributed with a posterior lobar predilection characteristic of CAA. CAA is comorbid with AD in as many as 95% of AD cases (Jellinger 2007). In this condition the β-amyloid peptide is deposited along the cerebral and meningeal vasculature in the walls of small and medium-sized arterioles. Vascular wall infiltration with these proteins appears to be associated with a structural instability of arterioles accounting for brain microbleed (BMB) and associated MR signal voids. In vivo evidence of CAA was limited until the introduction of GRE-T_2^* weighted MR imaging, which remains the clinical standard for detection of BMB which often result from CAA (Atlas 1988).

Though recent reviews of the BMB literature have attempted to codify the interpretation of these findings, the inconsistency of data sets, the lack of pathological confirmation and the need for better designed prospective studies to determine their clinical significance has been emphasized (Cordonnier 2006, 2007, Viswanathan 2006). Detection of BMB is improved by new, high-resolution, 3D GRE-T2* and SWI. SWI is an advance in T_2* weighted brain MR imaging that enhances contrast from local susceptibility tissue variations (Haacke 2004, 2005). At 1.5T, the SWI sequence was found to be four fold more sensitive for detection of traumatic BMB than conventional GRE-T_2^* and recent data in MCI subjects indicates again at least a four fold increase in BMB recognition by SWI compared to conventional GRE-T_2^* imaging (Haacke 2007, Tong 2003, 2004). To date, punctate signal voids have been observed in a number of diseases – by far the most common are hypertension and CAA. Those associated with hypertensive vasculopathy tend to be localized to basal ganglia, internal capsule, brain stem, and cerebellum, whereas those associated with CAA are generally smaller with a posterior lobar predilection (Rosand 2005 and Walker 2004).

Of the fifty patients enrolled in this study with mild cognitive impairment (MCI - the earliest clinically detectable stage of cognitive loss), 23 remained cognitively stable throughout the follow-up period while 27 progressed to dementia. Of the brain-regions of interest, only the left putamen demonstrated a significant loss of signal intensity in the cohort that progressed to dementia compared to both the stable MCI population and the normal control cases. Two or more BMB were observed in ten patients in the study. Of these ten, nine progressed to dementia while one remained stable at MCI. All nine who progressed to dementia had a progressive increase in the number of hypointensities, while

the one stable case did not have an increasing number. These findings indicate that CAA and microbleeds represent clinically important pathologies and are detectable in approximately one-third of dementia patients prior to the onset of cognitive loss.

One final study formed the background for this body of work. Longitudinal serum samples were collected from the patients described in the previous study. Proteomic analysis of peptides carried on albumin in the serum identified certain peptide breakdown products of heme degradation enzymes that were markedly elevated in MCI patients who would ultimately progress to dementia compared to those who remained stable. In particular, the ratio of biliverdin reductase B-related peptides to heme oxygenase 1-related peptides was markedly increased in the group that progressed to dementia. These findings may represent a valuable early biomarker of Alzheimer's disease, but they may also indicate abnormal activation of the heme degradation system in AD.

The findings from these studies provoke an important question: Could the absence of iron-overload in these cases indicate that iron dysregulation and overload is not inherently a feature of Alzheimer's disease, but rather of a comorbidity like CAA which produces microbleeding? Previous post-mortem tissue analyses of Alzheimer's disease brains in our laboratory failed to demonstrate an increase in either total iron concentration (in any studied region) or non-heme (chelatable) iron (Magaki 2007). Additionally, no dysregulation of iron regulatory proteins 1 or 2 could be demonstrated in our studies and no clear metabolic derangement has been consistently reported in the literature (Magaki 2007). However, heme-degradation pathway enzymes are reported to be increased in both AD brain and in peripheral serum samples from dementia patients (Premkumar

1995, Mueller 2010). CAA could potentially explain this pattern of findings and account for the source of pathological iron reported in numerous qualitative studies. While a wide spectrum of CAA severity is present in AD, at autopsy more than 95% of AD patients are found to have some degree of CAA pathology. Bleeding below the threshold of detection for our current MRI techniques has been reported and demonstrated to be associated with amyloid plaque formation (Cullen 2005). However, in our study, one-third of the dementia cases had detectable hypointensities thought to be CAA-related bleeding. AD accounts for about two-thirds of all dementia cases, meaning microbleeding may be a major disease mechanism in as many as half of all AD cases (Hendrie 1998).

Hypothesis and Aims of Current Studies

We proposed to clarify the degree to which iron is dysregulated in AD and to identify the source of abnormal iron. Several studies utilizing very different methodologies were required to answer these questions. We conducted a meta-analytic review of available literature to determine whether iron is actually increased in AD and to better understand how the belief that AD is a disease of iron-overload developed. Effective meta-analysis requires objective inclusion and exclusion criteria, so all studies encountered were included in the analysis unless there was an objective reason to exclude them. In particular, results reported from fixed tissue appeared to differ from results obtained from never-fixed specimens. We felt it was necessary to specifically confirm the effect of tissue fixation before excluding studies on fixed tissue from the analysis. Additionally, we extensively searched available literature, including studies in foreign

languages and studies which were not PubMed indexed. After confirming by meta-analysis that iron was not increased in quality-controlled studies of AD brain, we analyzed the citation patterns in key literature to better understand how the belief to the contrary developed.

Subsequently, we evaluated whether microvascular bleeding secondary to CAA accounts for the increased iron reported by some investigators in AD cases. This was accomplished by correlating brain iron levels and heme degradation pathway enzyme levels to the degree of CAA in post-mortem cases. If the hypothesis is true, non-heme iron measurements should increase in CAA-affected tissue and be associated with increases in heme-degradation pathway enzymes indicative of tissue exposure to blood. If iron overload is a feature of CAA rather than a more-general feature of AD, it is possible that chelation therapies will be more-effective for a subset of Alzheimer's patients with severe vasculopathy. Finally, because iron-overload appeared to be due primarily to microbleeding, we assessed whether hypointense foci in susceptibility weighted images accurately identified microhemorrhages in CAA tissue and observed the pathology present in these locations to better understand the mechanism of vascular degeneration associated with CAA.

The findings of these studies indicate that iron is not globally dysregulated in Alzheimer's disease, despite the dogmatic belief to the contrary in the field. When iron overload is present in a subset of AD brains, it correlates with microbleeding and CAA, and not with the presence of parenchymal hallmarks of AD. Microbleeding events can be detected by susceptibility weighted images *in vivo* which is a reasonable imaging biomarker of severe CAA. Finally, the mechanism associated with vascular degeneration

in CAA appears to be associated with the deposition of pro-oxidative copper and iron in the arteriolar walls and prominent late-complement activation – pathologies which may be directly associated with beta-amyloid deposition.

References

1. Aguero-Torres H, Fratiglioni L, Guo Z, et al (1999). Mortality from dementia in advanced age: a 5-year follow-up study of incident dementia cases. J Clin Epidemiol 52:737–743.

2. Alzheimer's Association (2010) 2010 Alzheimer's disease facts and figures. Alzheimer's Dement. 6:158-94.

3. Areosa S, Sherriff F, McShane R (2005) Memantine for dementia. Cochrane Database Syst Rev CD003154.

4. Atlas SW, Mark AS, Grossman RI, Gomori JM (1988) Intracranial hemorrhage: gradient-echo MR imaging at 1.5 T. Comparison with spin-echo imaging and clinical applications. Radiology 168:803-807.

5. Avramovich-Tirosh Y, Amit T, Bar-Am O, et al (2008) Physiological and pathological aspects of A-beta in iron homeostasis via 5'UTR in the APP mRNA and the therapeutic use of iron chelators. BMC Neuroscience 9:S2.

6. Brookmeyer R, Corrada MM, Curriero FC, Kawas C (2002) Survival following a diagnosis of Alzheimer disease. Arch Neurol 59:1764–1767.

7. Bush A, Tanzi R (2008) Therapeutics for Alzheimer's disease based on the metal hypothesis. Neurotherapeutics 5:421-32.

8. Castellani R, Honda , Zhu X, et al (2004) Contribution of redox-active iron and copper to oxidative damage in Alzheimer disease. Ageing Res Rev 3:319-26.

9. Cordonnier C, van der Flier WM, Sluimer JD, et al (2006) Prevalence and severity of microbleeds in a memory clinic setting. Neurology 66:1356-1360.

10. Cordonnier C, Al-Shahi Salman R, Wardlaw J (2007) Spontaneous brain microbleeds: systematic review, subgroup analyses and standards for study design and reporting. Brain 130:1988-2003.

11. Crapper McLachlan D, Dalton A, et al (1991) Intramusclar desferrioxamine in patients with Alzheimer's disease. Lancet 337:1304-8.

12. Cuello A, Bruno M, Allard S, et al (2010) Cholinergic involvement in Alzheimer's disease. A link with NGF maturation and degradation. J Mol Neurosci 40:230-5.

13. Devanand D, Sano M, Ming-Xin T, et al (1996) Depressed mood and the incidence of Alzheimer's Disease in the elderly living in the community. Arch Gen Psych 53:175-82.

14. Cullen KM, Kocsi Z, Stone J (2005) Pericapillary haem-rich deposits: evidence for microhaemorrhages in aging human cerebral cortex. J Cereb Blood Flow Metab 25:1656-1667.

15. Forloni G, Chiesa R, Smiroldo D, et al (1993) Apoptosis mediated neurotoxicity induced by chronic application of beta amyloid fragment 25-35. Neuroreport 4:523-6.

16. Ganguli M, Dodge HH, Shen C, et al (2005) Alzheimer disease and mortality: a 15-year epidemiological study. Arch Neurol 62:779–784.

17. Haacke EM, Xu Y, Cheng YC, Reichenbach JR (2004) Susceptibility weighted imaging (SWI). Magn Reson Med 52:612-618.

18. Haacke EM, Cheng NY, House MJ, et al (2005) Imaging iron stores in the brain using magnetic resonance imaging. Magn Reson Imaging. 23:1-25.

19. Haacke EM, DelProposto ZS, Chaturvedi S, et al (2007) Imaging cerebral amyloid angiopathy with susceptibility-weighted imaging. AJNR Am J Neuroradiol 28:316-317.

20. Hardy J, Higgins G (1992) Alzheimer's disease: the amyloid cascade hypothesis. Science 256:184-5.

21. Helmer C, Joly P, Letenneur L, et al (2001) Mortality with dementia: results from a French prospective community-based cohort. Am J Epidemiol 2001:642–648.

22. Helzner E, Scarmeas N, Cosentino S, et al (2008) Survival in Alzheimer's disease: a multiethnic population-based study of incident cases. Neurology 71:1489-95.

23. Hendrie H (1998) Epidemiology of dementia and Alzheimer's disease. Am J Geriatr Psychiatry 6:S3-18.

24. Holmes C, Boche D, Wilkinson D, et al (2008) Long-term effects of Abeta42 immunisation in Alzheimer's disease: follow-up of a randomized, placebo-controlled phase 1 trial. Lancet 372:216-23.

25. Honson N, Kuret J (2008) Tau aggregation and toxicity in taupathic neurodegenerative diseases. J Alz Dis 14:417-22.

26. Huang X, Moir R, Tanzi R, et al (2004) Redox-active metals, oxidative stress and Alzheimer's disease pathology. Ann NY Acad Sci 1012:153-63.

27. Jellinger KA, Lauda F, Attems J (2007) Sporadic cerebral amyloid angiopathy is not a frequent cause of spontaneous brain hemorrhage. Eur J Neurol 14:923-8.

28. Kalia M (2003) Dysphagia and aspiration pneumonia in patients with Alzheimer's disease. Metabolism Clin Exp 52:36-8.

29. Kirsch W, McAuley G, Holshouser B, et al (2009) Serial susceptibility weighted MRI measures brain iron and microbleeds in dementia. J Alz Dis 17:599-609.

30. Landau S, Harvey D, Madison C, et al (2010) Comparing predictors of conversion and decline in mild cognitive impairment. Neurology in press.

31. Lannfelt L, Blennow K, Zetterberg H, et al (2008) Safety, efficacy and biomarker findings of PBT2 in targeting Abeta as a modifying therapy for Alzheimer's disease; a phase IIa, double blind randomized placebo controlled trial. Lancet Neurol 7:779-86.

32. Lovell M, Robertson J, Teesdale W, et al (1998) Copper, iron and zinc in Alzheimer's disease senile plaques. Journal of Neurological Science 158:47-52.

33. Lyketsos C, DelCampo L. Steinberg M, et al (2003) Treating depression in Alzheimer disease: efficacy and safety of sertraline therapy and the benefits of depression reduction: the DIADS. Arch Gen Psych 60:737-46.

34. Magaki S, Raghavan R, Mueller C, et al (2007) Iron, copper and iron regulatory protein 2 in Alzheimer's disease and related dementia. Neuroscience Letters 418:72-6.

35. Molina-Holgado F, Gaeta H, Williams R, Francis P (2007) Metals ions and neurodegeneration. Biometals 20:639-54.

36. Molsa PK, Marttila RJ, Rinne UK (1995) Long-term survival and predictors of mortality in Alzheimer's disease and multi-infarct dementia. Acta Neurol Scand 91:159–164.

37. Mueller C, Zhou W, Vanmeter A, et al (2010) The heme degradation pathway is a promising serum biomarker source for the early detection of Alzheimer's disease. J Alz Dis. 19:1081-91.

38. Premkumar D, Smith M, Richey P, et al (1995) Induction of heme oxygenase-1 mRNA and protein in neocortex and cerebral vessels in Alzheimer's disease. J Neurochem 65:1388-402.

39. Rosand J, Muzikansky A, Kumar A, et al (2005) Spatial clustering of hemorrhages in probable cerebral amyloid angiopathy. Ann Neurol 58:459-462.

40. Samanta M, Wilson B, Santhi K, et al (2006) Alzheimer disease and its management: a review. Am J Ther 13:516-26.

41. Schrag M, Sharma S, Brown-Borg H, Ghribi O (2008) Hippocampus of Ames dwarf mice is resistant to beta-amyloid-induced tau hyperphosphorylation and changes in apoptosis-regulatory protein levels. Hippocampus 18:239-44.

42. Squitti R, Rossini P, Cassetta E, et al (2002) D-penicillamine reduces serum oxidatitive stress in Alzheimer's disease patients. Eur J Clin Inv 32:51-9.

43. Tong KA, Ashwal S, Holshouser BA, et al (2003) Hemorrhagic shearing lesions in children and adolescents with posttraumatic diffuse axonal injury: improved detection and initial results. Radiology 227:332-339.

44. Tong KA, Ashwal S, Holshouser BA, et al (2004) Diffuse axonal injury in children: clinical correlation with hemorrhagic lesions. Ann Neurol. 56:36-50.

45. Viswanathan A, Chabriat H (2006) Cerebral microhemorrhage. Stroke 37:550-555.

46. Walker DA, Broderick DF, Kotsenas AL, Rubino FA (2004) Routine use of gradient echo MRI to screen for cerebral amyloid angiopathy in elderly patients. AJR Am J Roentgenol 182:1547-1550.

47. Wolfson C, Wolfson DB, Asgharian M, et al (2001) A reevaluation of the duration of survival after the onset of dementia. N Engl J Med 344:1111–1116.

48. Zilka N, Novak M (2006) The tangled story of Alois Alzheimer. Bratisl Lek Listy 107:343-5.

CHAPTER TWO

THE EFFECT OF FORMALIN FIXATION ON THE LEVELS OF BRAIN TRANSITION METALS IN ARCHIVED SAMPLES

Matthew Schrag[1], April Dickson[1], Arshad Jiffry[1], David Kirsch[1], Harry V. Vinters[2] and Wolff Kirsch[1]

[1]Loma Linda University, Neurosurgery Center for Research, Loma Linda, California
[2]University of California Los Angeles, Department of Pathology and Laboratory Medicine, Los Angeles, California

Abstract

Reports that iron, zinc and copper homeostasis are in aberrant homeostasis are common for various neurodegenerative diseases, particularly for Huntington's disease, Parkinson's disease and Alzheimer's disease. Manipulating the levels of these elements in the brain through the application of chelators has been and continues to be tested therapeutically in clinical trials with mixed results. Much of the data indicating that these metals are abnormally concentrated in Alzheimer's disease and Parkinson's disease brain tissue was generated through the analysis of post-mortem human tissue which was archived in formalin. In this study, we evaluate the effect of formalin fixation of brain on the levels of three important transition metals (iron, copper and zinc) by atomic absorption spectroscopy. Paired brain specimens were obtained at autopsy for each case; one was conserved by formalin archival (averaging four years), the other was rapidly

frozen. Both white and grey matter samples were analyzed and the concentrations of iron and zinc were found to decrease with fixation. Iron was reduced by 40% ($p<0.01$), and zinc by 77% ($p<0.0001$); copper concentrations increased by 37% ($p<0.05$) by the paired T-test. The increase in copper is likely due to contamination from trace copper in the formalin. These results indicate that transition metal data obtained from fixed tissue may be heavily distorted and care should be taken in interpreting this data.

Introduction

The measurement of trace metals in human tissue has revealed numerous insights into both normal physiology and disease. Brain iron concentration increases with age, reaching a plateau at about age 55 (Hallgren and Sourander 1958). Disturbances in the levels of various metals including iron in the brain are reported to be associated with many neurodegenerative disorders, including Huntington's disease, amyotrophic lateral sclerosis, Alzheimer's disease (AD) and Parkinson's disease (PD). In these diseases, iron is known to accumulate in the deep grey matter and iron accumulation in the neocortex has been suggested to contribute to the cognitive dysfunction associated with some of these diseases. Abnormal accumulation of iron in the AD brain could account for increased oxidative injury which is an early finding in Alzheimer's disease and increases in brain iron have in fact been reported early in this condition mirroring the oxidative changes (Smith 2010, Nunomura 2001), although several additional studies have failed to detect any abnormal changes in brain iron in AD compared to age-matched controls at various stages of the disease (Hallgren and Sourander 1960, Ward and Mason 1987, Magaki 2007). Additionally, beta-amyloid peptides which aggregate to form senile

plaques in Alzheimer's and Parkinson's diseases, avidly bind to iron, zinc and copper. When these metals are bound, the toxicity of beta-amyloid is reported to markedly increase (Rottkamp 2001). Pharmacologically manipulating the levels and/or distribution of these metals in the brain is becoming a clinical reality for Alzheimer's disease and Parkinson's disease through the use of chelators and metallophores – several of which are in clinical trials (Crapper McLachlan 1991, Squitti 2003, Lannfelt 2008). Initial results have been mixed; modest improvement in secondary measures like the performance of activities of daily living has been reported, but no agent has yet produced an improvement in cognition.

Reports that iron, zinc and possibly copper are abnormally concentrated in neocortical brain in Alzheimer's and that all three metals are deposited in beta-amyloid plaques were primarily generated from analysis of post-mortem, fixed tissue through histochemical and radioanalytical techniques (such as particle induced X-ray emission tomography) (Goodman 1953, Lovell 1998). The reliability of this data set requires that formalin archival of tissue does not disturb the levels of these transition metals. We noted that previous reports of iron concentrations from both normal and diseased brains which utilized fixed specimens appear to report substantially lower concentrations than studies which use never-fixed specimens analyzed with equivalent techniques (Lovell 1998, Diebel 1996). To evaluate whether this observation represents an artifact introduced through the fixation technique, we have evaluated paired brain samples taken from the temporal lobe of Alzheimer's disease patients to determine whether samples stored in formalin have equivalent levels of three key transition metals – iron, copper and zinc.

Materials and Methods

Post mortem tissue was donated from the Alzheimer's Disease Research Center Brain Bank at the University of California, Los Angeles. All patients and/or their surrogates had consented to tissue donation prior to autopsy. The research protocol was approved by the Institutional Review Board of Loma Linda University Medical Center (approval #54174). Both frozen and formalin-archived tissue was collected from the middle temporal gyrus of four severe Alzheimer's disease brains. Tissue samples were isolated with a diamond blade scalpel and titanium and/or nylon forceps (to avoid contamination) and collected as 30-60 mg specimens of isolated grey or white matter. From fixed tissue, the surface of tissue blocks was dissected away to remove any tissue which might have been exposed to iron-containing instruments through the autopsy procedure.

Tissue was ashed for analysis by standard techniques. Briefly, brain tissue was immersed in concentrated nitric acid (300 microliters) overnight, then incubated in a water bath at 80 degrees Celsius for 20 minutes. The resulting solution was allowed to cool to room temperature and hydrogen peroxide (300 microliters, 10M solution) was added to dissolve lipid components. After thirty minutes incubation at room temperature, the sample was heated to 70 degrees Celsius in the water bath for 15 minutes. The resultant solution was allowed to cool for 10 minutes, then vortexed thoroughly and stored until analysis.

Atomic absorption spectrums were measured with a Varian SpectrAA 220Z atomic absorption spectrometer and processed with SpectrAA software v.4.1. Standard iron and copper curves were produced from 25, 50, 75 and 100 parts per billion solutions

of standard iron or copper in nitric acid (Arcos Organics, New Jersey). Standard curve for zinc was produced from 250, 500, 750 and 1000 parts per billion solutions of standard zinc in nitric acid (Solutions Plus Inc, Missouri). The spectrometer was zeroed to a maximum of 0.005 mean absorbance. For total iron measurements samples were diluted 1:40, for zinc measurements samples were diluted 1:10 and for copper samples were diluted 1:20. Standard furnace settings recommended by Varian were used for the analysis. All sample values were the mean of six measurements. Concentrations are calculated to reflect the concentration of the metal in micrograms per gram of native tissue (wet weight). Significance was determined by the two-tailed, paired Student's T test, with $\alpha = 0.05$.

Results

Two samples were analyzed from each of four brains which were severely affected by Alzheimer's disease (Braak and Braak stage VI) (Braak and Braak 1997). One frozen and one formalin-fixed temporal lobe specimen were obtained from each case for comparison; the mean duration of archival was four years (range 3-6). Each specimen was divided into grey and white matter which were analyzed separately. Six measurements were collected for each sample and the mean of the values was reported in Figure 1. The mean percent relative standard deviations (%RSD) over these repeated measures were 0.8% for iron, 12.5% for zinc and 1.8% for copper. The %RSD for zinc was wider because the concentration in fixed specimens approached the threshold of detection for this element (%RSD fixed = 20.8, %RSD frozen = 4.1%).

Micrograms iron / gram tissue (wet weight)
100
90
80
70
60
50
40
30
20
10
0
■ = grey matter
□ = white matter
Frozen brain specimen
Fixed brain specimen
Micrograms zinc / gram tissue (wet weight)
45
40
35
30
25
20
15
10
5
0
Frozen brain specimen
Fixed brain specimen
Micrograms copper / gram tissue (wet weight)
20
8
6
4
2
0
Frozen brain specimen
Fixed brain specimen

Figure 1: Effect of long-term formalin archival on transition metal levels in paired Alzheimer's disease brain samples

Iron levels were found to decrease by about 43% upon fixation in formalin ($p=0.008$), zinc levels were shown to decrease with fixation by about 75% ($p<0.0001$) and copper increased by 37% ($p=0.03$). All of these effects appeared to be independent of whether the tissue is collected from grey matter or white matter. Lines between specimens indicate they were taken from the same brain.

Iron levels in the fixed tissue were significantly lower than in the frozen specimens ($p=0.008$ by paired T-test). Seven of the eight specimens examined were found to have decreased iron after fixation, while one remained essentially unchanged. On average, iron concentration was 43% lower in the fixed tissue (mean difference 26.2 μg/g tissue, 95% CI 9.1-43.3 μg/g tissue) and both grey and white matter were affected equally. Brain zinc levels were also found to be notably decreased after fixation ($p<0.0001$). This change also affected both grey and white matter and resulted in a mean decrease in zinc of 19.8 μg/g tissue (95% CI 13.9-25.8 μg/g tissue). Brain copper was found to be increased in the fixed specimens ($p=0.03$). This finding was unexpected – seven out of eight specimens contained higher levels of copper than their frozen counterparts and the mean increase in copper was 1.65 μg/g tissue (95% CI 0.21-3.09 μg/g).

Discussion

Previous studies have shown that formalin fixation affects the levels of transition metals in various organs, although it has frequently been argued that most transition metals in the brain are not affected by fixation. This was primarily determined either by analysis after a brief fixation period or by indirect means such as determining the concentration of trace elements in the formalin in which the organ was stored for comparison to clean formalin (Andrasi 1990, Bush 1995, Gallein 2008). This approach evaluates transition metal leaching and is obviously sensitive to dilutional variation, evaporation and contamination from other sources. Additionally, because transition metal concentrations in most tissues vary considerably between individuals, a non-paired

analysis may mask the effect of formalin. The most sensitive approach is to obtain paired samples from each case, one of which is stored by freezing, the other by formalin archival for several years.

The findings of this study demonstrate that formalin archival of brain samples affects the concentration of several transition metals. Both iron and zinc were found be significantly depleted after archival in formalin. Copper, however, was found to increase with formalin fixation. This increase in copper may be due to contamination of formalin with copper. While copper levels in formalin are reported to be approximately 2% the level found in brain (0.1 ppm vs 5 ppm) (Andrasi 1990, Gellein 2007), the Alzheimer's disease brain is depleted of copper and over-expresses copper binding proteins such as ceruloplasmin which may increase the tissue's copper binding capacity and could in theory explain the accumulation of copper in the tissue with fixation (Loeffler 1996). Reports from the literature also indicate that copper levels dramatically increase in AD brain with fixation, although this was not noted in control tissue which would support this hypothesis (see Table 1).

The effect of fixation on brain iron has not been previously well-documented, although we noted that studies which analyzed fixed brain reported different levels of metals than those analyzing never-fixed brain. Iron levels detected using a micro-PIXE (particle induced x-ray emission) analysis of formalin fixed Alzheimer's disease amygdala were 38.8 µg / g wet tissue while other studies from the same laboratory using quantitative analyses of never-fixed, Alzheimer's disease amygdala found a mean iron concentration of 65.5 µg / g wet tissue (Lovell 1998, Samudralwar 1995, Deibel 1996, Cornett 1998, Thompson 1988). These studies showed that fixed tissue from the same

Table 1: Effect of short-term fixation on transition metal concentrations in the amygdala reported in the literature

Study and method	[Iron] control	[Iron] AD	[Zinc] control	[Zinc] AD	[Copper] control	[Copper] AD
Fixed tissue Lovell 1998 - micro-PIXE, 24hr formalin exposure	**18.9 +/- 5.3** N = 5	**38.8 +/- 9.4** N = 9	**22.6 +/- 2.8** N = 5	**51.4 +/- 11.0** N = 9	**4.4 +/- 1.5** N = 5	**19.3 +/- 6.3** N = 9
Never-fixed tissue	**49.2 +/- 3.3** N = 56	**65.5 +/- 3.8** N = 101	**14.5 +/- 0.5** N = 69	**18.2 +/- 0.7** N = 119	**4.1 +/- 0.3** N = 11	**2.7 +/- 0.3** N = 10
Thompson 1988 - INAA	48.9 +/- 3.0	60.6 +/- 4.9	14.1 +/- 0.5	17.0 +/- 0.8	-	-
Samudralwar 1995 - INAA	50.8 +/- 3.7	70.8 +/- 4.0	16.7 +/- 0.5	21.4 +/- 0.5	-	-
Deibel 1996 - INAA	48.6 +/- 2.2	70.8 +/- 6.4	15.2 +/- 0.6	19.8 +/- 1.0	4.1 +/- 0.3	2.7 +/- 0.3
Cornett 1998 - INAA	49.0 +/- 4.0	64.0 +/- 3.0	13.6 +/- 0.5	17.6 +/- 0.6	-	-
Rulon 2000 - AA	-	-	15.7 +/- 0.5	16.6 +/- 1.0	-	-
Percent change *(Two-tailed T test)*	***-61 %*** *p<0.0001*	***-41 %*** *p<0.0001*	***+56 %*** *p<0.0001*	***+182 %*** *p<0.0001*	***+7.3 %*** *p=0.52*	***+615 %*** *p<0.0001*

All six studies listed were published from the same laboratory at the University of Kentucky. One study analyzed fixed tissue; the others analyzed never-fixed tissue – all used quantitative analytical methods. The never-fixed results are pooled in the second row and listed individually below. Measurements represent microgram metal per gram tissue, wet weight (results from Deibel 1996 were converted from dry weight measurements to wet weight). Errors listed are standard deviation. AD = Alzheimer's disease, PIXE = particle induced x-ray emission, INAA = instrumental neutron activation analysis, AA = atomic absorption. "Percent change" indicates the difference between measurements of "Never-fixed" and "Fixed" tissue samples.

brain region contained 41% less iron than comparable never-fixed tissue, which is strikingly consistent with the 43% reduction we found in the paired samples in this study. Additionally, iron concentration in control tissue was found to decrease by even more (never-fixed 49.2 micrograms/gram versus fixed 18.9 micrograms/g – a 61% reduction, $p<0.0001$). The effects on copper levels in these studies were more severe in AD brain than what we report here. While fixed and frozen amygdala tissue from control brain was not significantly affected (4.1 vs 4.4 micrograms/gram, $p=0.52$), AD tissue was reported to contain 2.7 micrograms copper/gram in never-fixed tissue and 19.3 micrograms/gram in fixed tissue – a 615% increase (Lovell 1998, Deibel 1996). Finally, zinc levels were also found to be altered between the studies, although they did not match the results of our study. Fixation increased zinc levels by 54% in control tissue and by 179% in AD tissue (Lovell 1998, Thompson 1988, Samudralwar 1995, Deibel 1996, Cornett 1998, Rulon 2000). Our results found that zinc was depleted by 75% in temporal lobe tissue from AD patients. The discrepancy in these results may indicate that effects of fixation differ between brain regions, or with the length of fixation. Additionally, we noted a wide variance in the effect of fixation on tissue concentrations of all three metals, which makes it difficult to simply calculate a correction for fixation. Regardless, formalin fixation (even briefly) appears to destabilize the concentration of multiple metal species and may affect normal and diseased brain differently. It is therefore necessary to cautiously interpret transition metal data derived from fixed tissue and future studies should be limited to fresh or frozen specimens.

Altered homeostasis of iron, zinc and/or copper has been suggested to be involved in many neurodegenerative diseases; however, reports of metals concentration in these

tissues have been remarkably disparate in their conclusions. Before seriously considering the use of chelators or other compounds to manipulate the homeostasis of these essential biometals, it will be necessary to determine whether and to what degree they are truly dysregulated. This requires a critical evaluation of the available data. Because a significant portion of that data was generated from fixed tissue, it may be necessary to re-examine the fundamental assumptions about the role of metals in various neurodegenerative diseases.

References

1. Andrasi E, Nadasdi J, Molznar Z, et al (1990) Determination of main and trace element contents of human brain by NAA and ICP-AES methods. Biol Trace Elem Res 26/7:691-8.

2. Braak H, Braak E (1991) Neuropathological stageing of Alzheimer-related changes. Acta Neuropathol 82:239-59.

3. Bush V, Moyer T, Batts K, Parisi J (1995) Essential and toxic element concentrations in fresh and formalin-fixed human autopsy tissues. Clin Chem 41/2:284-94.

4. Cornett C, Markesbery W, Ehmann W (1998) Imbalances of trace elements related to oxidative damage in Alzheimer's disease brain. Neurotoxicology 19:339-45.

5. Crapper McLaughlan D, Dalton A, Kruck T, et al (1991) Intramusclar desferrioxamine in patients with Alzheimer's disease. Lancet 337:1304-8.

6. Deibel M, Ehmann W, Markesbery W (1996) Copper, iron and zinc imbalances in severely degenerated brain regions in Alzheimer's disease: possible relation to oxidative stress. Journal of Neurological Science 143:137-42.

7. Hallgren B, Sourander P (1958) The effect of age on the non-haemin iron in the human brain. J Neurochem 3:41-51.

8. Hallgren B, Sourander P (1960) The non-haemin iron in the cerebral cortex in Alzheimer's disease. J Neurochem 5:307-10.

9. Gellein K, Flaten T, Erikson K, et al (2008) Leaching of trace elements from biological tissue by formalyn. Biol Trace Elem Res 121:221-5.

10. Goodman L (1953) Alzheimer's disease; a clinico-pathologic analysis of 23 cases with a theory on pathogenesis. J Nerv Ment Dis 118:97-130.

11. Lannfelt L, Blennow K, Zetterberg H, et al (2008) Safety, efficacy and biomarker findings of PBT2 in targeting Abeta as a modifying therapy for Alzheimer's disease; a phase IIa, double blind randomized placebo controlled trial. Lancet Neurol 7:779-86.

12. Loeffler D, LeWitt P, Juneau P, et al (1996) Increased regional brain concentrations of ceruloplasmin in neurodegenerative disorders. Brain Res 738:265-74.

13. Lovell M, Robertson J, Teesdale W, et al (1998) Copper, iron and zinc in Alzheimer's disease senile plaques. Journal of Neurological Science 158:47-52.

14. Nunomura A, Perry G, Aliev G, et al (2001) Oxidative damage is the earliest event in Alzheimer Disease. J Neuropathol Exp Neurol 60:759-67.

15. Rottkamp C, Raina A, Zhu X, et al (2001) Redox-active iron mediates amyloid-beta toxicity. Free Radic Biol Med 30:447-50.

16. Rulon L, Robertson J, Lovell M, et al (2000) Serum zinc levels and Alzheimer's disease. Biol Trace Elem Res 75:79-85.

17. Samudralwar D, Diprete C, Ni B, et al (1995) Elemental imbalances in the olfactory pathway in Alzheimer's disease. Journal of Neurological Science 130;139-45.

18. Squitti R, Rossini P, Cassetta E, et al (2002) D-penicillamine reduces serum oxidatitive stress in Alzheimer's disease patients. Eur J Clin Inv 32:51-9.

19. Thompson C, Markesbery W, Ehmann W, et al (1988) Regional brain trace-element studies in Alzheimer's disease. Neurotoxicology 9:1-8.

CHAPTER 3

MAPPING IRON, ZINC AND COPPER IN THE ALZHEIMER'S DISEASE BRAIN: A QUANTITATIVE META-ANALYSIS

Matthew Schrag[1], Claudius Mueller[2], Mark A. Smith[3], and Wolff Kirsch[1]

[1]Loma Linda University School of Medicine and the Neurosurgery Center for Research, Loma Linda, California
[2]George Mason University, Center for Applied Proteomics and Molecular Medicine, Manassas, Virginia
[3]Case Western Reserve University, Department of Pathology, Cleveland, Ohio

Abstract

Dysfunctional homeostasis of transition metals is believed to play a role in the pathogenesis of Alzheimer's disease (AD). Brain copper, zinc, and particularly iron overload are widely accepted features of AD which have led to the hypothesis that oxidative stress generated from aberrant homeostasis of these transition metals might be a pathogenic mechanism behind AD. This meta-analysis compiled and critically assessed available quantitative data on brain iron, zinc and copper levels in AD patients compared to aged controls. The results were heterogeneous as a result of a series of heavily cited articles from one laboratory that reported large increases in iron in AD neocortex. Seven laboratories failed to reproduce these findings ($p=0.76$) – the pooled effect size reported by these studies was -0.05. Zinc was not increased in the neocortex. Copper was significantly depleted in AD ($p=0.0003$). In light of these findings, it will be important to

re-evaluate the hypothesis that transition metal overload accounts for oxidative injury noted in AD.

Introduction

The distribution and homeostasis of transition metals in Alzheimer's disease (AD) brain and their potential role in the etiology of neurodegeneration has been debated for six decades or more. Goodman presented one of the earliest arguments for a role of iron in AD in 1953 with a detailed pathological/histological description of a series of post-mortem AD cases. He reported increased Prussian/Turnbull's blue reactivity indicating abnormally high levels of tissue iron in a few of these patients. From these findings, he hypothesized that a defect in iron management may underlie late-onset cognitive loss in these cases. Hallgren and Sourander in 1958 and 1960 published the first quantitative analyses of brain iron in Alzheimer's disease patients using colorimetric techniques. This failed to demonstrate a significant increase in tissue levels of non-heme iron in AD brain. However, like Goodman, they noted that many of the specimens showed increased reactivity to histological iron stains. In the intervening decades, brain iron overload gradually became widely accepted as a feature of AD (Gerlach 1994, Benzi 1995, Smith 1997, Schipper 1999, Cuajungco 2000). Additionally, the observation that iron, zinc and copper were concentrated in beta-amyloid plaques led to the hypothesis that oxidative stress generated from aberrant homeostasis of these transition metals and pathologic metal-protein interactions might be mechanisms behind the aggregation and toxicity of senile plaques, ultimately leading to (or contributing to) the neurodegeneration associated with AD (Lovell 1998, Smith 1997, Markesbery 1999). In vitro studies demonstrated

that iron, zinc and copper at near-physiologic conditions each bind beta-amyloid and are capable of precipitating it into aggregates (Bush 1994). The discovery that chelating these metals from plaques reduced plaque toxicity and increased amyloid solubility in vitro further supported the metals hypothesis and became a basis for the therapeutic use of chelators in neurodegenerative conditions (Schubert 1995, Cherny 1999, Rottkamp 2001). Interest in manipulating brain levels of transition metals has risen, resulting in the development of many pharmacologic chelators and a number of clinical trials (Crapper McLachlan 1991, Lannfelt 2008, Liu 2010, Squitti 2002).

In the year 2000, one of the most-cited review articles on the subject of metals in AD declared that "a consensus has emerged in the literature that copper, zinc and iron are elevated in the AD-affected neocortex" (Bush 2000). The purpose of this study is to evaluate if that consensus is accurate. The issue remains that most available data on brain transition metal concentrations is qualitative, and quantitative studies have generally lacked adequate power to determine whether changes are significant. Additionally, several of the most prominently cited papers in the field have studied tissue that has been fixed, which has been shown to compromise the integrity of the data (Lovell 1998, Jellinger 1990, Schrag 2010). This has made it increasingly important to compile and critically assess available quantitative data on brain iron, zinc and copper levels in AD patients compared to aged controls.

Methods

Literature Search

Literature search was conducted by the first author. Appropriate articles were assembled by systematic queries of NCBI (PubMed), ISI Web of Science, OVID and GoogleScholar databases on the 8th of January 2010. Additionally, we reviewed the citation lists from each article retrieved for the meta-analysis and from relevant review articles. The indexes of certain journals were manually reviewed, including Journal of Radioanalytical and Nuclear Chemistry, Trace Elements in Medicine, Trace Elements and Electrolytes, and Microelement. Articles published in any year up to the date of search and in any language were included, as long as they were indexed in the databases described. Quantitative analytical techniques were included in the analysis; semi-quantitative approaches were excluded. Acceptable quantitative techniques included atomic absorption spectroscopy, inductively coupled plasma mass spectrometry or atomic emission spectroscopy, particle-induced x-ray emission, neutron activation analysis and colorimetric assays normalized to tissue weight. These methods have been shown to consistently produce equivalent results (Jervis 1985, Zhang 1997, Stedman 1997). Search terms therefore included a technique keyword (such as "neutron activation") and "Alzheimer's disease." General search of high-yield keyword combinations, such as "iron," "Alzheimer's" and "human brain" were also conducted. Abstracts were reviewed to collect only reports which compared human Alzheimer's disease brain to aged control brain for total iron, zinc and/or copper levels in any brain region. Finally, when possible we contacted an author from each study to request access to any unpublished data and to clarify methodological details. We were made aware of two unpublished datasets; these

could not be recovered for inclusion in this meta-analysis, but were described as finding no significant differences between groups.

Exclusion Criteria

Exclusion criteria were non-quantitative analysis (including normalizing element concentration to protein concentration), tissue fixation (for any duration of time), the absence of neuropathological diagnosis and inappropriate control tissue (all cases were required to be over age 55). Iron has been shown to increase in the brain with age in neurologically normal subjects; however, it reaches a relatively steady state by about age 55, which is why this was chosen as a cut-off (Hallgren and Sourander 1958, Markesbery 1984). Neuropathologic diagnosis was considered necessary because the clinical diagnosis of AD is only about 61-84% specific for AD (Gay 2008, Brunnstrom 2009). Tissue fixation has been shown to alter, sometimes dramatically, the concentrations of brain metals, either through leaching (iron is reduced on average by 40% in formalin fixed brain, zinc by as much as 75%), or by concentrating elements through tissue dehydration or by deposition of metal contaminants which may be present in formalin (particularly for copper) (Schrag 2010). Finally, normalization of metal levels to protein concentration was considered unreliable because one study found that much lower concentrations of protein were isolated from AD tissue compared to normal brain (Loeffler 1995).

Data Analysis

The studies which were included reported metals concentrations as either micromolar concentration or micrograms of metal per milligram of tissue. Tissue samples were either dessicated or native (referred to as dry weight or wet weight) -- wet weight was chosen as the standard measure for this study because it is the physiologically relevant mass. Because dry weight to wet weight conversion ratios have been extensively published for essentially all brain regions in both Alzheimer's disease and control brain, all dry weight measures were converted to wet weight measures. This conversion affected only two studies and the conversion ratios are included in supp. Table 4 (Andrasi 2000, Deibel 1998). Data from individual studies were collected as means, standard deviations, and numbers of brains in each group. Effect size was calculated by Hedge's g (with a small N bias correction) in a random effects model. Results were presented by brain region as weighted mean concentrations, and effect sizes. Studies were weighted in the analysis by inverse variance. Heterogeneity was assessed by Q-test with alpha = 0.05. The metal levels reported for the neocortex were nearly equivalent region-to-region, which enabled analysis of these regions jointly as well as individually. The pooled neocortical dataset included frontal lobe, temporal lobe, parietal lobe and hippocampal measurements. Normalcy of distribution was assessed with Lilliefors test for the pooled neocortical data (Lilleifors 1967). Figures were constructed using an Excel-based software add-on, MIX 1.7 (Bax 2007).

Results

Thirty-two studies were identified in the primary screen; twenty studies remained after the application of objective exclusion criteria. All studies evaluated for inclusion in the meta-analysis were reported in the annotated references with explanations of the rationale for inclusion or exclusion. In general, clinical data and demographic information were limited to age, sex and neuropathological diagnosis at death; comorbid diseases were generally not described. For this reason, evaluation of potential confounders was limited. Additionally, only one of the studies reported the use of blinding in any part of the study (Ward and Mason 1987). The neuropathologic diagnoses in all cases were limited to parenchymal Alzheimer's disease pathology -- vascular amyloid deposition and Lewy body pathologies were not described.

The main statistical measure we chose to describe the effect of AD on brain iron was Hedge's G, hereafter called simply "effect size." This statistical tool describes the difference between two groups (here the metal concentration in control brain vs. AD brain) as a proportion of the pooled standard deviation of the two groups. An effect size of 1 indicates the experimental group is one standard deviation higher than the control group. Because of the methodological differences and heterogeneity between the studies, a random effects model was chosen for the analysis. For datasets which were not significantly heterogenous, the random effects model yielded equivalent results to the fixed effects model and analysis in a fixed effects model would not alter the conclusions of the study.

When neocortical brain regions were analyzed together, the effect of Alzheimer's disease on brain iron approached significance (Fig 1; effect size = 0.23, 95%CI -0.07-

0.53, p=0.13). However, this analysis was complicated by significant heterogeneity. Heterogeneity in the iron dataset appeared to derive primarily from data published by the University of Kentucky (U of K) (Fig 2). When hippocampus, frontal, temporal and parietal lobes were merged to produce a cumulative dataset for analysis of neocortical iron, the heterogeneity between the U of K studies (4 studies) and all others (11 studies from 7 independent laboratories) became most evident, Q=26.0 (p=0.017) – the combined effect size reported by U of K studies alone was 0.67 (95%CI 0.35-1.00, p<0.0001) while the combined effect size reported by all other studies was -0.05 (95%CI -0.34-0.25, p=0.76); the latter we feel is the most-accurate estimate of the true effect of AD on neocortical iron (Fig. 2). With the exclusion of U of K studies, heterogeneity was reduced to non-significant levels as assessed by the Q test and no evidence of non-normal distribution was present by the Lilliefors test.

Region by region analysis (after the exclusion of the outlier data source) revealed significantly increased brain iron in Alzheimer's disease only in the putamen (supp. Table 1). Putamen iron levels were increased by 21.4% (effect size 1.14, 95% CI 0.50-1.78). While only one study apart from those from the U of K measured iron levels in the amygdala (and it had a very small number of samples), the increase in iron concentration reported by the U of K was higher than that reported by the independent study. Additional studies will be needed to determine the true effect size in the amygdala. The effect size for each neocortical region was non-significant (effect size hippocampus -0.32, 95%CI -0.76-0.11; frontal lobe -0.02, 95%CI -0.41-0.37; temporal lobe 0.56 95%CI -0.22-1.34; parietal lobe 0.35 95%CI -0.26-0.96).

There was insufficient data to adequately analyze the effect size of Alzheimer's disease on zinc for deep grey matter regions, although results seemed to parallel the changes in iron (strongest increases were reported for the putamen, globus pallidus and caudate nucleus). For neocortical regions, heterogeneity was found in the reports of zinc concentration although the heterogeneity was independent of the laboratory of origin (Fig 1). There was significant change in zinc concentration in the neocortex only in the parietal lobe (effect size hippocampus -0.08, 95%CI -1.00-0.85; frontal lobe 0.35, 95%CI -0.24-0.94; temporal lobe 0.47, 95%CI -0.13-1.07; parietal lobe 0.50, 95%CI 0.06-0.94).

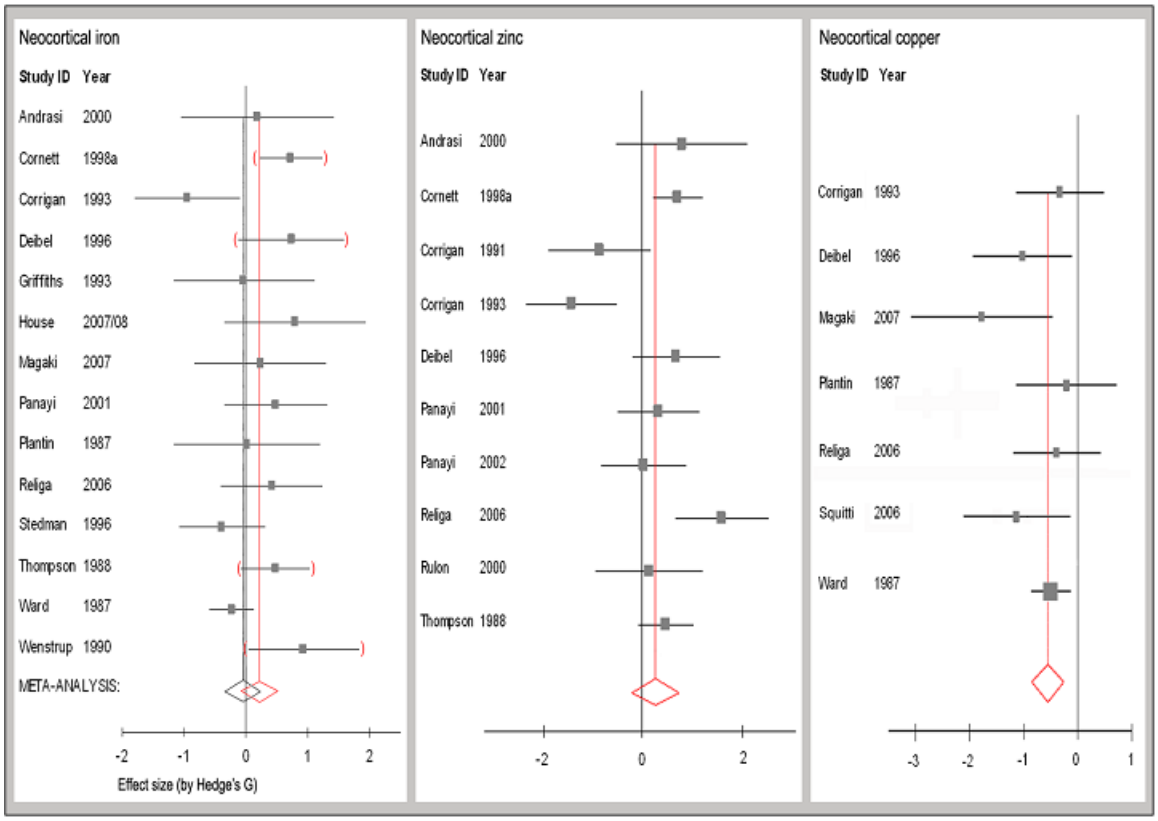
Neocortical iron
Study ID Year
Andrasi 2000
Cornett 1998a
Corrigan 1993
Deibel 1996
Griffiths 1993
House 2007/08
Magaki 2007
Panayi 2001
Plantin 1987
Religa 2006
Stedman 1996
Thompson 1988
Ward 1987
Wenstrup 1990
META-ANALYSIS:
-2 -1 0 1 2
Effect size (by Hedge's G)
Neocortical zinc
Study ID Year
Andrasi 2000
Cornett 1998a
Corrigan 1991
Corrigan 1993
Deibel 1996
Panayi 2001
Panayi 2002
Religa 2006
Rulon 2000
Thompson 1988
-2 0 2
Neocortical copper
Study ID Year
Corrigan 1993
Deibel 1996
Magaki 2007
Plantin 1987
Religa 2006
Squitti 2006
Ward 1987
-3 -2 -1 0 1

Figure 2: Meta-data of studies reporting the effect of Alzheimer's disease on neocortical iron, zinc and copper concentrations

Data from hippocampus, frontal, temporal and parietal lobes were combined to assess neocortical metal levels. Studies from the University of Kentucky (U of K) are indicated by red parentheses for iron data. The mean effect size indicated by red vertical lines includes data reported by U of K. The black vertical line indicates the meta-effect size for iron when this data source is excluded. There is no significant increase in neocortical iron in Alzheimer's brain: effect size = -0.05, 95%CI -0.34-0.25; n= 206 control, 251 AD. There is a trend toward an increase in neocortical zinc, although the dataset is significantly heterogenous: effect size = 0.26, 95% CI -0.22-0.75; n= 166 control, 118 AD. Copper levels are significantly depleted in Alzheimer's disease: effect size = -0.59, 95% CI -0.87- -0.31; n= 123 controls, 115 AD.

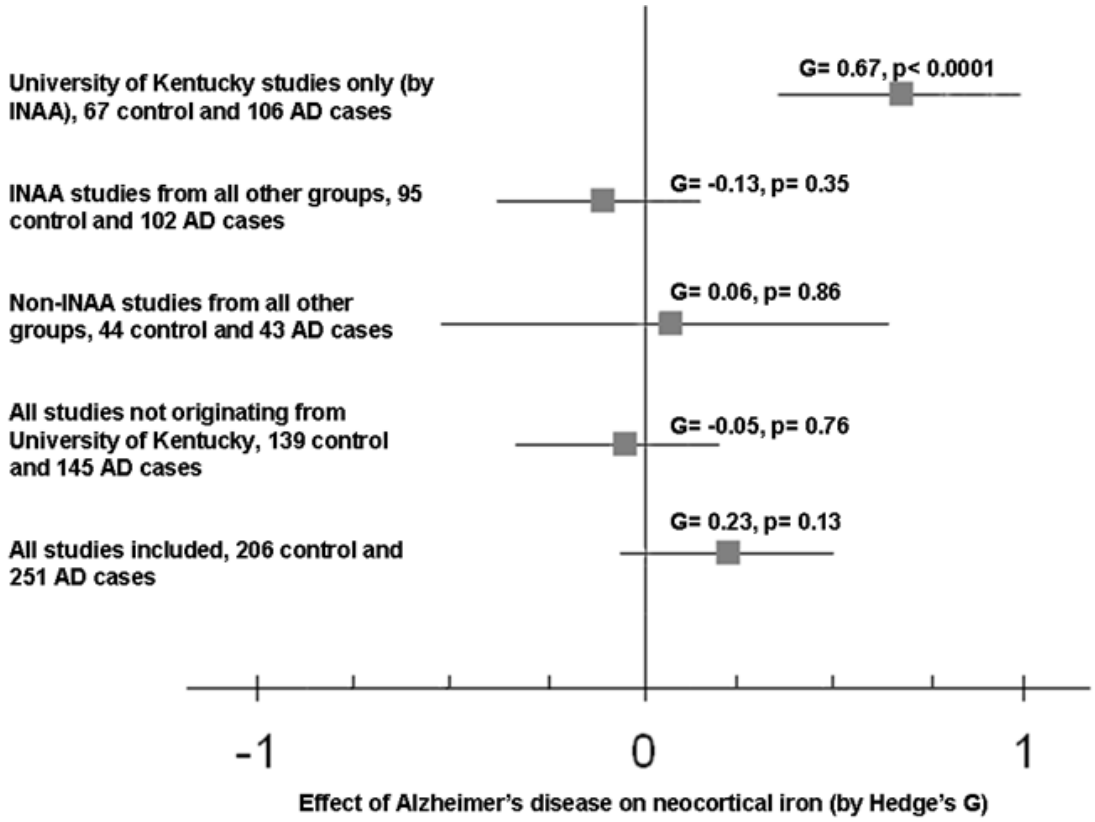
University of Kentucky studies only (by INAA), 67 control and 106 AD cases
G= 0.67, p< 0.0001
INAA studies from all other groups, 95 control and 102 AD cases
G= -0.13, p= 0.35
Non-INAA studies from all other groups, 44 control and 43 AD cases
G= 0.06, p= 0.86
All studies not originating from University of Kentucky, 139 control and 145 AD cases
G= -0.05, p= 0.76
All studies included, 206 control and 251 AD cases
G= 0.23, p= 0.13
-1
0
1
Effect of Alzheimer's disease on neocortical iron (by Hedge's G)

Figure 3: Laboratory of origin and not analytical technique appears to be the source of heterogeneity in measurements of neocortical iron in Alzheimer's disease.

Several individual studies indicated an increase in zinc concentration in each neocortical lobe (supp Table 2).

Copper levels were depleted in the AD group in most regions (supp. Table 3) and cumulatively neocortical copper was significantly reduced in AD (Fig.1; effect size -0.55, 95%CI -0.85- -0.25, p=0.0003). An additional study (conducted by the U of K) which was heavily cited and was excluded for tissue fixation, reported a dramatic increase in copper concentration (>400%) in AD amygdala compared to controls (Lovell 1998). However, a second report from the same laboratory reported copper was depleted in the amygdala with an effect size of -1.42, 95%CI -2.40- -0.44. The effect of Alzheimer's disease on hippocampal copper was -0.54, 95%CI -0.91- -0.16 and reported effect sizes for other neocortical regions ranged from -0.39 to -2.78.

Discussion

The data from this meta-analysis indicate that there is a wide-spread misconception in the scientific literature regarding the levels of several transition metals in AD brain. For iron levels, this misconception arose from the contributions of one laboratory which were remarkably dissimilar to other published reports and were heavily cited. Despite the fact that the U of K studies reported findings which were not reproduced by seven other laboratories, it was necessary to consider whether these discrepant reports could reflect the true effect size. However, we found no obvious quality measures between the studies which would account for the discrepancy. While brain iron concentration increases with aging and differences could therefore be attributed differences in age between control and AD groups, this was well-controlled in

study selection and control patients were over 55 years of age (Hallgren and Sourander 1958). The possibility that different analytical techniques could contribute to heterogeneous findings was also considered; however, the techniques employed in these studies have been shown to produce compatible results and five additional studies which did not originate at U of K also utilized INAA-based measurements (the technique employed in the U of K studies) without detecting significant changes (Andrasi 2000, Panayi 2001, 2002, Rulon 2000, Thompson 1988). This suggests the artifact was not dependent on the analytical technique employed (Fig 2). Moreover, no differences in the methodology of tissue preparation between these studies would be expected to produce the discrepant results observed here. While we were not been able to precisely identify the source of the artifact in this dataset, we felt confident in drawing conclusions from the non-U of K studies. We therefore concluded that Alzheimer's disease did not alter neocortical iron levels and there was no evidence for a global dysregulation in brain iron in Alzheimer's disease as has frequently been suggested. Iron was modestly elevated in the AD putamen over controls, but no other brain region appeared to be affected. The increases in tissue iron in the deep grey matter may be a significant component of Alzheimer's disease pathology, but they certainly do not account for the neocortical dysfunction observed in this disease. Moreover, AD is commonly comorbid with some degree of Lewy body disease which is strongly associated with increases in basal ganglia iron -- the findings in the putamen may be more reflective of this disease process (Hamilton 2000, Dexter 1991). Gradient echo T2* (GRE-T2*) and susceptibility weighted imaging (SWI) are iron-sensitive sequences that have been used to follow brain iron levels in AD patients (Chavan 2009, Kirsch 2009). Several large studies of this

technology have been conducted to evaluate the usefulness of following brain iron levels as a biomarker of AD. In these studies the putamen was the only region consistently found to contain increased levels of iron in AD (Kirsch 2009, Zhu 2009, Ding 2009). This is remarkably consistent with the results of this meta-analysis and validates the utility of this technology for noninvasively estimating tissue iron levels. However, increases in putamen iron are not specific to AD and therefore may not be particularly helpful in establishing a diagnosis.

Zinc levels reported in the neocortex were heterogeneous even after the exclusion of the University of Kentucky data. No significant increases were found for any region, although individual studies reported increases in the frontal and temporal cortex and the hippocampus. The heterogeneity of these results may be due to differences in tissue sampling.

Among the most important observations of this study is the prominent depletion of copper in AD. Insufficient data is currently available to enable a detailed regional assessment of alterations in copper levels in AD, but the available evidence suggests that copper is generally depleted in AD (although copper is noted to increase in the putamen by one study). There are widely discrepant results from U of K studies on the amygdala, one indicating decreased copper in AD (effect size -4.32, 95%CI -6.00- -2.63), one (excluded for tissue fixation) indicating more than four fold increased copper levels. The latter study is the most cited study on the subject of copper in AD and is the source for numerous articles reporting that copper levels are (several fold) increased in AD – several of which argue strongly in favor of clinical trials of metal chelation (Religa 2006, Cuajungco 2000, Rottkamp 2001, Bush 2000, Filiz 2008). It is important to clarify that

copper is not increased in AD brain. A clinical trial of D-penicillamine, a copper chelator, was unable to produce any clinical improvement in the treated cohort (in fact patients trended toward worse outcomes) and patients experienced numerous toxicities resulting in one death and the early suspension of the trial (Squitti 2002).

Focal alterations in metals distribution have been suggested by several studies to be associated with the primary pathologies of AD. All three metals evaluated here are reported to accumulate within senile plaques, although other studies call into question the consistency of this observation. One study found 30% of plaques had no detectable iron in them while a few of the largest plaques had high concentrations of magnetite. Because of the inhomogeneous distribution of metals in the brain, there is little doubt that sampling method is an important variable.

Based upon these cumulative findings and because of the disproportionate impact of outlier data on the literature, we feel it will be important to re-evaluate brain metals-overload hypotheses particularly when considering additional clinical trials of metal chelating/modulating therapies. It is fundamentally important that the application of metal-targeted pharmacology restores not only normal metal levels, but also normal transition metal physiology. For these reasons, we argue that further cautious study is necessary before exposing a large, vulnerable clinical population to potentially toxic chelating agents.

Annotated References

1. Andrasi E, Farkas E, Gawlik D, Rosick U, Bratter P (2000) Brain iron and zinc contents of German patients with Alzheimer's disease. Journal of Alzheimer's Disease 2:17-26.

INCLUDED: Iron and zinc were measured by INAA for hippocampus, frontal, parietal, occipital lobes, thalamus, caudate putamen and globus pallidus. Dry weight values were reported without dry to wet weight ratios; standard conversion ratios were applied. Results are from Eotvos University.

2. Andrasi E, Farkas E, Scheibler H, Reffy A, Bezur L (1995) Al, Zn, Cu, Mn and Fe levels in brain in Alzheimer's disease. Archives of Gerontology and Geriatrics 21:89-97.

EXCLUDED for formalin fixation: iron, zinc and copper were measured from ten brain regions by INAA and ICP-AES.

3. Collingwood J, et al (2005) In situ characterization and mapping of iron compounds in Alzheimer's disease tissue. Journal of Alzheimer's Disease 7:267-72.

EXCLUDED tissue fixation and semi-quantitative analysis: iron was measured by x-ray fluorescence in the frontal cortex of a single Alzheimer's case.

4. Connor J, Snyder B, Beard J, Fine R, Mufson E (1992) Regional distribution of iron and iron-regulatory proteins in the brain in aging and Alzheimer's disease. Journal of Neuroscience Research 31:327-335.

EXCLUDED for semi-quantitative methods (iron concentration normalized to protein concentration, not tissue weight): iron was measured by colorimetric assay in three brain regions.

5. Cornett C, Markesbery W, Ehmann W (1998a) Imbalances of trace elements related to oxidative damage in Alzheimer's disease brain. Neurotoxicology 19:339-45.

INCLUDED: Iron and zinc were measured by INAA in hippocampus, amygdala, frontal, parietal and temporal lobes and cerebellum. Results are from the University of Kentucky.

6. Cornett C, Ehmann W, Wekstein D, Markesbery W (1998b) Trace elements in Alzheimer's disease pituitary glands. Biological Trace Element Research 62:107-14.

INCLUDED: Iron and zinc were measured by INAA in pituitary. Results are from the University of Kentucky.

7. Corrigan F, Reynolds G, Ward N (1991) Reductions of zinc and selenium in brain in Alzheimer's disease. Trace Elements in Medicine 8:1-5.

INCLUDED: Iron, zinc and copper were measured for putamen, zinc measurements for caudate, temporal and frontal lobes by INAA. Results are from the University of Surrey.

8. Corrigan F (1993) Hippocampal tin, aluminum and zinc in Alzheimer's disease. BioMetals 6:149-54.

INCLUDED: Iron, zinc and copper were measured by ICP-MS in hippocampus (dentate gyrus only). Results are from the University of Surrey.

9. Danscher G, et al (1997) Increased amount of zinc in the hippocampus and amygdala of Alzheimer's diseased brains: a proton-induced x-ray emission spectroscopic analysis of cryostat sections from autopsy material. Journal of Neuroscience Methods 76:53-9.

EXCLUDED for semi-quantitative results**:** zinc was measured by PIXE in hippocampus and amygdala. Significant increases were reported in both regions. Results are from the University of Aarhus.

10. Dedman D, et al (1992) Iron and aluminum in relation to brain ferritin in normal individuals and Alzheimer's disease and chronic dialysis patients. Journal of Biochemistry 287:509-14.

EXCLUDED for semi-quantitative results: non-heme iron was measured by a colorimetric assay in the parietal lobe normalized to protein concentration. A significant increase in iron was reported. Results are the University of Sheffield.

11. Deibel M, Ehmann W, Markesbery W (1996) Copper, iron and zinc imbalances in severely degenerated brain regions in Alzheimer's disease: possible relation to oxidative stress. Journal of Neurological Science 143:137-42.

INCLUDED: Iron, copper and zinc measurements by INAA in the hippocampus, amygdala, temporal and parietal lobes and cerebrellum. Dry weight values were reported w/o dry to wet weight ratios; standard conversion ratios were applied. Results are from the University of Kentucky.

12. Ehmann W, Markesbery W, Alauddin M, Hossain T, Brubaker E (1986) Brain trace elements in Alzheimer's disease. Neurotoxicology 1:197-206.

EXCLUDED for absence of regional discrimination: iron and zinc measurements by INAA for bulk brain only. Results are from the University of Kentucky.

13. Griffiths P, Crossman A (1993) Distribution of iron in the basal ganglia and neocortex in postmortem tissue in Parkinson's disease and Alzheimer's disease. Dementia 4:61-5.

INCLUDED: Iron measurements by atomic absorption in frontal, parietal and temporal lobes, putamen, caudate, globus pallidus (lateral and medial separately) and substantia nigra. Results from University of Manchester.

14. House M, et al (2007) Correlation of proton transverse relaxation rates (R_2) with iron concentrations in postmortem brain tissue from Alzheimer's disease patients. Magnetic Resonance in Medicine 57:172-180.

INCLUDED: see next entry.

15. House M, St. Pierre T, McLean C (2008) 1.4T study of proton magnetic relaxation rates, iron concentrations and plaque burden in Alzheimer's disease and control postmortem brain tissue. Magnetic Resonance in Medicine 60:41-52.

INCLUDED: Because the number of cases in these two studies are small, the data has been merged and cited in the analysis as House (2007/08). Iron measurements are reported from atomic absorption studies of the hippocampus, amygdala, caudate, globus pallidus, thalamus, cingulated gyrus, corpus callosum, frontal, temporal, parietal and occipital lobes. Dry to wet weight ratios are reported for each region. Results are from University of Western Australia.

16. Leite R, Jacob-Filho W, Saiki M, Grinberg L, Ferretti R (2008) Determination of trace elements in human brain tissue using neutron activation analysis. Journal of Radioanalytical and Nuclear Chemistry 278:581-4.

EXCLUDED for lack of neuropathologic diagnosis of dementia cases: Iron and zinc were measured by INAA in frontal lobe and hippocampal tissue.

17. Loeffler D, et al (1995) Transferrin and iron in normal, Alzheimer's disease and Parkinson's disease brain regions. Journal of Neurochemistry 65:710-6.

INCLUDED although reported values were semi-quantitative (normalized to protein concentration), the amount of protein isolated per mass of tissue was also reported which enable conversion to the standard measure: iron measurement were obtained from a colorimetric assay for caudate, putamen, substanti nigra, globus pallidus and frontal lobe. Significant increases were reported in the frontal cortex and globus pallidus, however, when the results were recalculated to normalize to tissue weight, no significant changes remained. Results are from Wayne State University.

18. Lovell M, Robertson J, Teesdale W, Campbell J, Markesbery W (1998) Copper, iron and zinc in Alzheimer's disease senile plaques. Journal of Neurological Science 158:47-52.

EXCLUDED for tissue fixation: Iron, zinc and copper were measured in amygdala by microprobe-PIXE in the amygdala. Results are from University of Kentucky.

19. Magaki S, et al (2007) Iron, copper and iron regulatory protein 2 in Alzheimer's disease and related dementia. Neuroscience Letters 418:72-6.

INCDLUDED: Iron and copper measurements by atomic absorption reported for hippocampus and frontal lobe. Results are from Loma Linda University.

20. Panayi A, Spyrou N, Part P (2001) Differences in trace element concentrations between Alzheimer and "normal" human brain tissue using instrumental neutron activation analysis. Journal of Radioanalytic and Nuclear Chemistry 249:437-41.

INCLUDED: Iron and zinc were measured by INAA in frontal, parietal and temporal lobes. [Note: samples in this study were age-matched.] Results are from the University of Surrey.

21. Panayi A, Spyrou N, Iverson B, White M, Part P (2002) Determination of cadmium and zinc in Alzheimer's brain tissue using inductively coupled plasma mass spectrometry. Journal of Neurological Science 195:1-10.

INCLUDED: Zinc measurements were measured by ICP-MS for hippocampus, thalamus, frontal, parietal and temporal lobes. Controls as young as 38 were included in the control group -- the mean age of controls was 66.8 years versus a mean of 80.0 years for the AD group. Because only zinc

measurements were reported and zinc is less affected by ageing than iron, we decided to include this study. Results are from the University of Surrey.

22. Plantin L, Lying-Tunell U, Kristensson K (1987) Trace elements in the human central nervous system studied with neutron activation analysis. Biological Trace Element Research 13:69-75.

INCLUDED: Iron and copper were measured in the temporal lobe.

23. Rao K, Rao R, Shanmugavelu P, Menon R (1999) Trace elements in Alzheimer's disease: a new hypothesis. Alzheimer's Reports 2:241-6.

EXCLUDED: copper, iron and zinc measured by ICP-AES for hippocampus and frontal cortex. Age of control subjects was not reported. The study reported a more than 1000 fold increase in iron and a 12 fold increase in zinc in the AD hippocampus – these results are likely inaccurate in the context of other reported values.

24. Religa D, et al (2006) Elevated cortical zinc in Alzheimer's disease. Neurology 67:69-75.

INCLUDED: Iron, zinc and copper were measured by ICP-MS in the temporal lobe. Results are from Harvard University.

25. Rulon L, et al (2000) Serum zinc levels and Alzheimer's disease. Biological Trace Element Research 75:79-85.

INCLUDED: Zinc was measured by AA for the hippocampus, amygdala, temporal lobe and cerebellum. Results are from the University of Kentucky.

26. Samudralwar D, Diprete C, Ni B, Ehmann W, Markesbery W (1995) Elemental imbalances in the olfactory pathway in Alzheimer's disease. Journal of Neurological Science 130;139-45.

INCLUDED: Iron and zinc were measured by INAA for the olfactory system and amygdala. Results are from the University of Kentucky.

27. Squitti R, Quattrochi C, Forno G, Antuono P, et al (2006) Ceruloplasmin (2D PAGE) pattern and copper content in serum of Alzheimer's disease patients. Biomark Insights 1:205-13.

EXCLUDED: for semi-quantitative analysis.

27. Stedman J, Spyrou N (1997) Elemental analysis of the frontal lobe of "normal" brain tissue and that affected by Alzheimer's disease. Journal of Radioanalytical and Nuclear Chemistry 217:163-6.

INCLUDED: Iron and zinc were measured by INAA for the frontal lobe. Results are from the University of Surrey.

28. Tandon L, et al (1994) RNAA for arsenic, cadmium, copper and molybdenum in CNS tissue from subjects with age-related neurodegenerative diseases. Journal of Radioanalytical and Nuclear Research 179:331-9.

EXCLUDED for absence of regional discrimination: reported copper levels by RNAA in bulk brain samples only. Results are from the University of Kentucky.

29. Thompson C, Markesbery W, Ehmann W, Mao Y, Vance D (1988) Regional brain trace-element studies in Alzheimer's disease. Neurotoxicology 9:1-8.

INCLUDED: Iron and zinc measured by INAA for hippocampus, amygdala, and nucleus basalis of Meynert. Results are from the University of Kentucky.

30. Ward N, Mason J (1987) Neutron activation analysis techniques for identifying elemental status in Alzheimer's disease. Journal of Radioanalytical and Nuclear Chemistry 113:515-526.

INCLUDED: Iron and zinc were measured by INAA for hippocampus and bulk cortex. The study was blinded. NOTE: several subsequent papers (Religa 2006, Deibel 1996) questioned the reliability of this study suggesting that formalin-fixed tissue was used – this does not appear to be the case. The tissue was reportedly stored by refrigeration. The results obtained were consistent with those reported from other studies of non-fixed tissues and different from those that studies fixed tissues. This is the largest study in the analysis.

31. Wenstrup D, Ehmann W, Markesbery W (1990) Trace element imbalances in isolated subcellular fractions of Alzheimer's disease brains. Brain Research 533:125-31.

INCLUDED: Iron and zinc were measured by INAA for temporal lobe. Results are from the University of Kentucky.

32. Yoshimasu F, et al (1980) Studies on amyotrophic lateral sclerosis by neutron activation analysis—2. Comparative study of analytical results on Guam PD, Japanese ALS and Alzheimer's disease cases. Folia Psychiatrica et Neurologica 34:75-82.

EXCLUDED for fixation: reported copper levels by neutron activation analysis.

General References

33. Bax L, Yu L, Ikeda N, Moons K (2007) A systematic comparison of software dedicated to meta-analysis of causal studies. BMC Med Res Methodol 7:40.

34. Benzi G, Moretti A (1995) Are reactive oxygen species involved in Alzheimer's disease. Neurobiol Aging 16:661-74.

35. Brunnstrom H, Englund E (2009) Clinicopathological concordance in dementia diagnostics. Am J Geriatr Psych 17:664-70.

36. Bush AI, et al (1994) Rapid induction of Alzheimer Abeta amyloid formation by zinc. Science 265:1464-67.

37. Bush A (2000) Metals and neuroscience. Curr Opin Chem Biol 4:184-91.

38. Chavhan G, Babyn P, Thomas B, Schroff M, Haacke M (2009) Principles, techniques and applications of T2*-based MR imaging and its special applications. Radiographics 29:1433-49.

39. Cherny RA, et al (1999) Aqueous dissolution of Alzheimer's disease Abeta amyloid deposits by biometal depletion. J Biol Chem 274:23223-8.

40. Crapper McLachlan D, Dalton A, Kruck T, Bell M, Smith W, Kalow W, et al (1991) Intramusclar desferrioxamine in patients with Alzheimer's disease. Lancet 337:1304-8.

41. Cuajungco MP, Faget KY, Huang X, Tanzi RE, Bush A (2000) Metal chelation as a potential therapy for Alzheimer's disease. Ann N Y Acad Sci 920:292-304.

42. Dexter D, et al (1991) Alterations in the levels of iron, ferritin and other trace metals in Parkinson's disease and other neurodegenerative diseases affecting the basal ganglia. Brain 114:1953-75.

43. Ding, et al (2009) Correlation of iron in the hippocampus with MMSE in patients with Alzheimer's disease. J Mag Res Imaging 29:793-8.

44. Filiz G, et al (2008) The role of metals in modulating metalloprotease activity in AD brain. Eur Biophys J 37:315-21.

45. Gay B, Taylor K, Hohl U, Tolnay M, Staehelin H (2008) The validity of clinical diagnoses of dementia in a group of consecutively autopsied memory clinic patients. J Nutr Health Aging 12:132-7.

46. Gerlach M, Ben-Shachar D, Reiderer P, Youdim M (1994) Altered brain metabolism of iron as a cause of neurodegenerative diseases. J Neurochem 63:793-807.

47. Goodman L (1953) Alzheimer's disease; a clinico-pathologic analysis of 23 cases with a theory on pathogenesis. J Nerv Ment Dis 118:97-130.

48. Hallgren B, Sourander P (1958) The effect of age on the non-haemin iron in the human brain J Neurochem 3:41-51.

49. Hallgren B, Sourander P (1960) The non-haemin iron in the cerebral cortex of Alzheimer's disease. J Neurochem 5:307-10.

50. Hamilton R (2000) Lewy bodies in Alzheimer's disease: a neuropathological review of 145 cases using alpha-synuclein immunohistochemistry. Brain Pathol 10:378-84.

51. Jellinger K, Paulus W, Grundke-Iqbal I, Peiderer P, Youdim M (1990) Brain iron and ferritin in Parkinson's and Alzheimer's diseases. J Neural Transm Park Dis Dement Sect. 2:327-40.

52. Jervis RE, et al (1985) Trace elements in wet atmospheric deposition: application and comparison of PIXE, INAA and graphite furnace AAS techniques. Int J Environ Anal Chem 15:89-106

53. Kirsch W, et al (2009) Serial susceptibility weighted MRI measures brain iron and microbleeds in dementia. J Alz Dis 17:599-609.

54. Lannfelt L, et al (2008) Safety, efficacy and biomarker findings of PBT2 in targeting Abeta as a modifying therapy for Alzheimer's disease; a phase IIa, double blind randomized placebo controlled trial. Lancet Neurol 7:779-86.

55. Lilliefors H (1967) On the Kolmogorov-Smirnov test for normality with mean and variance unknown. J Am Stat Assoc 62:399-402.

56. Liu G, Men P, Perry G, Smith MA (2010) Nanoparticle and iron chelators as a potential novel Alzheimer therapy. Methods Mol Biol 610:123-44.

57. Markesbery W (1984) Brain trace elements concentrations in aging. Neurobiol Aging 5:19-28.

58. Markesbery W (1999) The role of oxidative stress in Alzheimer's disease. Arch Neurol 56:1449-52.

59. Rottkamp CA, et al (2001) Redox-active iron mediates amyloid-beta toxicity. Free Radic Biol Med 30:447-50.

60. Schipper H (1999) Glial HO-1 expressions, iron deposition and oxidative stress in neurodegenerative disease. Neurotox Res 1:57-70.

61. Schrag M, Dickson A, Jiffrey A, Kirsch D, Vinters HV, Kirsch W (2010) The effect of formalin fixation on the levels of brain transition metals in archived samples. Biometals in press.

62. Schubert D, Chevion M (1995) The role of iron in beta-amyloid toxicity. Biochem Biophys Res Commun 216:702-7.

63. Smith MA, Harris PL, Sayre LM, Perry G (1997) Iron accumulation in Alzheimer's disease is a source of redox-generated free radicals. Proc Nat Acad Sci 94:9866-8.

64. Squitti R, et al (2002) D-penicillamine reduces serum oxidatitive stress in Alzheimer's disease patients. Eur J Clin Inv 32:51-9.

65. Zhang J, et al (1997) Multi-element determination in earthworms with instrumental neutron activation analysis and inductively coupled plasma mass spectrometry: a comparison. J Radioanal Nucl Chem 223:149-55.

66. Zhu W, Zhong W, Wang W, Zhan C, et al (2009) Quantitative MR phase corrected imaging to investigate increased brain iron deposition in patients with Alzheimer's disease. Radiology 253:497-504.

TABLE 2 cont.: Effect of Alzheimer's disease on brain iron levels

Brain region	Studies/Methods	Number cases # control/# AD Total cases in bold *Cases w/o U of K.*	Effect size Hedge's g (95% CI) Merged effect (by inv. variance) *Effect size w/o Uof K*	[Fe] control µg/g wet weight Weighted mean *(Mean w/o UofK)*	[Fe] AD µg/g wet weight Weighted mean *(Mean w/o UofK))*	Comments
Hippocampus	Andrasi 2000 – INAA	5/5	0.22 (-1.03-1.46)	39.7 +/- 6.4	42.6 +/- 15.9	The studies in this group are not homogenous, Q=22.1 (p=0.002). Because the hippocampus is not homogenous in structure, this variation in findings may be contributed to by differences in sampling. However, exclusion of Univ. of Kentucky studies yields Q=5.0 (p=0.29).
	Cornett 1998a – INAA*	21/58	0.60 (0.09-1.11)	52.0 +/- 13.7	61.4 +/- 16.0	
	Corrigan 1993 – ICP-MS	12/12	-0.95 (-1.80- -0.10)	49.8 +/- 7.8	39.9 +/- 11.9	
	Deibel 1996 – INAA*	11/10	0.93 (0..3-1.85)	41.0 +/- 9.9	51.8 +/- 12.0	
	House 2008 – ICP-AES	2/2	0.83 (-4.28-5.95)	29.5 +/- 4.5	43.8 +/- 13.8	
	Magaki 2007 – AA	5/8	0.47 (-0.67-1.61)	47.0 +/- 6.0	49.0 +/- 2.0	
	Thompson 1988 – INAA*	23/27	0.47 (-0.09-1.04)	42.1 +/- 9.1	48.7 +/- 16.6	
	Ward 1987 -- INAA	60/58	-0.40 (-0.76- -0.03)	55.3 +/- 6.7	51.2 +/- 12.9	
	Meta-analysis	**139/181**	**0.18 (-0.31-0.66)**	**49.8 +/- 8.8**	**53.0 +/- 14.3**	
	Meta w/o U of K	*84/85*	*-0.33 (-0.76- 0.11)*	*52.5 +/- 6.8*	*48.7 +/-12.3*	
Olfactory bulb	Cornett 1998a – INAA*	21/58	0.94 (0.64-1.24)	43.0 +/- 32.0	49.0 +/- 22.8	These studies were both performed at the Univ of Kentucky with the same technique.
	Samudralwar 1995 –INAA*	35/46	5.60 (4.63-6.57)	27.1 +/- 21.3	60.3 +/-37.3	
Amygdala	Cornett 1998a – INAA*	21/58	0.68 (0.17-1.19)	49.0 +/- 18.3	64.0 +/- 22.8	
	Deibel 1996 – INAA*	11/10	1.43 (0.45-2.41)	48.6 +/- 7.3	70.8 +/- 20.2	
	House 2007/08 – AA	2/5	0.64 (-1.08-2.35)	35.4 +/- 0.1	41.9 +/- 9.6	
	Samudralwar 1995 –INAA*	9/19	1.23 (0.37-2.10)	50.8 +/- 11.1	70.8 +/- 17.4	
	Thompson 1988 – INAA*	15/14	0.74 (-0.02-1.49)	48.9 +/- 11.6	60.6 +/- 18.3	
	Meta-analysis	**58/106**	**0.88 (0.53-1.22)**	**48.7 +/- 7.2**	**64.4 +/- 20.7**	
	Meta w/o U of K	*2/5*	*0.64 (-1.08-2.35)*	*35.4 +/- 0.1*	*41.9 +/-9.6*	
Thalamus	Andrasi 2000 – INAA	5/5	0.36 (-0.89-1.61)	86.3 +/- 52.4	106.9 +/- 50.9	Total number of cases for this set is low and variance is quite high.
	House 2007/08 – AA	2/7	0.22 (-1.36-1.79)	41.7 +/- 1.5	44.0 +/- 10.2	
Caudate	Andrasi 2000 – INAA	5/5	2.20 (0.63-3.77)	61.4 +/- 21.9	145.5 +/- 42.0	Q=2.84 (p=0.24)
	Griffiths 1993 – AA	6/6	0.44 (-0.71-1.58)	99.6 +/- 6.6	105.3 +/- 15.6	
	House 2007/08 – AA	3/7	0.33 (-1.03-1.70)	98.5 +/- 15.5	108.0 +/- 28.6	
	Meta-analysis	**14/18**	**0.79 (-0.15-1.74)**	**85.7 +/- 15.4**	**113.3 +/- 28.0**	
Putamen	Andrasi 2000 – INAA	5/5	2.20 (0.63-3.77)	144.1 +/- 41.7	213.0 +/- 36.3	Q=1.74 (p=0.63)
	Corrigan 1991 – INAA	6/11	0.68 (-0.35-1.71)	91.7 +/- 5.9	96.6 +/- 7.3	
	Griffiths 1993 – AA	6/6	1.31 (0.06-2.56)	119.8 +/- 11.6	141.2 +/- 17.9	
	House 2007/08 – AA	2/5	1.23 (-0.16-2.62)	94.2 +/- 34.7	156.1 +/- 45.6	
	Meta-analysis	**13/16**	**1.14 (0.50-1.78)**	**110.1 +/- 24.7**	**139.1 +/- 28.2**	
Globus pallidus	Andrasi 2000 – INAA	5/5	1.47 (-0.02-2.95)	136.2 +/- 24.8	210.7 +/- 60.0	The study by Griffiths measured the lateral and medial nuclei separately. The lateral nucleus contained significantly more iron than the medial, and only the lateral nucleus showed a significant increase in iron in AD. Q=5.31 (p=0.07)
	Griffiths 1993 – AA	6/6	1.19 (-0.04-2.42)	185.4 +/- 14.6	213.0 +/- 26.5	
	House 2007/08 – AA	1/8	-0.64 (-1.92-0.72)	215.2 +/- 78.9	179.6 +/- 48.0	
	Meta-analysis	**12/19**	**0.67 (-0.61-1.94)**	**174.2 +/- 38.1**	**196.5 +/- 46.3**	

TABLE 2 cont.: Effect of Alzheimer's disease on brain iron levels

Substantia nigra	House 2007 – AA	1/2	-0.26	145.6	136.1 +/- 36.8	
	Griffiths 1993 – AA	6/6	0.76 (-0.41-1.94)	139.8 +/- 13.1	157.0 +/- 26.3	
Pituitary	Cornett 1998b – INAA*	15/43	0.76 (0.15-1.36)	71.0 +/- 19.0	79.0 +/- 5.0	
Nucleus basalis of Meynert	Thompson 1988 – INAA*	11/11	0. 18 (-0.66-1.02)	131 +/- 56.4	143 +/- 69.9	
Frontal lobe	Andrasi 2000 – INAA	5/5	-0.04 (-0.87-1.32)	54.9 +/- 10.4	54.5 +/- 9.4	The study by Magaki measured frontal white and grey matter separately. The concentration of iron in the white matter was significantly (2.2 times) higher than the grey, no significant changes were noted between the AD and control groups in either white or grey matter.
	Cornett 1998a – INAA*	21/58	0.55 (0.04-1.06)	52.0 +/- 13.7	60.9 +/- 16.8	
	Griffiths 1993 – AA	6/6	0.54 (-0.62-1.71)	41.8 +/- 8.2	49.0 +/- 15.2	
	House 2007/08 – AA	6/7	0.23 (-0.87-1.32)	44.0 +/- 32.3	49.7 +/- 12.2	
	Magaki 2007 – AA	6/8	0.0 (-1.06-1.06)	68.5 +/- 4.7	68.5 +/- 3.2	
	Panayi 2001 – INAA	8/16	0.07 (-0.78-0.92)	54.0 +/- 9.0	55.0 +/- 16.0	
	Stedman 1997–PIXE&INAA	15/18	0.12 (-0.57-0.80)	54.0 +/- 9.0	51.0 +/- 11.0	
	Meta-analysis	**62/115**	**0.19 (-0.12-0.50)**	**52.8 +/- 13.9**	**57.7 +/- 14.8**	
	Meta w/o U of K	***41/57***	***-0.02 (-0.41-0.37)***	***53.1+/- 14.0***	***54.0 +/- 12.4***	
Temporal lobe	Andrasi 2000 – INAA	5/5	2.12 (0.40-3.84)	50.7 +/- 4.6	59.4 +/- 2.5	This dataset is heterogeneous, Q=16.5 (p=0.035).
	Cornett 1998a – INAA*	21/58	1.07 (0.54-1.60)	51.0 +/- 13.7	67.7 +/- 16.0	
	Deibel 1996 – INAA*	11/10	0.52 (-0.35-1.39)	50.5 +/- 4.3	53.8 +/- 7.6	
	Griffiths 1993 – AA	6/6	-1.20 (-2.47-0.08)	50.1 +/- 8.5	39.4 +/- 8.0	
	House 2007/08 – AA	6/7	1.36 (0.10-2.61)	46.6 +/- 4.6	50.6 +/- 12.3	
	Panayi 2001 – INAA	9/12	1.00 (0.07-1.93)	49.0 +/- 9.0	59.0 +/- 10.0	
	Plantin 1987 -- INAA	6/5	0.01 (/1.17-1.20)	28.0 +/- 13.9	28.2 +/- 10.8	
	Religa 2006 – ICP-MS	14/10	0.42 (-0.40-1.24)	33.9 +/- 4.9	37.7 +/- 12.3	
	Wenstrup 1990 – INAA*	12/10	0.93 (0.04-1.82)	45.0 +/- 13.5	55.8 +/- 7.3	
	Meta-analysis	**90/123**	**0.68 (0.22-1.15)**	**46.6 +/- 9.9**	**59.3 +/- 13.1**	
	Meta w/o U of K	***42/45***	***0.56 (-0.22-1.34)***	***43.7+/- 7.9***	***49.3+/- 10.4***	
Parietal lobe	Andrasi 2000 – INAA	5/5	0.01 (-1.23-1.25)	49.4 +/- 29.3	49.6 +/- 26.1	
	Cornett 1998a – INAA*	21/58	0.75 (0.24-1.26)	56.0 +/- 18.3	69.0 +/- 16.8	
	Deibel 1996 – INAA*	11/10	0.63 (-0.25-1.52)	54.4 +/- 5.3	59.4 +/- 9.5	
	Griffiths 1993 – AA	6/6	0.24 (-0.89-1.39)	30.2 +/- 9.3	32.7 +/- 9.3	
	Panayi 2001 – INAA	9/12	0.58 (-0.31-1.47)	55.0 +/- 6.0	61.0 +/- 12.0	
	Meta-analysis	**52/91**	**0.59 (0.23-0.95)**	**50.4 +/- 15.4**	**63.4 +/- 15.8**	
	Meta w/o U of K	***20/23***	***0.35 (-0.26-0.96)***	***44.0 +/- 15.6***	***51.4+/- 15.4***	
Occipital lobe	Andrasi 2000 – INAA	5/5	-0.31 (-1.61-0.99)	58.1 +/- 7.5	49.9 +/- 26.8	
Cerebellum	Cornett 1998a – INAA*	21/58	0.33 (-0.66-1.06)	59.0 +/- 27.5	69.0 +/- 30.5	
	Deibel 1996 – INAA*	11/10	0.20 (-0.66-1.06)	55.2 +/- 17.2	57.8 +/- 3.2	

* study conducted at the University of Kentucky

TABLE 3: Effect of Alzheimer's disease on brain zinc levels

Brain region	Studies/Methods Meta-analysis	Number cases # control/# AD Total cases in bold	Effect size Hedge's g (95% CI) Merged effect (by inv. variance)	[Zn] control µg/g wet weight Weighted mean	[Zn] AD µg/g wet weight Weighted mean	Comments
Hippocampus	Andrasi 2000 – INAA	5/5	0.83 (-0.50-2.15)	12.0 +/- 3.6	16.1 +/- 3.6	Distribution is heterogeneous, Q=90.4 ($p<0.0001$). The methodology of tissue sampling was not consistent between these studies, which could produce variable results.
	Cornett 1998a – INAA*	21/58	0.60 (0.09-1.11)	15.2 +/- 4.6	18.0 +/- 4.6	
	Corrigan 1993 – ICP-MS	12/12	1.44 (0.52- 2.35)	8.1 +/- 2.9	12.8 +/- 3.4	
	Deibel 1996 – INAA*	11/10	0.55 (-0.32-1.43)	13.7 +/- 3.0	15.3 +/- 2.5	
	Panayi 2002 – ICP-MS	10/9	0.02 (-0.88-0.93)	14.7 +/- 3.9	14.6 +/- 3.9	
	Rulon 2000 – INAA*	5/5	0.61 (-0.67-1.90)	15.2 +/- 1.1	16.3 +/- 2.0	
	Thompson 1988 – INAA*	23/27	0.48 (-0.09-1.04)	11.4 +/- 1.9	15.9 +/- 12.5	
	Ward 1987 -- INAA	60/58	-2.01 (-2.45- -1.56)	8.4 +/- 1.1	6.6 +/- 0.6	
	Meta-analysis	**147/184**	**-0.08 (-1.00-0.85)**	**11.4 +/- 2.6**	**13.0 +/- 5.7**	
Amygdala	Cornett 1998a – INAA*	21/58	0.96 (0.44-1.48)	13.6 +/- 2.3	17.6 +/- 4.6	All studies from this region are from the Univ of Kentucky
	Deibel 1996 – INAA*	11/10	1.67 (0.65-2.70)	15.2 +/- 2.0	19.8 +/- 3.2	
	Rulon 2000 – INAA*	5/5	0.49 (-0.72-1.70)	15.7 +/- 1.1	16.6 +/- 2.2	
	Samudralwar 1995 –INAA*	9/19	2.27 (1.25-3.29)	16.7 +/- 1.5	21.4 +/- 2.2	
	Thompson 1988 – INAA*	23/27	0.83 (0.07-1.60)	14.1 +/- 2.4	17.0 +/- 4.2	
	Meta-analysis	**69/119**	**1.21 (0.67-1.75)**	**14.7 +/- 2.1**	**18.4 +/- 4.0**	
Olfactory bulb	Cornett 1998a – INAA*	21/58	0.48 (-0.02-0.99)	16.5 +/- 5.5	19.4 +/- 6.1	
	Samudralwar 1995 –INAA*	35/46	1.01 (0.55-1.49)	15.5 +/- 4.7	21.2 +/- 6.1	
Thalamus	Andrasi 2000 – INAA	5/5	0.19 (-1.05-1.43)	11.8 +/- 2.2	10.9 +/- 5.8	
Caudate	Andrasi 2000 – INAA	5/5	3.05 (1.22-4.87)	15.0 +/- 2.1	8.4 +/- 1.8	
	Corrigan 1991 – INAA	6/11	1.35 (0.26-2.44)	10.6 +/- 1.5	8.6 +/- 1.2	
Putamen	Andrasi 2000 – INAA	5/5	2.24 (0.66-3.82)	16.3 +/- 1.7	11.7 +/- 2.0	
	Corrigan 1991 – INAA	6/11	3.18 (1.72-4.63)	14.3 +/- 1.3	10.5 +/- 0.7	
Globus pallidus	Andrasi 2000 – INAA	5/5	-0.36 (-1.61-0.89)	19.8+/- 1.6	18.7 +/- 3.6	
Pituitary	Cornett 1998b – INAA*	15/43	0.39 (-0.20-0.99)	15.5 +/- 1.0	15.7 +/- 0.04	
Nucleus basalis of Meynert	Thompson 1988 – INAA*	11/11	2.57 (1.38-3.75)	11.4 +/- 1.3	15.9 +/- 2.0	

TABLE 3 cont.: Effect of Alzheimer's disease on brain zinc levels

Frontal lobe	Andrasi 2000 – INAA	5/5	1.81 (0.20-3.40)	11.0 +/- 1.9	14.9 +/- 2.0	
	Cornett 1998a – INAA*	21/58	0.74 (0.23-1.26)	12.5 +/- 2.7	14.7 +/- 3.0	
	Corrigan 1991 – INAA	5/11	-0.49 (-1.57-0.58)	10.3 +/- 1.1	9.8 +/- 0.9	
	Panayi 2001 – INAA	8/16	0.08 (-0.77-0.92)	12.5 +/- 1.8	12.7 +/- 2.7	
	Panayi 2002 – ICP-MS	9/10	0.03 (-0.87-0.93)	13.2 +/- 3.4	13.3 +/- 2.9	
	Meta-analysis	**48/100**	**0.35 (-0.24-0.94)**	**12.2 +/- 2.6**	**13.7 +/- 2.8**	
Temporal lobe	Andrasi 2000 – INAA	5/5	1.94 (0.29-3.60)	10.6 +/- 2.0	17.0 +/- 3.7	Data is heterogeneous, Q=23.5 ($p<0.0001$).
	Cornett 1998a – INAA*	21/58	0.79 (0.27-1.30)	14.1 +/- 3.2	17.5 +/- 4.6	
	Corrigan 1991 – INAA	6/11	-1.65 (-2.83- -0.47)	9.7 +/- 0.7	8.7 +/- 0.5	
	Deibel 1996 – INAA*	11/10	0.72 (-0.17-1.61)	11.7 +/- 1.0	13.1 +/- 2.5	
	Panayi 2001 – INAA	9/12	0.25 (-0.62-1.11)	14.0 +/- 3.9	14.9 +/- 3.2	
	Panayi 2002 – ICP-MS	9/11	0.15 (-0.73-1.04)	14.2 +/- 3.6	14.7 +/- 2.7	
	Religa 2006 – AA	14/10	1.57 (0.64-2.54)	11.2 +/- 1.9	25.8 +/- 13.7	
	Rulon 2000 – INAA*	7/6	0.12 (-0.13-1.07)	14.0 +/- 3.9	14.8 +/- 1.4	
	Meta-analysis	**82/123**	**0.47 (-0.13-1.07)**	**12.7 +/- 2.8**	**16.3 +/- 5.3**	
Parietal lobe	Andrasi 2000 – INAA	5/5	-0.34 (-1.59-0.91)	10.1 +/- 5.2	8.2 +/- 4.9	
	Cornett 1998a – INAA*	21/58	0.75 (0.23-1.26)	12.2 +/- 3.2	14.5 +/- 3.0	
	Deibel 1996 – INAA*	11/10	1.03 (0.10-1.95)	12.4 +/- 1.3	11.3 +/- 0.6	
	Panayi 2001 – INAA	8/14	0.62 (-0.27-0.78)	11.5 +/- 2.2	13.4 +/- 3.3	
	Panayi 2002 – ICP-MS	10/10	-0.09 (-0.97-0.78)	13.5 +/- 4.5	13.1 +/- 3.6	
	Meta-analysis	**55/97**	**0.50 (0.06-0.94)**	**12.0 +/- 3.3**	**13.7 +/- 3.1**	
Occipital lobe	Andrasi 2000 – INAA	5/5	-0.58 (-1.85-0.69)	9.6 +/- 4.8	12.0 +/- 2.2	
Cerebellum	Deibel 1996 – INAA*	5/5	0.50 (-0.77-1.77)	13.5 +/- 0.9	14.0 +/- 0.9	
	Rulon 2000 – INAA*	7/7	2.56 (1.14-3.97)	10.9 +/- 0.7	13.6 +/- 1.2	

* study conducted at the University of Kentucky

TABLE 4: Effect of Alzheimer's disease on brain copper levels

Brain region	Studies/Methods Meta-analysis	Number cases # control/# AD Total cases in bold	Effect size Hedge's g (95% CI) Merged effect (by inv. variance)	[Cu] control µg/g wet weight Weighted mean	[Cu] AD µg/g wet weight Weighted mean	Comments
Hippocampus	Corrigan 1993 – ICP-MS	12/12	-0.33 (-1.14-0.47)	5.1 +/- 1.1	4.5 +/- 2.2	All three studies utilize different sampling methods. Corrigan measured the dentate gyrus, Deibel a full hippocampal section at the level of the lateral geniculate body and Magaki isolated white matter from grey matter in the hippocampus. The data from Magaki are presented as a mean of white matter and grey matter measurements.
	Deibel 1996 – INAA*	11/10	-1.32 (-2.28- -0.36)	3.2 +/- 0.7	2.3 +/- 0.6	
	Magaki 2007 – AA	4/7	0.00 (-1.23-1.23)	4.4 +/- 0.4	4.4 +/- 1.0	
	Ward 1987 – INAA	60/58	-0.50 (-0.86- -0.13)	1.8 +/- 0.2	1.7 +/- 0.2	
	Meta-analysis	**87/87**	**-0.54 (-0.91- -0.16)**	**2.6 +/- 0.5**	**2.4 +/- 0.9**	
Amygdala	Deibel 1996 – INAA*	11/10	-1.42 (-2.40- -0.44)	4.1 +/- 1.0	2.7 +/- 0.9	
Putamen	Corrigan 1991 – INAA	6/11	1.21 (0.17-2.39)	2.2 +/- 0.5	2.8 +/- 0.3	
Frontal lobe	Magaki 2007 – AA	6/8	-2.78 (-4.39- -1.17)	7.1 +/- 1.3	4.0+/- 0.5	Magaki isolated white matter from grey matter in the frontal lobe. The data from Magaki are presented as a mean of white matter and grey matter measurements. Copper levels in white and grey matter were comparable.
	Plantin 1987 -- INAA	10/8	-1.45 (-2.53- -0.38)	3.5 +/- 0.8	2.1 +/- 1.0	
Temporal lobe	Deibel 1996 – INAA*	11/10	-1.28 (-2.24- -0.32)	4.0 +/- 0.6	3.2 +/- 0.6	
	Plantin 1987 -- INAA	10/7	-1.86 (-3.07- -0.66)	3.1 +/- 0.6	1.8 +/- 0.7	
	Religa 2006 – ICP-MS	14/10	-0.39 (-1.21-0.43)	2.8 +/- 1.4	2.3 +/- 1.0	
	Squitti 2006 -- AA	10/9		6.8 +/- 1.5	5.1 +/- 1.6	
	Meta-analysis	**45/36**	**-1.11 (-1.98- -0.24)**	**4.0 +/- 1.0**	**3.2 +/- 1.0**	
Parietal lobe	Deibel 1996 – INAA*	11/10	-1.28 (-2.24- -0.32)	4.1 +/- 0.6	3.8 +/- 0.9	
	Plantin 1987 -- INAA	10/8	-1.19 (-2.22- -0.16)	3.9 +/- 0.8	2.3 +/- 0.8	
Occipital lobe	Plantin 1987 – INAA	10/7	-0.99 (-2.02-0.05)	3.9 +/- 0.8	2.2 +/-1.2	
Cerebellum	Deibel 1996 – INAA*	11/10	-0.80 (-1.47- -0.43)	5.7 +/- 1.0	5.1 +/- 0.3	

* study conducted at the University of Kentucky

TABLE 5: Wet to dry ratios used in calculations

Brain region	Dry to wet ratio, control	Dry to wet ratio, AD	Number cases (control/AD)
Hippocampus	0.19	0.18	39/36
Amygdala	0.20	0.22	25/38
Thalamus	0.25	0.18	7/11
Caudate	0.19	0.19	7/9
Putamen	0.23	0.22	8/12
Globus pallidus	0.26	0.32	3/10
Frontal lobe	0.20	0.22	45/42
Parietal lobe	0.20	0.20	27/22
Temporal lobe	0.19	0.20	27/28
Occipital lobe	0.23	0.21	12/6
Cerebellum	0.20	0.21	4/3

Data assembled from Ehmann 1986, House 2007 & 2008, Panayi 2001, Samudralwar 1995, Stedman 1997 and Thompson 1988.
Ratios are weighted means between reported values.

CHAPTER 4

THE EFFECT OF CEREBRAL AMYLOID ANGIOPATHY ON IRON, COPPER AND ZINC IN ALZHEIMER'S DISEASE

Matthew Schrag[1], Andrew Crofton[1], Arshad Jiffry[1], David Kirsch[1], Matthew Zabel[1], April Dickson[1], Dylan W. Domaille[4], Xiao Wen Mao[2], Harry V. Vinters[3], Christopher J. Chang[4] and Wolff Kirsch[1]

[1]Neurosurgery Center for Research, Training and Education, Loma Linda University, Loma Linda, California
[2]Radiation Research Laboratories, Loma Linda University, Loma Linda, California
[3]Departments of Pathology and Laboratory Medicine (Neuropathology) and Neurology, David Geffen School of Medicine at University of California Los Angeles, Los Angeles, California
[4]Department of Chemistry and the Howard Hughes Medical Institute, University of California Berkeley, Berkeley, California

Abstract

Cerebral amyloid angiopathy (CAA) is a vascular lesion associated with Alzheimer's disease (AD), is present in as many as 95% of AD patients and produces MRI-detectable microbleeds in many of these patients. It is possible that CAA-related microbleeding is a source of pathological iron in the AD brain. Because the homeostasis of copper, iron and zinc are so intimately linked, we determined whether CAA contributes to changes in the brain levels of these metals. We obtained brain tissue at autopsy from the temporal lobes of AD patients with severe CAA to compare to AD patients without evidence of vascular amyloid. Patients with severe CAA had significantly higher non-heme iron levels. Histological analysis demonstrated that iron was deposited in the walls of large CAA-affected vessels. Zinc levels were significantly

elevated in grey matter in both the CAA and non-CAA AD tissue, but no vascular staining was noted in CAA cases. Copper levels were decreased in both CAA and non-CAA AD tissues and copper was found to be prominently deposited on the vasculature in CAA. Together, these findings demonstrate that CAA is a significant variable affecting transition metals in AD.

Introduction

There is considerable interest in understanding transition metal homeostasis in the brain, particularly in Alzheimer's disease (AD) research. The AD neocortex is frequently stated to contain increased iron levels at the tissue level. Numerous review articles have suggested that AD brain contains two to five fold more iron than control tissue (Avramovich-Tirosh 2008, Bush and Tanzi 2008, Molina-Holgado 2007, Huang 2004). Remarkably, most quantitative measurements of brain iron failed to show any increase in neocortical iron in AD (Andrasi 2000, Corrigan 1991, Griffiths and Crossman 1993, Hallgren and Sourander 1960, Magaki 2007, Panayi 2001, Plantin 1987, Religa 2006, Stedman and Spyrou 1997, Ward and Mason 1987).

Never-the-less, increases in iron levels in the deep grey matter structures of the brain in patients with AD have been clearly demonstrated and other disturbances in iron levels and distribution may be more easily detected in qualitative studies (Andrasi 2000, Corrigan 1991, Griffiths and Crossman 1993). However, despite extensive investigation, the source of this abnormal iron remains a matter of debate; it may represent a metabolic derangement, abnormal deposition or clearance or perhaps some other explanation.

Cerebral amyloid angiopathy (CAA) is a vascular manifestation of AD which is present in as many as 95% of AD patients and can produce MRI-detectable microbleeds even in patients with only mild cognitive impairment (Jellinger 2010, Kirsch 2007, Schrag 2010). Vascular amyloid deposition results in loss of vascular smooth muscle cells (particularly in arterioles), and thickening of the vessel wall with congophilic material. These changes result in fragility of the microvascular system, although the exact mechanism which undermines its stability is not known (Vinters 1987, Vinters 1996). Several studies have demonstrated that iron-rich deposits staining positive for beta-amyloid are preferentially distributed near vascular elements, which may suggest that microbleeding could be a catalyst for the formation of AD-like pathologic lesions (Goodman 1953, Cullen 2005, 2006). Because of the near-ubiquitous presence of CAA in the context of AD, it is possible that CAA-related microbleeding is a source (perhaps the major source) of pathological iron in AD brain. In this study we assessed this hypothesis by determining the levels of various metals by both analytical and qualitative techniques in groups of cases with severe AD and either severe or negligible CAA.

Materials and Methods

Tissue Selection

Post mortem tissue was obtained from the Alzheimer's Disease Research Center Brain Bank at the University of California, Los Angeles. All patients and/or their surrogates had consented to participate in research protocols prior to tissue donation. The research was approved by the Institutional Review Board of Loma Linda University Medical Center (approval #54174). Both frozen tissue specimens and fixed tissues were

available for study. Neuropathologic examination at the time of autopsy included Braak and Braak staging of AD and Vonsattel grading of CAA pathology (Vinters and Vonsattel 2000, Braak and Braak 1991, Greenberg 1997). Vonsattel staging describes the severity of CAA as follows: stage 1- β-amyloid deposition limited to the basement membrane of arterioles and primarily involving leptomeningeal vessels; stage 2- β-amyloid deposited between vascular smooth muscle cells and pathology extends to penetrating arterioles and stage 3- β-amyloid largely replaces vascular smooth muscle in arterioles. Microaneurysms and microhemorrhages often occur with Vonsattel stage 3 CAA.

Frozen tissue was isolated from the superior or middle temporal lobe gyrus for three groups of patients; six samples were obtained for an aged neurological control group, along with eight AD samples without evidence of significant CAA (Vonsattel grades 0-1) and eight AD samples with severe CAA (grade 3). Patient demographics are listed in Table 6.

Atomic Absorption Spectrometry

Metals measurements were conducted as previously described (Schrag 2010). Blocks of grey matter and white matter weighing between 30-60mg were cut from the donated specimens. For total iron, copper and zinc determination, tissue was prepared by nitric acid ashing. Brain tissue was covered in concentrated nitric acid (300µL) overnight, then incubated in a water bath at 80°C for 20 minutes. The solution was allowed to cool to room temperature for 10 minutes. Hydrogen peroxide (300 µL of 10M solution) was then added to dissolve the lipid components and allowed to incubate at

room temperature for 30 minutes. The mixture was then incubated at 70°C in the water bath for 15 minutes. The resulting solution was allowed to cool to room temperature for ten minutes, thoroughly vortexed, then frozen until needed.

For non-heme iron extraction, 260µL of 500µM EDTA was added to brain regions which were then homogenized. One hundred microliters of trichloroacetic acid (20% solution in 500µM EDTA) was added and thoroughly vortexed before incubating at 90°C for 30 minutes. Finally, 700µL of the EDTA solution was added and thoroughly vortexed. The resulting suspension was centrifuged at 13,000 g for 10 minutes and the supernatant was collected as the non-heme iron sample.

Atomic absorption spectra were measured with a Varian SpectrAA 220Z atomic absorption spectrometer and processed with SpectrAA software v.4.1 (Varian Inc., California). Standard iron and copper curves were produced from 25, 50, 75 and 100 parts per billion solutions of standard iron or copper in nitric acid (Arcos Organics, New Jersey). Standard curve for zinc was produced from 250, 500, 750 and 1000 parts per billion solutions of standard zinc in nitric acid (Solutions Plus Inc, Missouri). The spectrometer was zeroed to a maximum of 0.005 mean absorbance. For total iron measurements samples were diluted 1:40, for non-heme iron samples were diluted 1:20, for zinc measurements samples were diluted 1:10 and for copper samples were diluted 1:20. All sample values presented in Table 7 are the mean of six measurements.

Histology

Frozen sections were prepared for four of the patients from each group for histology. Histological slides were prepared on a Leica cryostat with either 14 or 20

micrometer thick sections of brain tissue containing both an intact portion of the cortical ribbon and adjacent white matter. Iron staining was accomplished with modified Prussian Blue and Turnbull's blue methods on the 20 micrometer thick sections. Prolonged incubation times were employed to increase the sensitivity of the techniques (Smith 1997 and Cullen 2005, 2006). Ideal incubation times for aged brain to balance signal to background-noise ratio were optimized to 48 hours. Frozen sections were allowed to dry at room temperature for ten minutes and then briefly fixed for 10 minutes in absolute methanol. While staining of never-fixed tissue is preferred to limit the possibility of leaching metals from the tissue, unfixed brain tissue was not stable throughout the long staining procedure. Methanol-fixation has been shown in a study using hepatocytes to preserve iron levels far better than formalin-containing fixatives (Okon 1998). Staining solutions for each probe were prepared as 5% potassium ferrocyanide (for Prussian Blue labeling of ferric iron) or 5% potassium ferricyanide (for Turnbull's blue labeling of ferrous iron) dissolved in an aqueous solution with 10% hydrochloric acid. After 24 hours' exposure, the staining solution was replaced with fresh solution for a further 24 hours. The sections were then washed in distilled deionized water, dehydrated through 100% ethanol, cleared in xylene and mounted in a resinous medium (Permount, Fisher Scientific). The slides were imaged on a Leica DM50 light microscope (Leica Microsystems, Illinois), at least five fields containing arterioles and five of capillaries were captured from each slide.

Zinc was visualized using a fluorescein-conjugated probe, ZP4, as follows. Frozen, 14 micron sections were allowed to dry at room temperature for 10 minutes and were then placed in PBS for 30 minutes. A 2 micromolar solution of the zinc probe in

PBS was prepared and gently pipetted over the section. After a ten minute incubation, the sections were washed three times in PBS for 10 minutes each. Care was taken to minimize agitation to prevent damage to the unfixed tissue section. A thin paraffin spacer was placed on the slide and the section was coverslipped with aqueous mounting medium containing DAPI. The slide was then immediately imaged on an Olympus confocal microscope (Olympus America Inc., Pennsylvania).

Copper was imaged using a turn-on probe with a boron-dipyrromethene (BODIPY) fluorophore, copper sensor 1 (CS1). The fluorescent yield from this probe has been reported to increase 10 fold upon binding to monovalent copper (Miller 2006, Zeng 2006, Domaille 2008). Sections were allowed to dry for ten minutes, permeabilized in Triton-X in PBS for ten minutes and finally washed gently in PBS for ten additional minutes. A 2 micromolar solution of the CS1 probe was prepared and pipetted over the section. After ten minutes, the excess probe was tapped off the slide which was then mounted with a thin paraffin spacer in aqueous mounting medium containing DAPI (Vector Labs, California). For colocalization of vascular copper deposits with beta-amyloid, we added a ten-minute incubation of the section in 1% Thioflavin-S solution followed by thorough washing to the procedure prior to the CS1 incubation.

Electrophoresis

Protein levels of heme degradation enzymes were determined by denaturing SDS-PAGE and western blot. Briefly, tissue samples were isolated containing roughly equal proportions of white and grey matter from the temporal lobe. The tissue was homogenized in an ice cold sucrose buffer containing a protease inhibitor cocktail. The

tissue was disrupted with seven strokes with a fitted Teflon pestle in a glass homogenization tube. Crude nuclear debris was cleared from the suspension by centrifugation at 1000g for 15 minutes. Total protein concentration was determined in the supernatant by the Bradford assay (Pierce Laboratories, Illinois). Samples were prepared for electrophoresis by adding 25% v/v loading buffer (Invitrogen, California) and 10% v/v beta-mercaptoethanol and heating at 95°C for ten minutes. Fifteen micrograms of total protein were loaded into each lane of a 10% polyacrylamide gel and electrophoresed at 100V in a MiniProtean Tetra System (BioRad Laboratories, California). The proteins were then transferred to a nitrocellulose membrane at 30V for four hours. The resulting blot was blocked in an albumin-based blocking buffer (Invitrogen) and probed with either mouse monoclonal beta-actin (1:1000), rabbit monoclonal heme oxygenase 1 (HO-1) (1:100), mouse monoclonal HO-2 (1:500), mouse monoclonal biliverdin reductase A (BLVD R A) (1:200) or mouse monoclonal BLVD R B (1:200) antibodies (all from Abcam, Cambridge, Massachusetts). After an overnight incubation at 4°C, the blots were thoroughly washed with TBS buffer containing 0.05% Tween-20 and a fluorescently labeled goat anti-mouse or rabbit secondary (IRDye, Licor) was applied. After a two-hour incubation the blots were washed again and visualized on an Odyssey Infrared Imaging System (Licor Biosciences, Nebraska). Optical density was determined using Odyssey 2.0 software and data were collected as the relative intensity of the band of interest compared to the corresponding loading control band.

Clear native acrylamide electrophoresis was conducted to validate staining from the CS1 copper probe. Non-denaturing conditions were required to ensure proteins retained any bound copper (Finney 2010). The homogenate was prepared as previously

described except EDTA was omitted from the protease inhibitor cocktail to prevent metal chelation. To 500 microliters of homogenate, 120 microliters of 20% digitonin was added to solubilize the membrane components. Crude nuclear debris was then removed by centrifugation at 1000g. Finally, 20 microliters of 50% glycerol and 0.1% Ponceau-S dye were added to the sample. Fifty micrograms of total protein were loaded into a gradient 4-13% acrylamide gel (prepared without SDS) and run on ice at 250V overnight. Running buffer consisted of 50 mM Tris, and 7.5 mM imidazole; 0.05 % deoxycholate and 0.05% Triton-X-100 were added to the cathode buffer.

The gel was probed with 2mM CS1 solution for ten minutes and copper-positive bands were detected by red fluorescence. Confirmation that fluorescent bands were in fact copper-positive was determined by incubating the gel with 1% bathocuproine sulfate (BCS), a copper chelator, for 48 hours and observing the reduction in fluorescence. Additionally, fluorescent bands were cut from the gel and analyzed for copper content as follows. The band of interest was carefully weighed and incubated with 600 microliters concentrated nitric acid for 2 hours. It was then heated to 80°C in a water bath for ten minutes. The resulting sample was then analyzed by atomic absorption spectrometry as previously described.

All measurements are reported as mean +/- standard deviation. Significance was assessed by the Students T test (two-tailed) with alpha of $p=0.05$.

TABLE 6: Patient demographics and neuropathologic findings

Patient group	Number of cases	Age	Sex	Neuropathologic characterization
Aged control (neurologically normal)	6	76 ± 12	5M 1F	Normal (age-related changes only)
Alzheimer's disease w/o significant cerebral amyloid angiopathy	8	86 ± 6	1M 7F	Braak and Braak stages V-VI Vonsattel grade 0-1
Alzheimer's disease w/ severe cerebral amyloid angiopathy	8	82 ± 7	4M 4F	Braak and Braak stages V-VI Vonsattel grade 3-3+

TABLE 7: Temporal lobe metal concentrations

Metal	Aged control	Alzheimer's disease w/o significant cerebral amyloid angiopathy	Alzheimer's disease w/ severe cerebral amyloid angiopathy
Total iron, white matter	58.89 ± 7.68	53.40 ± 9.68	70.20 ± 17.98$^{\Psi}$
Total iron, grey matter	46.22 ± 14.60	46.04 ± 9.48	52.44 ± 12.90
Non-heme iron, white matter	50.16 ± 25.47	51.52 ± 13.71	72.31 ± 20.66$^{\Psi}$
Non-heme iron, grey matter	34.19 ± 9.47	40.88 ± 13.33	53.49 ± 15.59*
Zinc, white matter	26.49 ± 5.65	28.98 ± 5.70	25.68 ± 7.33
Zinc, grey matter	16.05 ± 3.75	23.66 ± 5.99*	24.28 ± 4.50**
Copper, white matter	6.00 ± 1.10	4.28 ± 1.30*	4.41 ± 1.28*
Copper, grey matter	5.72 ± 1.20	3.74 ± 1.07**	3.94 ± 1.02*
Aluminum, white matter	1.82 ± 0.86	3.50 ± 1.91	2.63 ± 2.24
Aluminum, grey matter	2.94 ± 2.12	4.24 ± 3.82	2.45 ± 1.69

Data presented as µg metal/g wet tissue +/- standard deviation
*p<0.05, **p<0.01 compared to control
$^{\Psi}$p<0.05 compared to Alzheimer's disease w/o significant cerebral amyloid angiopathy

Results

Twenty-two brain samples were obtained from the temporal lobes of elderly humans at autopsy. Cases included in the study were carefully chosen based upon their neuropathologic findings. A group of cases with AD was assessed for the severity of vascular β-amyloid deposition. Eight cases demonstrating severe cerebral amyloid angiopathy were included in one group, eight with minimal to no cerebral amyloid angiopathy were included in another – all patients in both of these groups demonstrated severe parenchymal AD pathology. Additionally, six cases with no evident neuropathologic abnormalities and matching age distribution were included as controls (Table 6). This study design was chosen to delineate pathologic changes associated with vascular degeneration from the effects of parenchymal Alzheimer's pathology. The tissue was selected from the middle and superior temporal gyri, a region significant to AD, and was preserved by flash freezing over liquid nitrogen at the time of autopsy; the sample was never exposed to fixative.

The level of metals in the tissue was determined by atomic absorption spectrometry (Table 7). Total iron was measured because the majority of other measures of brain iron in AD reported in the literature have been performed by measuring total iron. However, because substantial blood remains trapped within the vasculature in this post-mortem tissue, measurement of non-heme (chelatable) iron was considered a more-reliable measure of tissue iron content. Total iron was found to be significantly increased in the group with CAA, compared to the AD group without CAA, in white matter measurements ($p=0.036$). Iron levels in the AD group without CAA were non-significantly lower than those in the control group. No significant differences were noted

in the grey matter measurements between the groups. Non-heme iron measurements confirmed the significant increase in white matter iron in the CAA group compared to the AD-only group ($p=0.032$) and the CAA group trended strongly toward an increase compared to normal controls as well ($p=0.097$). There was no difference in non-heme iron levels in the white matter between the AD-only group and the controls. In the grey matter, iron was again significantly increased in the group with CAA compared to the control group ($p=0.020$) while the AD-only group was not significantly different from the controls. In the absence of vascular pathology, no alteration in brain iron content could be detected in AD brain compared to normal aged control brain.

Histologically, Prussian blue and Turnbull's blue staining were used to determine the distribution of ferrous and ferric iron in these specimens. Turnbull's blue preferentially reacts with divalent iron and brightly stained the walls of arterioles in the CAA group while this staining was absent from specimens from both of the other groups (Fig. 4). Prussian blue staining of ferric iron was not prominent and did not stain the vasculature in any group except in areas of obvious hemorrhage (not shown). Little staining of amyloid plaques was noted, although demonstration of iron in amyloid plaques is typically accomplished with DAB-enhancement of iron stains, which was not done here.

To reinforce the hypothesis that iron deposition in AD is a result of microbleeding, we observed the levels of heme degradation enzymes (Fig. 5). The expression of several of these enzymes is inducible in the presence of extravascular heme and would therefore be expected to be elevated in the context of ongoing microbleeding. Two isoforms of heme oxygenase are responsible for catalyzing the degradation of heme

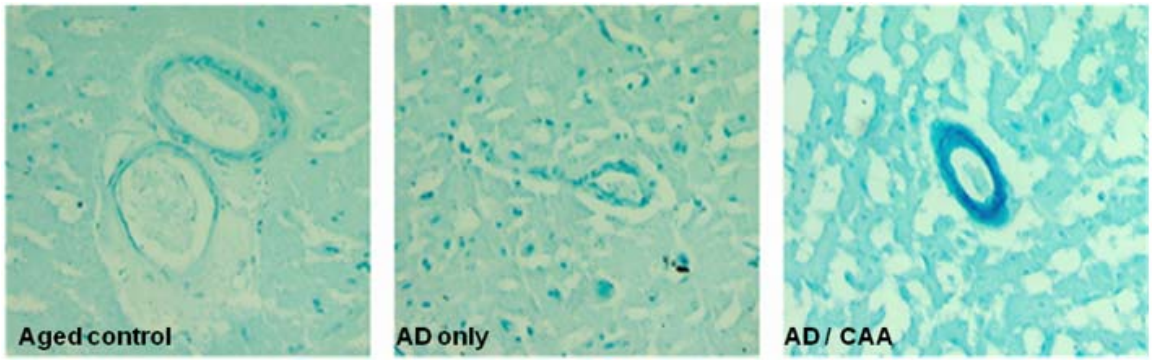
Aged control
AD only
AD / CAA

Figure 4: Iron is deposited on arterioles in cerebral amyloid angiopathic brain
Turnbull's blue stain of control, AD brain without CAA and AD brain with CAA demonstrates deposition of ferrous iron in the wall of an arteriole affected by CAA.

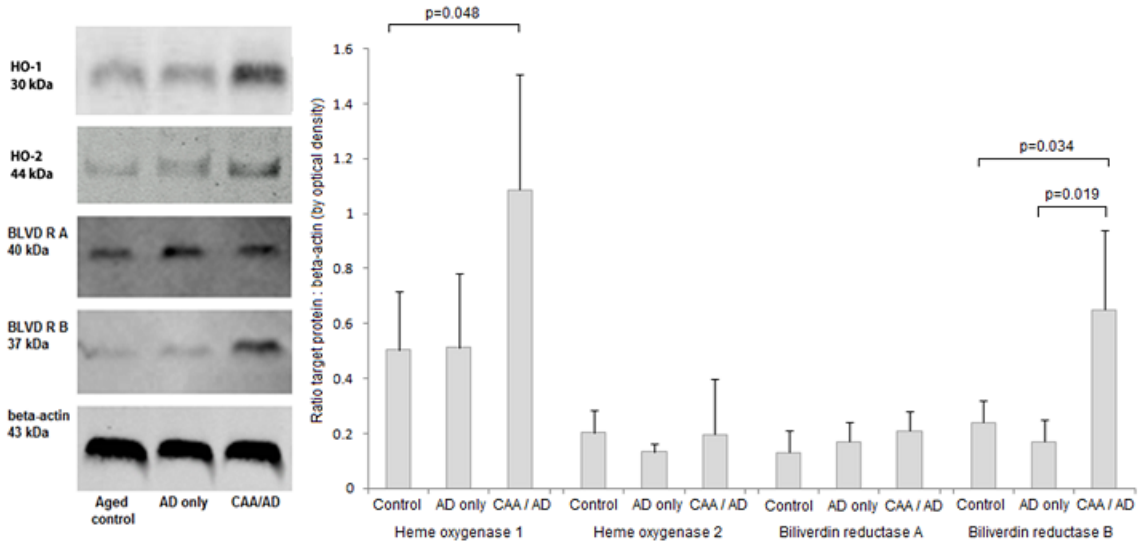
HO-1
30 kDa
HO-2
44 kDa
BLVD R A
40 kDa
BLVD R B
37 kDa
beta-actin
43 kDa
Aged control
AD only
CAA/AD
Ratio target protein : beta-actin (by optical density)
p=0.048
p=0.034
p=0.019
Control
AD only
CAA / AD
Heme oxygenase 1
Heme oxygenase 2
Biliverdin reductase A
Biliverdin reductase B

Figure 5: Heme degradation enzymes are induced in cerebral amyloid angiopathic brain but not in purely parenchymal Alzheimer's disease brain

Representative western blots for the major enzymes involved in heme degradation are shown at left above. One isoform each of heme oxygenase (HO-1) and biliverdin reductase (BLVD R B) are substantially elevated in tissue with severe CAA compared to both normal control tissue and AD tissue without CAA. There is no significant difference between AD without CAA and controls. These results support the hypothesis that increased iron in AD is primarily a result of microbleeding.

into biliverdin, carbon monoxide and free iron. HO-1 is the major inducible form, and HO-2 is generally constitutively expressed. HO-1 was significantly elevated in the group with CAA and was at comparable levels in both of the other groups. HO-2 levels were not significantly different between groups. As heme oxygenase is inducible by a variety of molecules, alterations in its expression are non-specific for microbleeding so we also studied the next enzymes in the heme degradation pathway, biliverdin reductases A and B. We found that while biliverdin reductase A levels were unchanged between groups, biliverdin reductase B levels were significantly increased in the CAA group over both the control and AD-only group, indeed more than three fold over the AD-only group. These findings strongly support the hypothesis that the increases in iron in the CAA group are the result of ongoing microvascular bleeding.

Zinc levels were also measured by atomic absorption spectrometry. No significant differences were noted among the groups in zinc measurements from the white matter. Both CAA and AD-only groups had significantly more zinc in the grey matter than the control group ($p=0.0035$ and $p=0.019$ respectively). Changes in zinc levels appear restricted to the grey matter. Histological analysis of zinc distribution with fluorescent probe ZP4 mirrored the findings of the atomic absorption with a moderate increase in staining of zinc in grey matter from the AD groups. No prominent labeling of the vasculature was noted in any of the groups (Fig. 6).

Copper measurements by atomic absorption spectrometry demonstrated significant abnormalities. Both CAA and AD-only group had significantly lower levels of copper in the white matter than the controls ($p=0.023$ and $p=0.031$ respectively). Changes in the grey matter were even more dramatic with both the CAA and AD-only

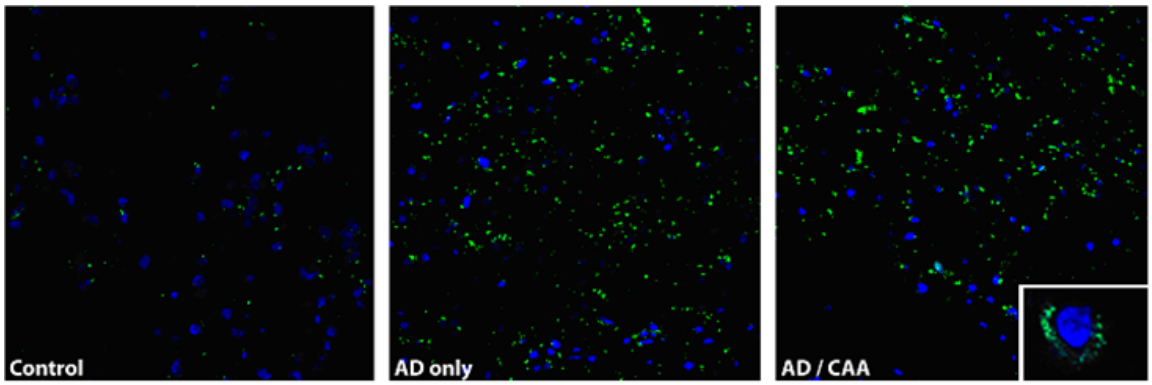
Control
AD only
AD / CAA

Figure 6: Increased non-synaptic zinc levels in grey matter in Alzheimer's disease
Non-synaptic zinc was visualized using the green fluorescent ZP4 probe. Zinc is concentrated in the grey matter of both AD groups compared to normal control. Non-synaptic zinc is primarily distributed in a perinuclear pattern as shown in the inset of the image on the right. Zinc deposition on the vasculature was not prominent in any group.

group again having less copper than the controls ($p=0.011$ and $p=0.0069$ respectively). To qualitatively assess the distribution of copper we used a recently developed copper probe, copper sensor 1 or CS1 (Miller 2006, Zeng 2006, Domaille 2008). This probe is a BODIPY-conjugated turn-on probe whose fluorescent yield is reported to increase by ten fold upon binding to monovalent copper. Notably, the probe is selective for monovalent copper only; no appreciable signal was reported by divalent copper. Because this probe had not been previously used in histological applications, we performed a number of control experiments to ensure that the fluorescent signal generated from this probe represented true copper binding (Fig. 7). We assessed the ability of the probe to detect protein-bound copper since virtually all copper in the brain is bound. To accomplish this, we electrophoresed brain protein homogenates under non-denaturing conditions (and without Coomassie dye which interferes with the fluorescent signal) and probed the resulting gel with CS1. Several bands were cut from the gel and analyzed by atomic absorption spectrometry and those that were fluorescent contained considerably more copper that those that were not. Forty-eight hour incubation of the gel with 1% BCS, a copper chelator, obliterated the fluorescent signal. Finally, we ran purified ceruloplasmin, a protein which selectively binds divalent copper, to veridy selective monovalent copper detection by the probe. No fluorescent signal was detected corresponding to the ceruloplasmin band on Coomanssie stain, although a considerable concentration of copper was detected by AA. When the probe was applied to brain tissue, BCS copper chelation of the tissue section obliterated any red-fluorescent signal. CS1 staining of tissue sections revealed discrete peri-nuclear puncta of intense red fluorescence in all three groups. This pattern of staining is consistent with the pattern of

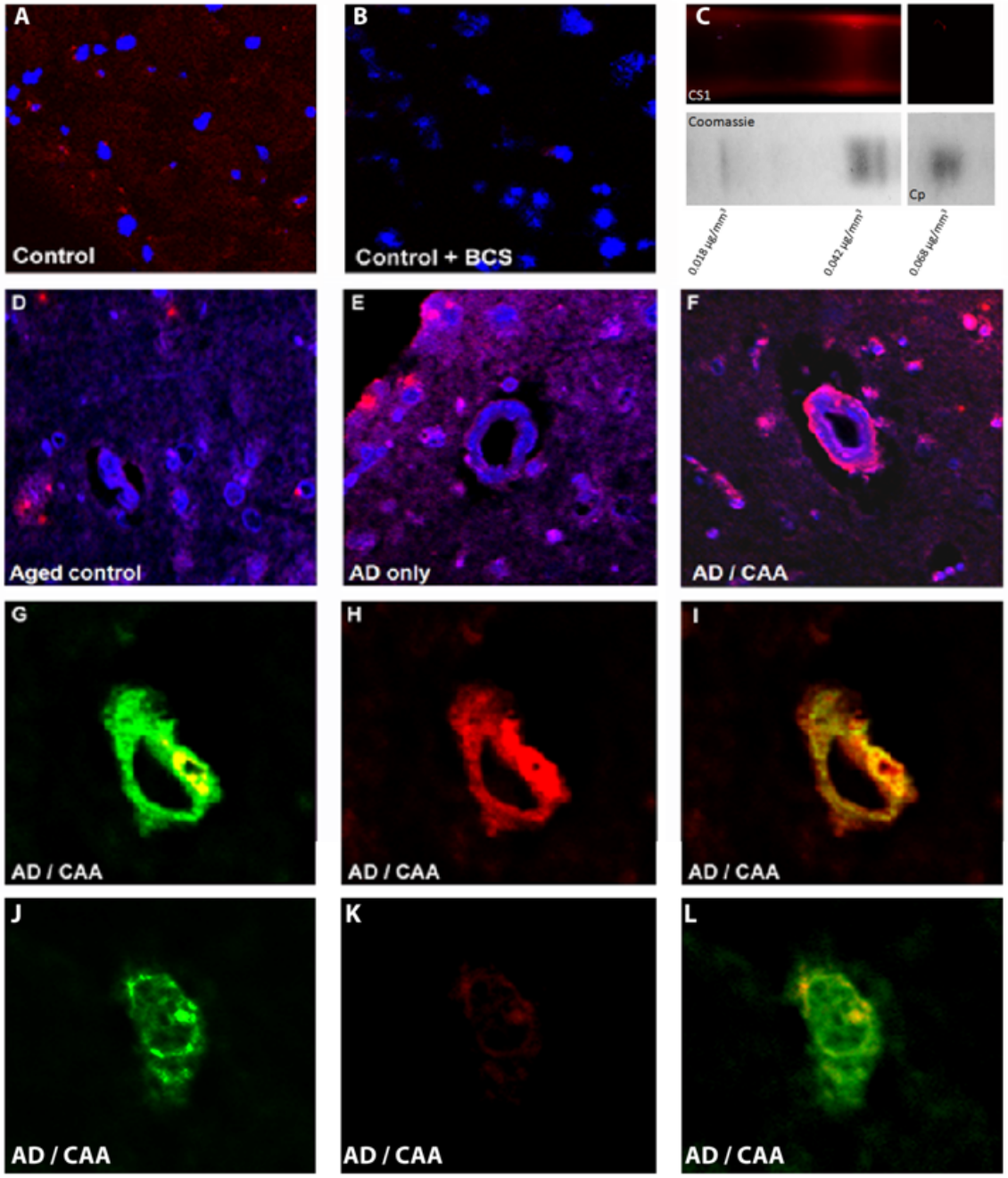
A
Control
B
Control + BCS
C
CS1
Coomassie
Cp
0.018 µg/mm²
0.042 µg/mm²
0.068 µg/mm²
D
Aged control
E
AD only
F
AD / CAA
G
AD / CAA
H
AD / CAA
I
AD / CAA
J
AD / CAA
K
AD / CAA
L
AD / CAA

Figure 7: Copper is concentrated in vascular elements in CAA
Images A and B show control brain cortex stained with CS1 probe (red) and DAPI. Image B was stained after the tissue was incubated in BCS, a selective copper chelator. BCS incubation reduces fluorescence from the CS1 probe, confirming that the bulk of the red signal is from copper binding. Image C shows a portion of a native protein electrophoresis of a brain homogenate. A band binding the CS1 probe was located. An adjacent protein band (determined by Coomassie staining) along with the positive band were analyzed by atomic absorption spectroscopy. The concentration of copper in the positive band was more than double that in the negative band. Additionally, purified ceruloplasmin (Cp in image C) which is known to bind divalent copper did not fluoresce upon CS1 incubation, confirming the valence selectivity of the probe. Images D, E and F show CS1 and DAPI staining of control, AD only and AD with CAA brain respectively. Monovalent copper is prominently deposited on vessels in the CAA case. Images G, H, I and J, K, L show thioflavin staining of beta-amyloid (G and J) overlaid on CS1 stain for copper (H and K) in CAA-affected brain. Copper appears to strongly colocalize with thioflavin staining of beta-amyloid (green) in a CAA vessel, but only weakly in beta-amyloid plaque.

staining of key copper-binding proteins reported in other studies. Importantly, in the CAA group remarkable staining of the vasculature was observed in the grey matter. Both capillaries and arterioles were stained and the copper staining was noted to colocalize with the fluorescence from the thioflavin-S stain for beta-amyloid.

For historical interest, we also measured aluminum in these tissues – no significance difference between the groups was detected, but variance in aluminum levels was high for all groups.

Discussion

The metabolism of iron in the brain and how it changes with aging and AD has been studied in depth. Total iron levels increase throughout the brain with age under normal conditions, particularly in the putamen, reaching a relatively steady concentration by about the sixth decade of life (Hallgren and Sourander 1958, Markesbery 1984). Elevated levels of tissue metals can cause neuronal injury through a number of mechanisms. Both iron and copper are redox active metals, capable of generating free-radicals as they cycle between valence states. Oxidative injury in the form of lipid peroxidation, protein crosslinking and DNA damage have been reported as early pathologic findings in the process of Alzheimer's neurodegeneration -- injuries which result from uncontrolled reactive oxygen species whose formation could be catalyzed by abnormal free iron (Markesbery 1999 and Smith 2007). Additionally, the β-amyloid plaques characteristic of AD have been described as a sort of "metals sink" because copper, zinc and in particular iron are thought to be concentrated at their cores (Goodman 1953, Lovell 1997). While many, perhaps even most, β-amyloid plaques in human brain

contain no more iron than normal brain tissue (in fact, one study found 30% had no detectable iron whatever), some plaques (particularly larger ones) have been shown to contain high concentrations of a reactive iron oxide, magnetite (Dhenain 2002, Collingwood 2008). Iron-binding appears to increase the toxicity of β-amyloid -- when amyloid is incubated with a strong metal chelator prior to its application to neurons *in vitro*, its toxic effects are dramatically ameliorated (Rottkamp 2001). For this reason, therapies to manipulate brain iron levels have been tested in human trials (Crapper McLachlan 1991, Lannfelt 2008).

Pathologic accumulation of iron has been hypothesized to be a result of abnormal expression patterns of iron regulatory proteins (IRPs), the master regulators of brain iron (Smith 1998). The expression of IRPs is directly affected by tissue iron levels and alters the expression of numerous iron binding proteins, including storage molecules like ferritin, iron transport molecules like transferrin, transferrin-receptor and divalent metal transporter 1 and certain key proteins related to AD, including amyloid precursor protein. IRPs bind to iron-response elements in untranslated regions (UTRs) of the affected genes, upregulating gene expression if they bind in a 5' UTR, downregulating expression when binding is in a 3' UTR (Leipuviene 2007, Rogers 2008, Avramovich-Tirosh 2008). This elaborate system intricately regulates the homeostasis of brain iron and appears to remain largely intact in the AD brain. We previously showed that the level and pattern of expression of IRP1 and IRP2 are unchanged in AD brain compared to normal aged brain and while reports vary, the majority of evidence suggests ferritin, transferrin and transferrin-receptor levels are essentially unchanged (Magaki 2007, Connor 1992, Beard 1993, Loeffler 1995). Because the metabolic handling of iron appears to be essentially

intact in AD, we chose to assess whether abnormal deposition of iron through microbleeding may account for the qualitative increases reported by various investigators.

The novel component of the design of this study is the stratification of AD cases by the degree of vascular amyloid pathology to determine whether the increased iron often reported in AD is associated with, or the result of, parenchymal or vascular pathology. CAA pathology in AD exists as a spectrum ranging from nearly undetectable in some cases to the predominant neuropathologic abnormality in others (Greenberg 1997). For this reason, the stratification employed here is somewhat arbitrary; it is a useful distinction.

The current study, in the context of previous work, leaves little doubt that iron deposition in AD may be linked to microvascular bleeding or leakage. Iron levels were only increased in the CAA group and this increase was found to be associated with vascular accumulation of ferrous iron. Moreover, the heme degradation enzymes HO-1 and BLVDR B were significantly elevated in the CAA group over both the normal controls and the non-CAA AD cases. Increases in heme oxygenase 1 in AD have been previously well-documented, but the finding of increased biliverdin reductase B is a new observation and quite interesting. This reductase, in addition to its role in heme degradation, functions as both a dual specificity serine/threonine/tyrosine kinase and a leucine zipper-type transcription factor which promotes the expression of heme oxygenase 1 among other targets (Lerner-Marmarosh 2005, Florczyk 2008). These features hint at a more prominent role for this molecule in the pathologies of AD than has previously been appreciated. Curiously, in a recently published prospective study peptide

fragments from both heme oxygenase 1 and biliverdin reductase B were shown to be elevated in serum of subjects with mild cognitive impairment who subsequently progressed to late-onset dementia in comparison to subjects with equally severe mild cognitive impairment who remained cognitively stable (Mueller 2010). We have now shown that both enzymes are directly involved in vascular AD pathology – that they are detectable in peripheral blood samples makes them potentially valuable as biomarkers of AD. CAA-related microbleeding is additionally often detectable by susceptibility weighted MRI at early stages of cognitive impairment (Kirsch 2009, Schrag 2010). Iron modulation has been considered as a potential therapy for AD, although initial clinical trials have not yet shown an improvement in cognitive performance (Crapper McLachlan 1991, Lannfelt 2008). Because these biomarkers are available, future clinical trials may be designed to treat a subset of patients with identifiable microbleeding rather than all patients presenting with cognitive decline.

The significance of zinc levels in the neocortex of brain affected by AD has been debated for decades. Several studies have shown an increase in zinc in AD neocortex (Cornett 1998, Corrigan 1993, Deibel 1996, Religa 2006, Ward and Mason 1987) while others have found no significant increase (Andrasi 2000, Panayi 2002) and one study found a decrease in zinc (Corrigan 1991). Our result demonstrates that zinc is increased in AD only in grey matter. Previous studies have examined tissue samples that included both grey and white matter together, so discrepancies may be due to differences in tissue sampling. While a previous study convincingly showed that zinc was deposited on the vasculature in an animal model of CAA, our results suggest that alterations in zinc may not be strongly associated with vascular β-amyloid in human CAA (Friedlich 2004).

Copper levels are generally reported to decrease in AD (Diebel 1996, Magaki 2007). One often-cited study reports an increase in copper, although this is likely artifactual due to tissue fixation, which has been shown to increase apparent tissue copper levels in AD (Lovell 1998, Schrag 2010). Our results demonstrate a significant decrease in copper in both white and grey matter across both AD groups studied. Monovalent copper was also noted to be deposited on vascular elements affected by CAA using a novel fluorescent probe. Curiously, no staining of copper was noted in β-amyloid plaques in these studies which may mean that copper associated with plaques is primarily in the divalent form. The perinuclear punctate staining pattern of monovalent copper was observed in specimens from all three groups of cases and likely represents an endoplasmic reticular and trans-golgi distribution (Yang 2005). A similar pattern of staining has been observed for several key neuronal copper binding proteins including ATP7A, ATOX1, and Steap2 which are associated with these subcellular structures (Tokuda 2009, El Meskini 2007, Prohaska 2004). The CS1 probe has enabled this initial histological analysis of monovalent copper in AD and will no doubt lead to future studies clarifying the neurobiology and neuropathology of brain copper.

For decades there has been substantial interest in the role of metals in AD and in manipulating the homeostasis of these metals as therapy -- this interest will likely continue. However, clinical trials of chelators and chelator-like compounds have demonstrated substantial toxic effects and one has claimed the life of a patient-participant (Squitti 2002). For this reason, more detail is needed in the analysis of the role of these metals and the associated metabolic pathways in disease to identify the best ways to intervene.

Acknowledgements

This research was funded by the National Institutes of Health (AG20948). Harry V. Vinters is supported in part by P01 AG12435, P50 AG16570 and the Daljit S. and Elaine Sarkaria Chair in Diagnostic Medicine. Christopher J. Chang is an investigator with the Howard Hughes Medical Institute and is funded through the NIH (GM79465). None of the authors report conflicts of interest related to this material.

References

1. Andrasi E, Farkas E, Gawlik D, et al (2000) Brain iron and zinc contents of German patients with Alzheimer's disease. Journal of Alzheimer's Disease 2:17-26.

2. Avramovich-Tirosh Y, Amit T, Bar-Am O, et al (2008) Physiological and pathological aspects of Abeta in iron homeostasis via 5'UTR in the APP mRNA and the therapeutic use of iron-chelators. BMC Neurosci 9 suppl:S2.

3. Braak H, Braak E (1991) Neuropathological stageing of Alzheimer-related changes. Acta Neuropathol 82:239-59.

4. Bush A, Tanzi R (2008) Therapeutics for Alzheimer's disease based on the metal hypothesis. Neurotherapeutics 5:421-32.

5. Collingwood J, Chong R, Kasama T, et al (2008) Three-dimensional tomographic imaging and characterization of iron compounds within Alzheimer's plaque core material. J Alz Dis 14:235-45.

6. Connor J, Snyder B, Beard J, et al (1992) Regional distribution of iron and iron-regulatory proteins in the brain in aging and Alzheimer's disease. Journal of Neuroscience Research 31:327-335.

7. Cornett C, Markesbery W, Ehmann W (1998) Imbalances of trace elements related to oxidative damage in Alzheimer's disease brain. Neurotoxicology 19:339-45.

8. Corrigan F, Reynolds G, Ward N (1991) Reductions of zinc and selenium in brain in Alzheimer's disease. Trace Elements in Medicine 8:1-5.

9. Corrigan F (1993) Hippocampal tin, aluminum and zinc in Alzheimer's disease. BioMetals 6:149-54.

10. Crapper McLachlan D, Dalton A, Kruck T, et al (1991) Intramusclar desferrioxamine in patients with Alzheimer's disease. Lancet 337:1304-8.

11. Cullen K, Kocsi Z, Stone J (2005) Pericappillary haem-rich deposits: evidence for microhemorrhages in aging human cerebral cortex. J Cereb Blood Flow Metab 25:1656-67.

12. Cullen K, Kocsi Z, Stone J (2006) Microvascular pathology in the aging human brain: evidence that senile plaques are sites of microhemorrhages. Neurobiol Aging 27:1786-96.

13. Dedman D, Treffry A, Candy J, et al (1992) Iron and aluminum in relation to brain ferritin in normal individuals and Alzheimer's disease and chronic dialysis patients. Journal of Biochemistry 287:509-14.

14. Deibel M, Ehmann W, Markesbery W (1996) Copper, iron and zinc imbalances in severely degenerated brain regions in Alzheimer's disease: possible relation to oxidative stress. Journal of Neurological Science 143:137-42.

15. Dhenain M, Privat N, Duyckaerts C, Jacob R (2002) Senile plaques do not induce susceptibility effects in T2*-weighted MR microscopic images. NMR Biomed 15:197-203.

16. Domaille D, Que E, Chang CJ (2008) Synthetic fluorescent sensors for studying the cell biology of metals. Nature Chem Biol 4:168-75.

17. El Meskini R, Crabtree K, Cline L, et al (2007) ATP7A (Menkes protein) functions in axonal targeting and synaptogenesis. Mol Cell Neurosci 34:409-21.

18. Finney L, Chishti Y, Kharet T, et al (2010) Imaging metals in proteins by combining electrophoresis with rapid x-ray fluorescence mapping. ACS Chem Biol 5:577-87.

19. Florczyk U, Jozkowicz A, Dulak J (2008) Biliverdin reductase: new features of an old enzyme and its potential therapeutic significance. Pharm Reports 60:38-48.

20. Friedlich A, Lee J, van Groen T, et al (2004) Neuronal zinc exchange with the blood vessel wall promotes cerebral amyloid angiopathy in an animal model of Alzheimer's disease. J Neurosci 24:3453-9.

21. Goodman L (1953) Alzheimer's disease; a clinico-pathologic analysis of 23 cases with a theory on pathogenesis. J Nerv Ment Dis 118:97-130.

22. Greenberg S, Vonsattel JP (1997) Diagnosis of cerebral amyloid angiopathy. Stroke 28:1418–1422.

23. Griffiths P, Crossman A (1993) Distribution of iron in the basal ganglia and neocortex in postmortem tissue in Parkinson's disease and Alzheimer's disease. Dementia 4:61-5.

24. Hallgren B, Sourander P (1958) The effect of age on the non-haemin iron in the human brain J Neurochem 3:41-51.

25. Hallgren B, Sourander P (1960) The non-haemin iron in the cerebral cortex of Alzheimer's disease. J Neurochem 5:307-10.

26. Huang X, Moir R, Tanzi R, et al (2004) Redox-active metals, oxidative stress and Alzheimer's disease pathology. Ann NY Acad Sci 1012:153-63.

27. Jellinger K (2010) Prevalence and impact of cerebrovascular lesions in Alzheimer's and Lewy Body diseases. Neurodegener Dis 7:112-115.

28. Lannfelt L, Blennow K, Zetterberg H, et al (2008) Safety, efficacy and biomarker findings of PBT2 in targeting Abeta as a modifying therapy for Alzheimer's disease; a phase IIa, double blind randomized placebo controlled trial. Lancet Neurol 7:779-86.

29. Leipuviene R, Theil E (2007) The family of iron responsive RNA structures regulated by changes in cellular iron and oxygen. Cell Mol Life Sci 64:2945-55.

30. Leite R, Jacob-Filho W, Saiki M, et al (2008) Determination of trace elements in human brain tissue using neutron activation analysis. Journal of Radioanalytical and Nuclear Chemistry 278:581-4.

31. Lerner-Marmarosh N, Shen J, Torno M, et al (2005) Human biliverdin reductase: a member of the insulin receptor substrate family with serine/threonine/tyrosine kinase activity. Proc Natl Acad Sci 102:7109-14.

32. Loeffler D, Connor J, Juneau P, et al (1995) Transferrin and iron in normal, Alzheimer's disease and Parkinson's disease brain regions. Journal of Neurochemistry 65:710-6.

33. Lovell M, Robertson J, Teesdale W, et al (1998) Copper, iron and zinc in Alzheimer's disease senile plaques. Journal of Neurological Science 158:47-52.

34. Magaki S, Raghavan R, Mueller C, et al (2007) Iron, copper and iron regulatory protein 2 in Alzheimer's disease and related dementia. Neuroscience Letters 418:72-6.

35. Markesbery W (1984) Brain trace elements concentrations in aging. Neurobiol Aging 5:19-28.

36. Miller E, Zeng L, Domaille W, Chang C (2006) Preparation and Use of Coppersensor-1, a Synthetic Fluorophore for Live-Cell Copper Imaging. Nature Protocols 1:824-827.

37. Molina-Holgado F, Gaeta H, Williams R, Francis P (2007) Metals ions and neurodegeneration. Biometals 20:639-54.

38. Panayi A, Spyrou N, Iverson B, et al (2002) Determination of cadmium and zinc in Alzheimer's brain tissue using inductively coupled plasma mass spectrometry. Journal of Neurological Science 195:1-10.

39. Panayi A, Spyrou N, Part P (2001) Differences in trace element concentrations between Alzheimer and "normal" human brain tissue using instrumental neutron activation analysis. Journal of Radioanalytic and Nuclear Chemistry 249:437-41.

34. Plantin L, Lying-Tunell U, Kristensson K (1987) Trace elements in the human central nervous system studied with neutron activation analysis. Biological Trace Element Research 13:69-75.

41. Prohaska J, Gybina A (2004) Intracellular copper transport in mammals. J Nutrition 134:1003-6.

42. Religa D, Strozyk D, Cherny R, et al (2006) Elevated cortical zinc in Alzheimer's disease. Neurology 67:69-75.

43. Rogers J, Bush A, Cho H, et al (2008) Iron and the translation of the amyloid precursor protein (APP) and ferritin mRNAs: riboregulation against neurol oxidative damage in Alzheimer's disease. Biochem Soc Trans 36(Pt6):1282-7.

44. Rottkamp C, Raina A, Zhu X, et al (2001) Redox-active iron mediates amyloid-beta toxicity. Free Radic Biol Med 30:447-50.

45. Schrag M, Dickson A, Jiffry A, et al (2010) The effect of formalin fixation on the levels of brain transition metals in archived samples. BioMetals in press.

46. Schrag M, McAuley G, Pomakian J, et al (2010) Correlation of hypointesities in susceptibility-weighted images to tissue histology in dementia patients with cerebral amyloid angiopathy: a post-mortem MRI study. Acta Neuropathol 119:291-302.

47. Smith DG, Cappai R, Barnham KJ (2007) The redox chemistry of the Alzheimer's disease amyloid beta peptide. Biochim Biophys Acta 1768:1976-90.

48. Smith M, Harris P, Sayre L, Perry G (1997) Iron accumulation in Alzheimer disease is a source of redox-generated free radicals. Proc Natl Acad Sci 94:9866-8.

49. Smith MA, Wehr K, Harris P, et al (1998) Abnormal localization of iron regulatory protein in Alzheimer's disease. Brain Res 788:232-6.

50. Stedman J, Spyrou N (1997) Elemental analysis of the frontal lobe of "normal" brain tissue and that affected by Alzheimer's disease. Journal of Radioanalytical and Nuclear Chemistry 217:163-6.

51. Squitti R, Rossini P, Casseta E, et al (2002) D-penicillamine reduces serum oxidative stress in Alzheimer's disease patients. Eur J Clin Invest 32:51-9.

52. Tandon L, Ni B, Ding X, et al (1994) RNAA for arsenic, cadmium, copper and molybdenum in CNS tissue from subjects with age-related neurodegenerative diseases. Journal of Radioanalytical and Nuclear Chemistry 179:331-9.

53. Tokuda E, Okawa E, Ono S (2009) Dysregulation of intracellular copper trafficking pathway in a mouse model of mutant copper/zinc superoxide dismutase-linked familial amyotrophic lateral sclerosis. J Neurochem 111:181-91.

54. Vinters HV (1987) Cerebral amyloid angiopathy: a critical review. Stroke 18:311-26.

55. Vinters HV, Wang Z, Secor D (1996) Brain parenchymal and microvascular amyloid in Alzheimer's disease. Brain Pathol 6:179-95.

56. Vinters HV, Vonsattel JP (2000) Neuropathologic features and grading of Alzheimer-related and sporadic CAA. In: Verbeek MM, de Wall RMW, Vinters HV, editors. *Cerebral amyloid angiopathy in Alzheimer's disease and related disorders.* Dordrecht, the Netherlands; Kluwer Academic: pp. 137–155.

57. Ward N, Mason J (1987) Neutron activation analysis techniques for identifying elemental status in Alzheimer's disease. Journal of Radioanalytical and Nuclear Chemistry 113:515-526.

58. Yang L, McRae R, Henary M, et al (2005) Imaging of the intracellular topography of copper with a fluorescent sensor and by synchrotron x-ray fluorescence microscopy. Proc Natl Acad Sci 102:11179-84.

59. Zeng L, Miller E, Pralle A, et al (2006) A selective turn-on fluorescent sensor for imaging copper in living cells. J Am Chem Soc 128:10-1.

CHAPTER 5

CORRELATION OF HYPOINTENSITIES IN SUSCEPTIBILITY WEIGHTED MAGNETIC RESONANCE IMAGES TO TISSUE HISTOLOGY IN DEMENTIA PATIENTS WITH CEREBRAL AMYLOID ANGIOPATHY

Matthew Schrag[1], Grant McAuley[1], Justine Pomakian[2], Claudius Mueller[1,3], Harry V. Vinters[2], E. Mark Haacke[4,5,6], Barbara Holshouser[4], Daniel Kido[4], and Wolff Kirsch[1]

[1]Neurosurgery Center for Research; Loma Linda University, Loma Linda, California
[2]Department of Pathology and Laboratory Medicine and Department of Neurology, David Geffen School of Medicine at the University of California Los Angeles, Los Angeles, California
[3]Center for Applied Proteomics and Molecular Medicine, George Mason University, Manassas, Virginia
[4]The Magnetic Resonance Imaging Institute for Biomedical Research, Detroit, Michigan
[5]Department of Radiology; Loma Linda University School of Medicine, Loma Linda, California
[6]Department of Radiology; Wayne State University, Detroit, Michigan

Abstract

Neuroimaging with iron-sensitive MR sequences (gradient echo T_2* (GRE-T_2*) and susceptibility weighted imaging (SWI)) identifies small signal voids that are suspected brain microbleeds (BMB). Though the clinical significance of these lesions remains uncertain, their distribution and prevalence correlates with cerebral amyloid angiopathy (CAA), hypertension, smoking, and cognitive deficits. Investigation of the pathologies that produce signal voids is necessary to properly interpret these imaging findings. We conducted a systematic correlation of SWI identified hypointensities to tissue pathology in *post mortem* brains with AD and varying degrees of CAA. Autopsied brains from eight Alzheimer's disease patients, six of which showed advanced CAA,

were imaged at 3T; foci corresponding to hypointensities were identified and studied histologically. A variety of lesions was detected; the most common lesions were acute microhemorrhage, hemosiderin residua of old hemorrhages, and small lacunes ringed by hemosiderin. In lesions where the bleeding vessel could be identified, ß-amyloid immunohistochemistry confirmed the presence of ß-amyloid in the vessel wall. Significant cellular apoptosis was noted in the perifocal region of recent bleeds along with heme oxygenase 1 activity and late complement activation. Acutely extravasated blood and hemosiderin were noted to migrate through enlarged Virchow-Robin spaces propagating an inflammatory reaction along the local microvasculature – a mechanism that may contribute to the formation of lacunar infarcts. Correlation of imaging findings to tissue pathology in our cases indicates that a variety of CAA related pathologies produce MR-identified signal voids and further supports the use of SWI as a biomarker for this disease.

Introduction

In vivo evidence of cerebral amyloid angiopathy (CAA) was limited until the introduction of gradient echo T_2^* (GRE-T_2^*) weighted magnetic resonance (MR) imaging, which remains the clinical standard for detection of brain microbleeds (BMB) which often result from CAA (Atlas 1988). BMB are detected as focal signal intensity losses, presumably secondary to iron-containing hemosiderin residua of hemoglobin breakdown. Though recent reviews of the BMB literature have attempted to codify the interpretation of these findings, the inconsistency of data sets, the lack of pathological confirmation and the need for better designed prospective studies to determine their

clinical significance has been emphasized (Viswanathan 2006, Cordonnier 2007a, 2007b). Detection of BMB is improved by new, high-resolution, 3D GRE-T2* and susceptibility weighted imaging (SWI). SWI is an advance in T_2* weighted brain MR imaging that enhances contrast from local susceptibility tissue variations (Haacke 2004, 2005). At 1.5T, the SWI sequence was found to be four fold more sensitive for detection of traumatic BMB than conventional GRE-T_2^* and recent data in MCI subjects indicates again at least a four fold increase in BMB recognition by SWI compared to conventional GRE-T_2^* imaging (Tong 2003, 2004, Sehgal 2005, Haacke 2007).

To date, punctate signal voids have been observed in a number of diseases – by far the most common are hypertension and CAA. Those associated with hypertensive vasculopathy tend to be localized to basal ganglia, internal capsule, brain stem, and cerebellum, whereas those associated with CAA are generally smaller with a posterior lobar predilection (Walker 2004, Rosand 2005). CAA is comorbid with Alzheimer's disease (AD) in as many as 95% of AD cases (Jellinger 2007). In this condition the β-amyloid peptide is deposited along the cerebral and meningeal vasculature in the walls of small and medium-sized arterioles. This peptide appears to induce a local inflammatory response ranging from subtle changes to, in extreme cases, a granulomatous angiitis with apoptotic death of vascular smooth muscle cells (Aliev 2002, Anders 1997). Studies of CAA autopsy material have confirmed these findings and the presence of other (non-β-amyloid) proteins such as cysteine protease inhibitor (cystatin) in CAA vessel walls (Anders 1997). Vascular wall infiltration with these proteins appears to be associated with a structural instability of arterioles accounting for BMB and associated MR signal

voids; however, the biologic and molecular mechanisms for β-amyloid accumulation, inflammatory and oxidative responses, and vascular weakening are unclear at present.

Recent evidence has shown that the presence of BMB predicts reduced global cognitive function and is a risk factor for progression of mild cognitive impairment to outright dementia (Yakishiji 2008, Kirsch 2009). Additionally, one study noted a significant correlation between patients with at least one hypointensity in GRE-T2* imaging and those homozygous for the Apolipoprotein E ε4 gene, a well-known risk factor for Alzheimer's disease (Sveinbjornsdottir 2008). Remarkably, there have been very few verifications of the histopathology of radiologically identified BMB, and none utilizing the newer sensitive sequences (Cordonnier 2007a). There are currently three reports in the published literature that describe the pathology of hypointensities in MR images; all three rely upon GRE-T2* imaging and most evaluate hypertensive patients. A recent case report isolated eight microbleeds from a single, elderly hypertensive patient (Tatsumi 2008). Tanaka and colleagues studied hypointensities in three relatively young autopsy cases, two involving hypertension and one a large mass in the brain indicating that hemosiderin granules were found corresponding to hypointensities, except in one case where a microaneurysm was found (1999). The largest correlative study evaluated eleven cases, but was only able to correlate imaging findings to pathologic abnormalities in six. The hypointensities in that study were associated with hematomas and/or hemosiderin granules. However, only two of the cases had CAA and one of them was also hypertensive; neither of the patients was identified as having been clinically demented during life (Fazekas 1999).

More recently, SWI has been used to study trauma; in this venue, numerous papers have shown SWI to be particularly sensitive for detecting blood products (Tong 2003, 2004). Still, none of the many works in this area have correlated the imaging findings seen in trauma with histology. Our study represents the first correlation of SWI focal hypointensities to tissue pathology in *post mortem* human CAA-affected brain.

Materials and Methods

Patient Characteristics

Post-mortem tissue was obtained from the Alzheimer's Disease Research Center Brain Bank at the University of California, Los Angeles (Harry V. Vinters). All patients or their surrogates had consented to participate in research protocols prior to tissue donation. The research protocol was approved by the Institutional Review Board of Loma Linda University Medical Center (approval #54174). The average age of participants was 79.9 years with a standard deviation of 9.3 years; four were male, four female. All patients had long clinical histories of dementia. AD pathology was classified by Braak and Braak staging guidelines and CAA pathology was graded by Vonsattel's criteria. Briefly, grade 1 CAA involves ß-amyloid deposition primarily in a fine rim on the basement membrane. Grade 2 disease extends to allocortical and cerebellar vessels and deposition of ß-amyloid among smooth muscle cells partially replacing the tunica media. Grade 3 disease involves total replacement of arteriolar vascular smooth muscle (Greenberg 1997). Autopsy findings confirmed Braak and Braak pathology at stage VI and Vonsattel pathology at grade 3 for four of the brains. Two cases were found to have severe CAA pathology (grade 3) out of proportion to AD pathology. These are included

as relatively "pure" cases of CAA. Two had stage VI AD pathology, but negligible CAA – these were included as AD controls. In addition to the eight demented cases, two neurologically normal, aged control brains were scanned along with the others and no hypointensities were detected in them. One of the patients with severe CAA and AD died of an acute intracerebral hemorrhage; the affected lobe was excluded from analysis. None of the patients had a history of hypertension, traumatic brain injury or other causes of BMB. Cases with Lewy bodies detected on pathologic examination were excluded. Patient demographics, clinical duration of dementia (when known) and the imaging findings are listed in Table 8.

Tissue Preparation

Three, 1cm coronal sections were obtained from each of eight human brains at autopsy; slices were taken through the frontal, temporo-parietal and occipital lobes. Because lesions frequently occur near the periphery of tissue specimens in CAA, they are easily obscured in post-mortem imaging by the artifact produced at the air-tissue interface. To eliminate this interface and movement artifacts in imaging and to improve the ease of handling delicate tissue, the formalin fixed brain slices were embedded in blocks of 4% agarose gel. Agarose is an aqueous suspension that effectively contrasts to the fixed tissue in MR images and eliminates the phase disturbance. The encased tissue is well-preserved, and the gel block is easier to orient within the MR scanner and eliminates tissue movement, which was encountered when specimens were imaged in liquids. Agarose did not penetrate the tissue and was neatly separated from the specimen after imaging was completed. Air bubbles mimic the signal voids of focal iron, so care

TABLE 8: Patient demographics and locations of microbleeds on MR

Case# age/sex	Clinical severity of dementia	B&B*/ Vonsattel grade	Lesion locations: Cortical grey matter	Lesion locations: Deep grey matter	Lesion locations: White matter	Cause of death
1. 89/M	14 yrs / severe	VI / 0	-	-	-	Pneumonia
2. 81/M	Severe / slow progression	VI / 0	-	-	-	Pneumonia
3. 61/M	2 yrs / rapid progression	IV / 3+	1	-	4	Complications of malnutrition
4. 85/F	Slow progression	V / 3+	-	1	4	Coronary artery disease
5. 73/F	Severe	VI / 3	-	-	3	Unknown
6. 90/M	Severe / slow progression	VI / 3	-	1	4	Emphysema/pneumonia
7. 74/F	Severe / slow progression	VI / 3	7	2	2	Massive intracerebral hemorrhage in the right frontal/parietal lobes
8. 86/F	8 yrs / slow progression	VI / 3	4	1	4	Pneumonia

*B&B=Braak and Braak score

was taken to thoroughly remove any bubbles which might complicate interpretation of the MR scans.

Imaging Parameters

MR imaging was performed on a 3T scanner in the coronal plane (Siemens). The following parameters were used: echo time, 20ms; repetition time, 30ms; flip angle, 15°; slice thickness, 2mm; matrix size 256mmx256mm; in plane resolution, 0.5mmx0.5mm. The images were reviewed by two experienced interpreters blinded to autopsy diagnoses and any conflicts were settled by the senior neuroradiologist at Loma Linda University Medical Center, Dr. Daniel Kido. An explanation of hypointensity reporting criteria has been published previously and is comparable to other established protocols (Kirsch 2009, Cordonnier 2008). Briefly, hypointensities were identified as regions 5.7 mm or less in diameter of relative signal void (Greenberg 2009). Additionally, hypointensities were evaluated for continuity with blood vessels, and location within a sulcus. If either were present, the hypointensity was interpreted as vascular in origin or an artifact from an air bubble and was not counted.

Dissection and Histology

The focal points of interest were located within the tissue block by orienting to tissue architecture and cutting at the depth estimated from the slice thickness of the MR images, thus enabling accurate dissection and consistent recovery of the lesion. Thirteen, well-dissected microbleeds, 5 cortical and 8 at the grey-white junction with at least one specimen from each CAA case, were measured with precision calipers through the widest point to record their diameters for comparison to apparent size in the MR images.

For immunohistochemistry, markers were observed on adjacent sections for each of ten histological specimens -- representing two acute bleeds with intact erythrocytes, five old hematomas, two cavitary specimens and one bleed in the basal ganglia. These specimens were embedded in paraffin in the usual fashion. Serial sections were cut at a thickness of 8 μm through the region of interest and mounted on slides for hematoxylin and eosin staining, immunohistochemical and fluorescent studies. The sections were deparaffinized in three exchanges of xylene, rehydrated through serial alcohol exchanges, and permeabilized in 0.01% TritonX in PBS. Antigen retrieval was performed by heating sections in a microwave three times for three minutes each while submerged in a 0.01% citrate solution. The sections were then treated with 1% hydrogen peroxide in PBS and incubated with a blocking solution of 1.5% normal serum (also in PBS). Sections were then incubated with the primary antibody of choice in 4% normal serum overnight at 4°C. After washing with PBS, sections were incubated with the secondary antibody for two hours, washed in additional exchanges of PBS and treated with diaminobenzidine/ hydrogen peroxide (DAB) for ten minutes (Vector Laboratories). They were then rinsed for 3 min in PBS, dehydrated through serial alcohols, cleared to xylene and coverslipped with mounting resin (Permount, Fisher). Antibodies used were those against Aβ1-42 (1:100, Abcam), CD68 (1:100, Dako), HO-1 (1:250, Biomol) and complement C6 (1:500, Quidel).

For visualizing iron, sections were stained by the enhanced Prussian Blue method by immersing the sections in a mixture of equal parts of 20% hydrochloric acid and 10% potassium ferrocyanide solution for 20 min. All sections were washed in 3 changes of distilled water and incubated with DAB (Vector Laboratories). They were counterstained

with hematoxylin for 5 min, rinsed twice in distilled water, and dehydrated through 95% and 100% alcohol. Slides were cleared in xylene, and mounted with resinous mounting medium.

Fluorescent studies were performed on four microbleed specimens -- two acute bleeds and two old hematomas. In order to more thoroughly characterize heme oxygenase 1 (HO-1) levels around lesions, we double labeled sections for HO-1 and MAP-2, a marker of neurons. Sections (8 μm) cut through the lesion were deparaffinized in 3 changes of xylene and washed in PBS for 15 min. They were then treated with 0.3% hydrogen peroxide in methanol for 30 min and incubated with a blocking solution of 2% normal goat serum in PBS. Subsequently, sections were incubated overnight at 4°C with mAb to HO-1 (1: 100, BioMol) followed with FITC-conjugated goat anti-mouse secondary antibody (1: 500) for 30 min at room temperature. After three 5 min rinses in PBS, sections were blocked with 5% normal mouse serum. After 2 h incubation with MAP-2 monoclonal antibody (1: 500, Abcam) sections were rinsed three times in PBS for 5 min each and incubated with Texas Red conjugated goat anti-mouse secondary antibody in PBS for 30 min temperature. Sections were then rinsed in PBS, coverslipped with Vectashield containing DAPI (Vector Laboratories) and observed under a confocal microscope (Olympus). Apoptosis detection was performed using the terminal deoxynucleotidyl transferase-mediated dUTP nick end labeling (TUNEL) technique (Vector Laboratories). Five fields at a magnification of 100 × were captured adjacent to each lesion and compared to fields at least five diameters away from the lesion. Statistically significant differences were determined by the Student t-test.

Results

Radiologic-histopathologic Correlation

Thirty-eight lesions were detected in SWI images from our cases (Fig.8 and Table 8). The lesions ranged from 0.5 to 5 mm in diameter, and in ten lesions intact erythrocytes were found. In sixteen specimens, old hematomas were found which contained dark brown cellular debris positive for Prussian Blue staining. In seven of the specimens, small cavities were found at the site indicated by the MR image. At three sites, no pathology was visible on gross inspection, but hemosiderin granules and hematoiden deposition were detected at microscopy. At one site a dissection in the wall of a grossly distended vessel was discovered and blood within the vessel wall apparently produced the hypointensity on SWI. One additional hypointensity was caused by a microaneurysm (Fig. 9). The vast majority of lesions (79%) appeared near the cortical ribbon in two key distributions – just beneath the grey-white junction (eighteen lesions, recorded in Table 8 as white matter lesions) and in the superficial cortex where pial arterioles penetrate the grey matter (twelve lesions). Representative examples of each are present in the adjacent lesions in Figure 8a-c. Deep white matter lesions were rarely observed (three of the thirty-eight total specimens) and all had an atypical cavitary appearance.

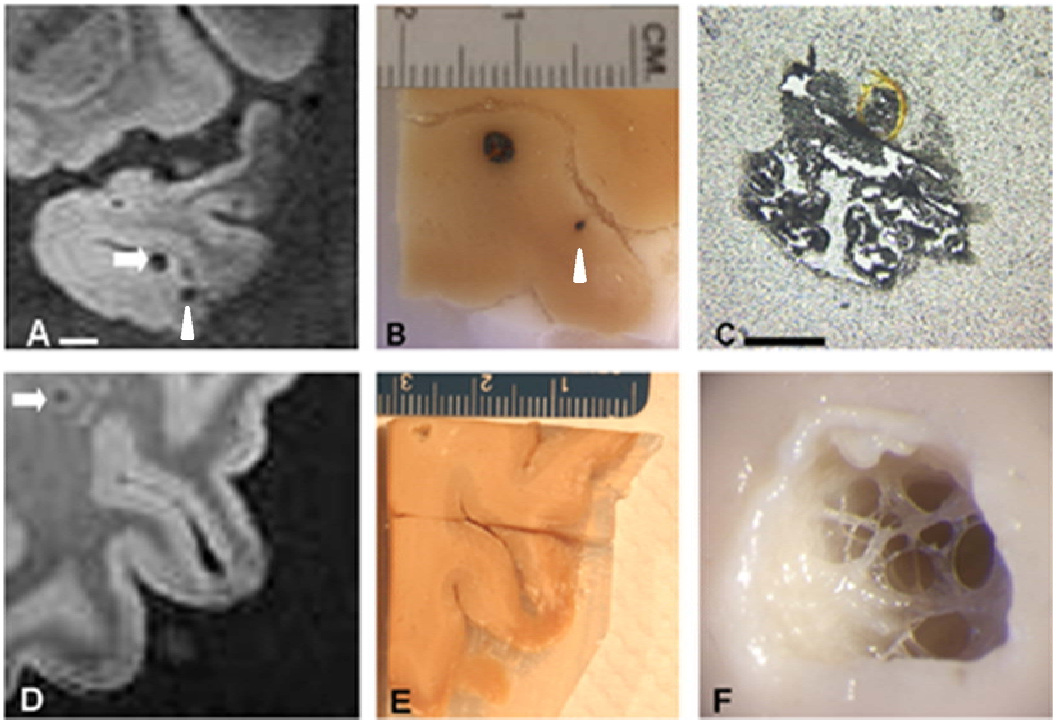
A
B
C
D
E
F

Figure 8: Correlation of hypointensities and tissue pathology
The stepwise isolation of two lesions is illustrated above. In image A, a hypointensity in SWI is noted in the left temporal lobe (scale bar = 5mm). The corresponding lesion is shown in image B. This hematoma is typical of those located in grey matter, the blood does not diffuse into the tissue, but remains encapsulated within a pseudocapsule (scale bar =1mm). A second lesion is present in this tissue block; the size of this lesion is overestimated by SWI, illustrating the "blooming effect" of this technology (arrowheads in a & b). Another hypointesity located in the white matter of the left parietal lobe is indicated in image D (scale is equal to image A). The corresponding lesion has been dissected in image E and is shown under a dissecting microscope in image F. The final image shows a cavitary lesion trabeculated by vascular elements. Further histologic workup of the lesion demonstrated hemosiderin granules within a gliotic capsule (see Fig. 13).

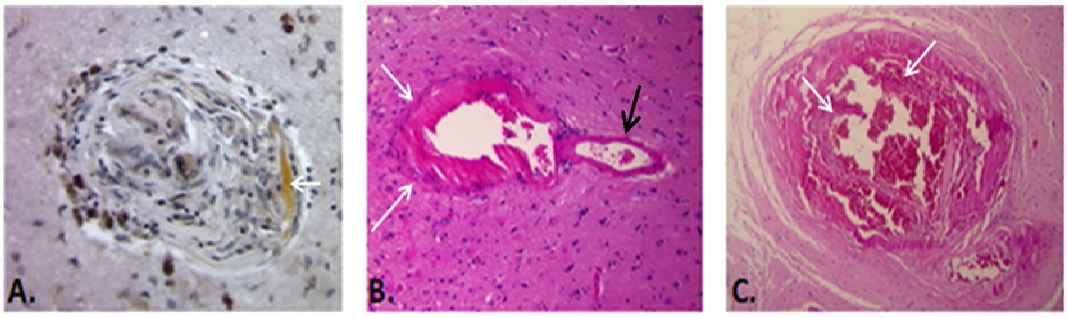
A.
B.
C.

Figure 9: MR hypointensities without grossly visible pathology
The vast majority of hypointensities were associated with hemorrhages visible upon dissection; however a few required more extensive investigation. Shown in image A is a well-healed lesion consisting of focal scarring with hemosiderin deposits stained by DAB enhanced Prussian Blue stain. Hematoiden deposition is also noted in the lesion (white arrow). Image B shows an arteriolar aneurysm (white arrows indicate the dome of the aneurysm; black arrow indicates the "parent" artery). Image C shows a severely dilated vessel with a dissection in the endothelium and blood in the vessel wall (arrows point the ruptured endothelial layer).

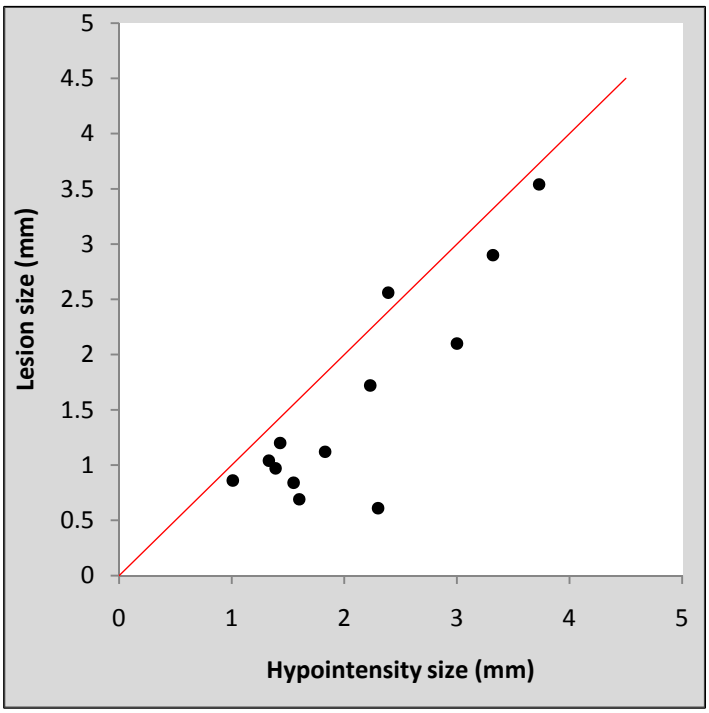
Lesion size (mm)
Hypointensity size (mm)
0
0.5
1
1.5
2
2.5
3
3.5
4
4.5
5
0
1
2
3
4
5

Figure 10: The "blooming effect" of signal voids induced by hemosiderin-iron
The theoretical equality of lesion size to MR hypointensity size is graphed in red. The actual measurements are shown in the scatter plot and almost all the lesions are smaller than their associated MR finding. The signal voids averaged 1.58+/-0.75 times the size of the associated lesion.

Figure 10 compares the size of lesions to their apparent size in SWI. SWI consistently over-estimated the diameter of small lesions in what has previously been termed the "blooming effect;" hypointensities in this study were 1.57+/- 0.75 times the size of the corresponding lesion. This discrepancy was most notable with smaller lesions where the hypointensity could appear more than three times the diameter of the actual lesion. This effect is illustrated in images A and B of Figure 8 which show one lesion which appeared nearly accurately sized on SWI and another which was significantly magnified by the MR image. This effect may make quantifying the volume of hemorrhage from these MR images unreliable for BMB on the order of the voxel size.

CAA-Related Vascular Damage

In several hemorrhages it was possible to determine which vessel ruptured. In these cases specific observation of the underlying vascular pathology was possible. We also examined the vasculature near sites of hemorrhage when examination of the ruptured vessel was not possible. ß-amyloid immunostaining demonstrated that ß-amyloid deposition was present in the walls of involved vessels. Hematoxylin and eosin staining revealed significant morphologic changes in vessels associated with hemorrhage and the surrounding arterioles. The vessel walls were noted to be thickened, profoundly acellular, and lacking evidence of a musclaris layer. The pathology primarily involved arterioles, capillaries were only sparsely affected.

CD68 immunostaining revealed activated microglia or macrophages on nearly all of the larger parenchymal vessels in a cortical/subcortical distribution. Little vascular staining was present in the deep grey matter. Complement activation on vessels was

assessed with an antibody against complement component C6, the first component of the membrane attack complex (MAC) that stably inserts into the cell membrane. Once C6 is bound to C5b in the cell membrane, the MAC is activated, inevitably leading to cell lysis. The arterioles in CAA brain stained intensely against the C6 marker. This staining was associated with evidence of medial intima degeneration – the characteristic target-shaped vessel morphology associated with severe CAA. Arterioles in the basal ganglia did not react with the C6 antibody.

Evidence of Peri-Hematoma Inflammation

Evidence for the presence of heme oxygenase 1, an inducible, pro-oxidative enzyme that catalyzes the degradation of heme into biliverdin, carbon monoxide and free iron, was noted around many hematomas in the form of hematoiden, a bright yellow pigment. This pigment intensely stained the injured vessels in numerous lesions as illustrated in Figure 11. Representative microbleeds were evaluated with immunohistochemical staining against HO-1. Intense staining of the hematoma was noted in every case along with variable reactivity of the adjacent parenchyma. More prominent staining of this adjacent tissue was noted near recent bleeds; however, some HO-1 activity was noted even around old bleeds without evidence of intact erythrocytes. With fluorescent staining against HO-1, numerous non-neuronal cells in the perihematomal region stained strongly positive for HO-1 around both old and recent hematomas. No heme oxygenase activity was noted around the cavitary lesions. CD68 is a marker for cells of monocyte lineage and will stain microglia, macrophages and neutrophils. While intense reactivity of this antibody was noted in the vessels associated

with each lesion, acute bleeds stained less intensely than old hematomas. Old hematomas were stained throughout the lesions and in perivascular spaces in which hemosiderin was deposited. Finally, TUNEL staining for apoptotic cells was undertaken on four of the lesions (images not shown). Because formalin archived tissue was used in this study, significant auto-fluorescence was present in the sections. To be considered apoptotic, a cell had to be both marked with the TUNEL probe and demonstrate a pyknotic or fragmented nucleus by DAPI staining. The region immediately adjacent to the hematoma was noted to contain significantly more apoptotic cells than the background -- a nearly four-fold increase. The apoptosis rate in the background tissue of severe CAA/AD patients was 0.93% (+/- .39%); 3.9% (+/- 1.6%) of the cells adjacent to the hematomas met criteria for apoptosis ($p<0.01$).

Formation of Secondary Ischemia and White Matter Lesions

Cavitary, lacune-like lesions were present in one of seven deep grey matter lesions (14%), and six of twenty-one white matter lesions (29%). Three of these lesions occurred in deep white matter, three were in subcortical white matter. These sites were ringed by scarred vascular elements and a gliotic capsule containing hemosiderin granules. Cavitary lesions in the deep white matter were larger (3-5mm in diameter) than the subcortical cavitary lesions (1-2mm). Several additional lacunar infarcts and numerous microinfarcts were encountered in the tissue which did not appear on SWI as hypointensities.

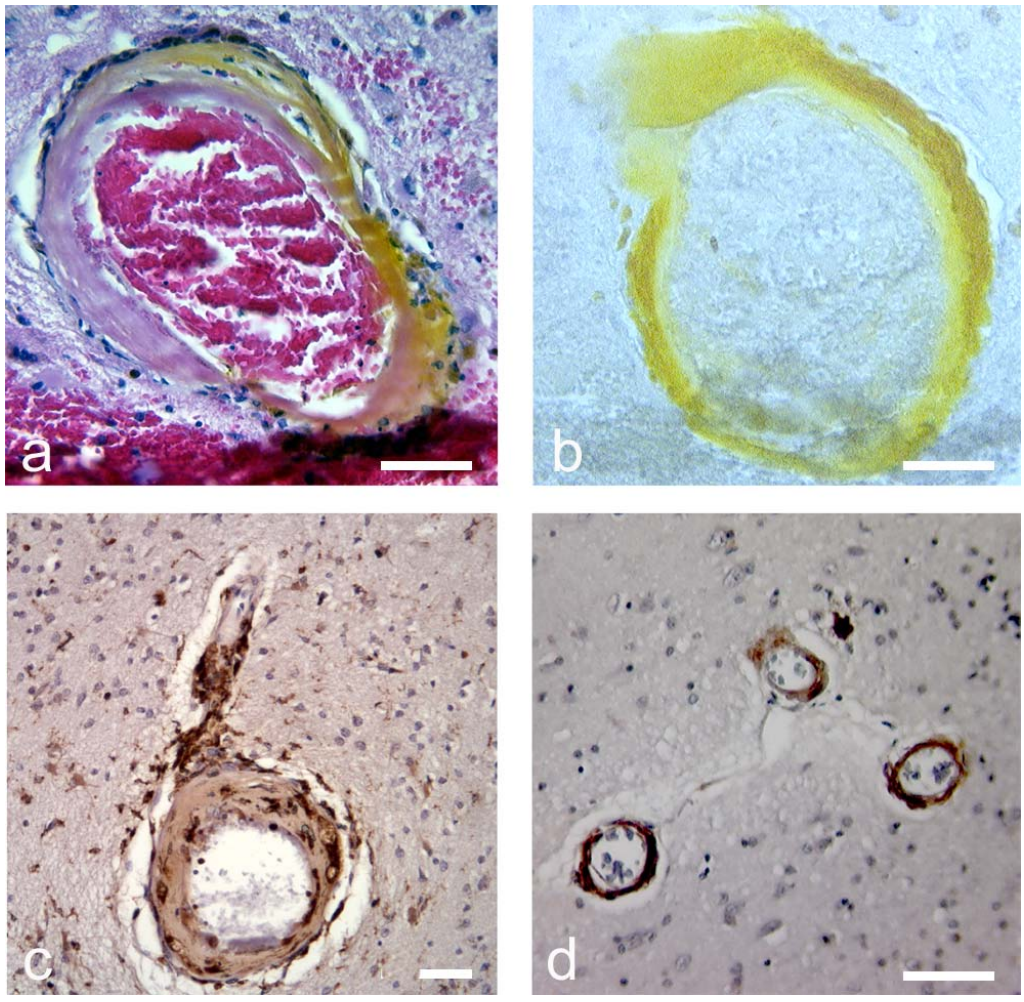
a
b
c
d

Figure 11: Vascular damage associated with CAA and hemorrhage
Images A shows the vessel associated with the lesion in Figure 7c. The vessel wall is hypocellular, eosinophilic and is surrounded by prominent macrophages. The arteriole is stained a brilliant yellow by the endogenous pigment hematoiden (a breakdown product of biliverdin indicating the presence of heme oxygenase activity). Image B represents an immunohistochemical stain of the same vessel demonstrating the presence of ß-amyloid 1-42 in the vessel wall. Image C represents an immunohistochemical stain against CD68, a marker of macrophages and microglia, demonstrating intense microglial activation around vascular elements and macrophages in the vessel wall. Image D shows immunohistochemistry for complement C6. The microvessels in CAA stain strongly for C6 in the tunica media.

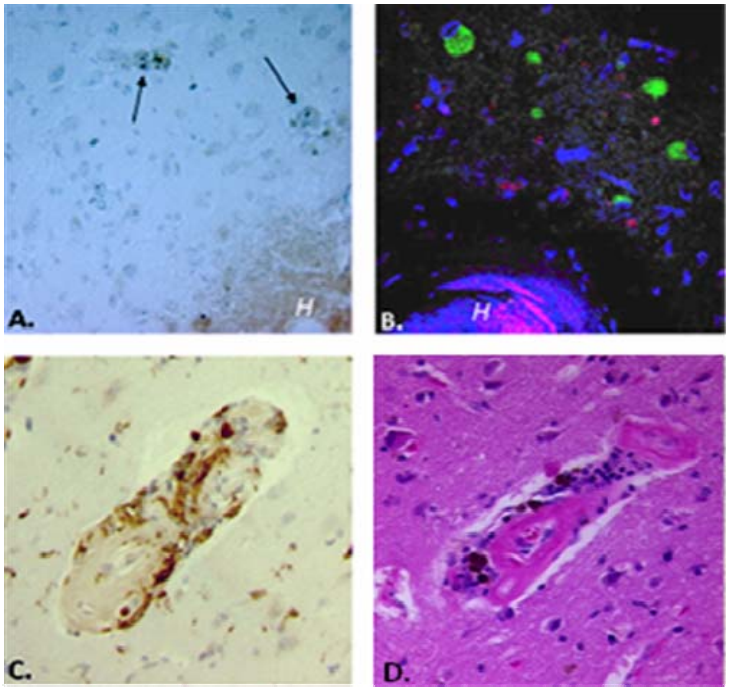
A.
H
B.
H
C.
D.

Figure 12: The local tissue reaction
Immunhistochemical staining highlights the local inflammatory response produced by a hematoma. Image A is stained by DAB over an anti-HO1 primary antibody and illustrates intense HO-1 reactivity within a hematoma and extending into the surrounding parenchyma (H indicates hematoma). Image B is a merged fluorescent study with MAP2/TexasRed staining in red to mark neurons, DAPI in blue to mark all cell nuclei and anti-HO1/FITC in green showing the presence of heme oxygenase 1; the hematoma is visible in the inferior portion of the photo as non-specific staining (again labeled H). Perinuclear HO-1 expression is noted in the peri-focal zone in non-neuronal cells. Image C shows CD68 reactivity indicating a prominent microglial response around a vessel and hemosiderin deposition mainly in macrophages in the vessel wall. H&E of an adjacent section of the identical vessel is shown in image D with perivascular heme-degradation products (arrows).

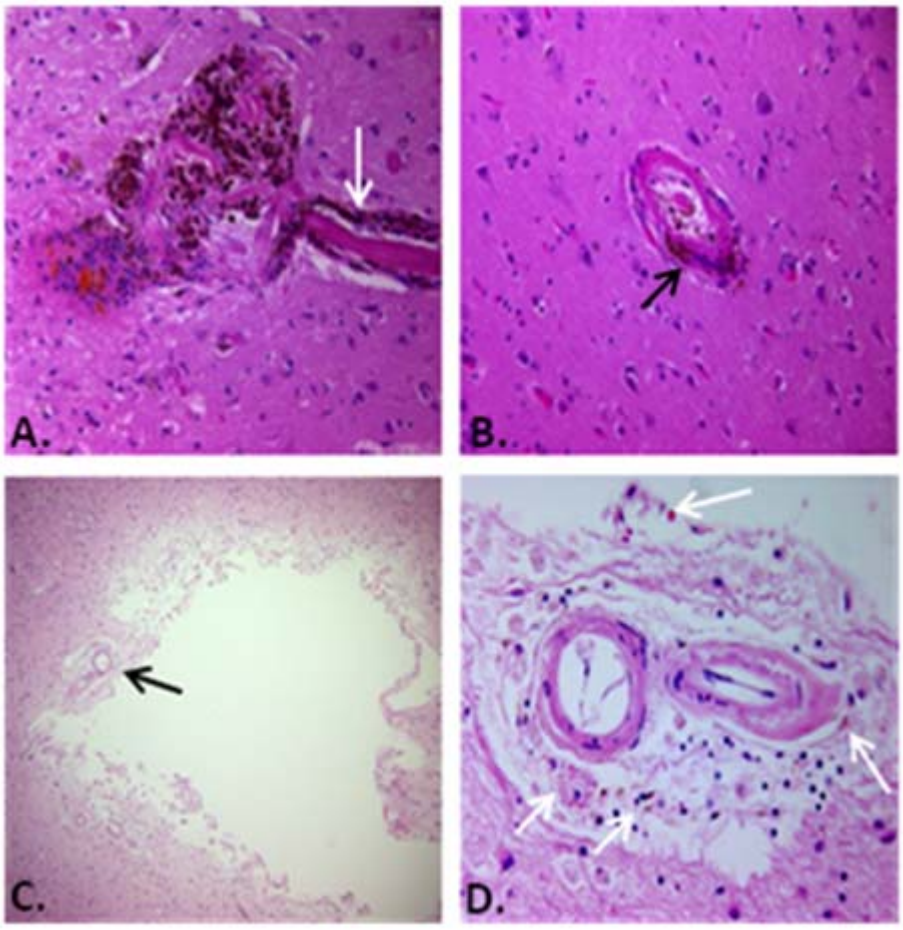
A.
B.
C.
D.

Figure 13: Perivascular hemosiderin deposition may contribute to subsequent ischemic changes. Image A shows a hemorrhage around a degenerated arteriole with hematoiden deposition (yellow/orange material), significant local inflammation and hemosiderin both in the lesion and tracking in the perivascular space along the arteriole (white arrow). Image B shows another vessel, ~500 microns distant from the lesion in image A, with extensive perivascular hemosiderin (arrow). Hemosiderin was present around both capillaries and arterioles at a distance of more than twice the diameter of the lesion and was accompanied by inflammatory cells. Image C shows another lesion that appeared as a hypointensity in SWI (the cavitary lesion shown in Fig. 8d,e,f) and on pathological examination proved to be a lacunar infarct. Image D shows in detail the vessels indicated by the arrow in image C. These vessels are also surrounded by numerous inflammatory cells and macrophages interspersed with hemosiderin granules (arrows).

In acute bleeds in the white matter, hemorrhage products were noted to seep into the surrounding tissue whereas hematomas discovered in grey matter were generally well-circumscribed lesions surrounding an injured vessel. Blood was noted to propagate along perivascular spaces away from the hemorrhage, bathing the regional vessels in blood and blood degradation products. These vessels were surrounded by small, basophilic immune cells and numerous macrophages/activated microglia (Fig. 13). Similar pathologic abnormalities were found around the larger vascular components entering sites of ischemic cavitary lesions. No intact erythrocytes or evidence of acute blood was detected in or near any of the cavitary lesions. However, granular hemosiderin deposits and hemosiderin-laden macrophages were noted in the gliotic capsule around the lesion, so the lesions were interpreted as old, healed hemorrhage sites. Vessels were noted to cross nearly all of the cavitary lesions, but they appeared scarred, emerged from a fibrotic matrix and contained no residual blood suggesting a possible secondary ischemic pathology contributing to the appearance of the lesions. (See Fig. 13)

Discussion

Post mortem MRI is valuable both as a research method and in clinical pathology (Nicholl 2007). Several approaches to *post-mortem* MR imaging have been utilized, from scanning native, unfixed tissue to scanning fixed tissues bathed in liquid to embedding tissues in gels (Fazekas 1999, Schmierer 2007). Embedding tissues improves control and quality of the images and protects and preserves the specimens (Pfefferbaum 2004). As neuroimaging techniques advance, it is important that imaging findings are carefully correlated to tissue pathology. *Post mortem* imaging enables a definitive

approach to this process. While fixation of the brain certainly alters its magnetic resonance properties, these changes have been well-studied and can be accommodated within standard imaging protocols (Carvlin 1989, Blamire 1999). The architecture of the brains in our study remains clearly visualized with good signal-to-noise ratio at the current parameters. Moreover, iron pools have been shown to be stably preserved in formalin-archived tissue, so it is unlikely that the lesions of interest in this study were compromised by the fixation process (Bush 1995).

In this study, blood and/or hemosiderin was encountered corresponding to every signal void in susceptibility weighted images, but the size of the signal void did not reflect closely the size of the hemorrhage. There is wide variation in BMB size, location, and presumed clinical significance. Very small BMB with diameters of 50-200 μm are widespread in the AD brain, but BMB visible by 1.5T GRE-T_2^* range from 3-10 mm in diameter in the MR image (Cullen 2005). There is general agreement among radiologists that BMB are homogeneous round signal losses with diameters less than 5 mm, though some reports include lesions up to 10 mm in apparent diameter (Koenncke 2006). A recent report determined that hemorrhages fall in a bimodal distribution between macro and microhemorrhages with the critical separating value being 5.7mm (Greenberg 2009). Those detectable by SWI at 3T in this study are as small as 1mm in apparent diameter on the scans, and 0.3-0.4 mm measured diameter in the tissue. SWI consistently overestimated the size of bleeds in what has been termed a "blooming effect." In our specimens, the blooming effect magnified the smallest bleeds by as much as 300%. Because of this phenomenon, the apparent size of the lesion on MR is an unreliable estimate of the extent of tissue injury.

The underlying pathologic lesions we discovered correlating to hypointensities was quite varied. The vessels associated with bleeding demonstrated pathologies classically associated with CAA including vessel wall thickening, ß-amyloid replacement of vascular smooth muscle, microaneurysms and, most frequently, frank hemorrhage. ß-amyloid has been shown in *in vitro* studies to be particularly toxic to vascular smooth muscle cells, which may explain the relative acellularity of the muscularis layer in the involved arterioles (Davis 1999). Complement activation was also noted as a prominent part of the vascular pathology, and may be a mechanism of or contribute to amyloid toxicity in the vessel wall. The presence of late complement component C6 surrounding diseased vessels and hemorrhages is a notable finding. Numerous studies have examined the role of the complement system in Alzheimer's disease; it has been established that Abeta binds to both C1q and C3 of the classical complement pathway, activating the early portion of the cascade (Yasojima 1999, Terai 1997). However, the cascade is only activated through C3 in the tissue parenchyma; the lytic portion has not been noted to play a major role in the inflammation induced by beta-amyloid plaques (Cadmen 1997). However, we found that the lytic pathway is observed prominently in the vessel wall. Cultured human cerebrovascular cells have been shown to secrete all the components of the late complement cascade and C6 in particular is upregulated in the presence of β-amyloid (Walker 2008). The Alzheimer's brain is primed for a complement reaction; with elevated parenchymal levels of activated early complement, the introduction of the terminal proteins through vascular injury and hemorrhage may trigger significant cellular loss. The presence of activated MAC in this pathology may make this cascade of future therapeutic interest.

Several sites thought to be microvascular bleeding on SWI were found to be associated with cavitary lesions resembling small lacunar infarcts. Iron deposits were found in the gliotic capsule around these lesions which presumably produced the signal void appreciated on SWI (Fig. 13c,d). In a few cases, particularly larger lesions, a hyperintense halo was present around the hypointensity (Fig. 8). A correlation between microbleeds and lacunar infarcts has been established by a number of imaging studies; in fact, one recent study found the presence of a lacunar infarct the strongest predictor of microbleeds in neurologically healthy adults, stronger than all traditional vascular risk factors (Igase 2009). The cause of this phenomenon is not entirely clear from previous studies. Central nervous system microvasculopathies are well-associated with lacunar infarcts, causing a disturbance in the penetrating arteries feeding white matter tracts, interrupting this important terminal blood supply (Fisher 1991). Recently, the severity of CAA pathology was shown to correlate with the prevalence of microinfarcts in both grey and white matter (Soontornniyomkij 2009). Several observations here may help clarify the pathological mechanism underlying these lesions and why they are so closely associated with microhemorrhages. The tissue response to microhemorrhage is an intense inflammatory reaction. We found that a rim of activated microglia forms around the hemorrhage, complement is activated and HO-1 is induced. This ultimately results in significantly increased cell death including the loss of neurons about the lesions. It has been well-described that extracellular fluids in the brain migrate along the vascular bed in a retrograde fashion through perivascular spaces and are reabsorbed at the level of the arterioles (Schley 2006). These Virchow-Robin spaces are significantly dilated in CAA which could facilitate the movement of perivascular contents (Roher 2003). As shown in

Figure 9, blood from hemorrhagic lesions propagates through the perivascular space predisposing to an inflammatory reaction along a significant portion of the local vasculature. This pattern of spread also has been noted in MR studies looking at the symptomatic perforating artery adjacent to a lacunar infarct (Wardlaw 2001). Additionally, the toxic milieu is confined differently in white matter and grey matter. The Virchow-Robin spaces in grey matter are invested with two meningeal membranes, one basal lamina closely investing the vessel, one investing the glia limitans at the parenchymal surface. In the white matter, the parenchymal membrane is absent, which seems to facilitate the migration of hemorrhagic blood products through the white matter, while it is generally confined to a hematoma in the grey (Pollock 1997). This may result in a more aggressive inflammatory response in the white matter, increasing the probability of spasm or scarring of the vascular supply. These features could conceptually account for the ischemic appearance of some lesions, particularly in the white matter. We observed significant scarring in vessels surrounded by hemosiderin as they enter the lacune-like portion of BMB.

This study is an important step in validating the interpretation of hypointensities in SWI as brain microbleeds. A number of studies now argue in favor of the use of these signal hypointensities as a biomarker of CAA. This may be justified, but we offer a few cautions. First, while hypointensities in this study were associated with CAA pathologies (microbleeding, microaneurysm and endoluminal defect) there are rarely causes for hypointensities that are unrelated to this pathology, including microthrombi, calcifications and air emboli. Additionally, while the distribution of lesions in CAA is characteristic, other disease processes can also produce microhemorrhages. The presence

of hypointensities should be interpreted in light of the clinical setting and the presence of a single hypointensity in a normotensive patient who is cognitively normal may be of little clinical importance (Knudsen 2001). However, the presence of multiple BMBs is rarely, if ever, benign and likely does represent microvascular bleeding. Detectable bleeding in a distribution consistent with CAA likely indicates significant additional bleeding below the threshold currently detectable by clinical imaging studies (Cullen 2005).

BMB are clearly an important "lesion." Some studies indicate that over 95% of AD patients are found at autopsy to have some degree of CAA pathology (Greenberg 1997). Roughly one-third of patients with AD have MR detectable microbleeds, and patients whose cognitive loss is primarily associated with this sort of bleeding may respond to different sorts of treatment modalities. These lesions have also been noted early in the process of cognitive loss and have a prognostic value for the progression of mild cognitive impairment to dementia. When viewed as an ongoing, progressive process, it is not difficult to believe that CAA and microvascular bleeding play a significant role in the cognitive dysfunction ascribed to Alzheimer's disease. Ultimately, we continue to wait for effective therapeutic strategies for dementia to emerge, but this imaging technique offers *in vivo* diagnostic potential to a significant portion of Alzheimer's patients and accurate diagnosis is a prelude to therapy.

Acknowledgements

This research was funded by the National Institutes of Health (AG20948). Harry V. Vinters is supported in part by P01 AG12435, P50 AG16570 and the Daljit S. and Elaine Sarkaria Chair in Diagnostic Medicine. E. Mark Haacke is a consultant to Siemens Corporation. None of the other authors have real or potential conflicts of interest related to this work. We thank Zachary Taylor who was an undergraduate summer researcher in our lab, as well as Cindy Dickson, April Dickson and Jackie Knecht for administrative assistance and for editing the manuscript.

Abbreviations

GRE-T2* = gradient echo T2*; SWI = susceptibility weighted imaging; MR = magnetic resonance; BMB = brain microbleed; CAA = cerebral amyloid angiopathy; AD = Alzheimer's disease; HO-1 = heme oxygenase 1.

References

1. Aliev G, Smith MA, Seyidov D, et al (2002) The role of oxidative stress in the pathophysiology of cerebrovascular lesions in Alzheimer's disease. Brain Pathol 12:21-35.

2. Anders K, Wang Z, Kornfeld M, et al (1997) Giant cell arteritis in association with cerebral amyloid angiopathy: immunohistochemical and molecular studies. Hum Pathol 89:1237-46.

3. Atlas SW, Mark AS, Grossman RI, Gomori JM (1988) Intracranial hemorrhage: gradient-echo MR imaging at 1.5 T. Comparison with spin-echo imaging and clinical applications. Radiology 168:803-807.

4. Blamire A, Rowe J, Styles P, McDonald B (1999) Optimising imaging parameters for post mortem MR imaging of the human brain. Acta Radiol 40:593-7.

5. Bush V, Moyer T, Batts K, Parisi J (1995) Essential and toxic element concentrations in fresh and formalin-fixed human autopsy tissues. Clin Chem 41/2:284-294.

6. Cadmen E, Puttfarcken P (1997) Beta-amyloid peptides initiate the complement cascade without producing a comparable effect on the terminal pathway in vitro. Exp Neurol 146:388-94.

7. Carvlin M, Asato R, Hackney D, et al (1989) High-resolution MR of the spinal cord in humans and rats. Am J Neuroradiol 10:13-7.

8. Cordonnier C, van der Flier WM, Sluimer JD, et al (2006) Prevalence and severity of microbleeds in a memory clinic setting. Neurology 66:1356-1360.

9. Cordonnier C, Al-Shahi Salman R, Wardlaw J (2007) Spontaneous brain microbleeds: systematic review, subgroup analyses and standards for study design and reporting. Brain 130:1988-2003.

10. Cordonnier C, Potter G, Jackson C, et al (2008) Improving interrater agreement about brain microbleeds: development of the Brain Observer MicroBleed Scale. Stroke 40:94-9.

11. Cullen KM, Kocsi Z, Stone J (2005) Pericapillary haem-rich deposits: evidence for microhaemorrhages in aging human cerebral cortex. J Cereb Blood Flow Metab 25:1656-1667.

12. Davis J, Cribbs DH, Cotman CW, Van Nostrand WE (1999) Pathogenic amyloid-beta protein induces apoptosis in cultured human cerebrovascular smooth muscle cells. Amyloid 6:157-64.

13. Fazekas F, Kleinert R, Roob G, et al (1999) Histopathologic analysis of foci of signal loss on gradient-echo T2*-weighted MR images in patients with spontaneous intracerebral hemorrhage: evidence of microangiopathy-related microbleeds. AJNR Am J Neuroradiol 20:637-642.

14. Fisher C (1991) Lacunar infarcts - a review. Cerebrovascular Dis 1:311-20.

15. Greenberg S, Vonsattel JP (1997) Diagnosis of cerebral amyloid angiopathy. Stroke 28:1418-1422.

16. Greenberg S, Nandigam R, Delgado P, et al (2009) Microbleeds versus macrobleeds: evidence for distinct entities. Stroke 40:2382-6.

17. Haacke EM, Xu Y, Cheng YC, Reichenbach JR (2004) Susceptibility weighted imaging (SWI). Magn Reson Med 52:612-618.

18. Haacke EM, Cheng NY, House MJ, et al (2005) Imaging iron stores in the brain using magnetic resonance imaging. Magn Reson Imaging. 23:1-25.

19. Haacke EM, DelProposto ZS, Chaturvedi S, et al (2007) Imaging cerebral amyloid angiopathy with susceptibility-weighted imaging. AJNR Am J Neuroradiol 28:316-317.

20. Igase M, Tabara Y, Igase K, et al (2009) Asymptomatic cerebral microbleeds seen in healthy subjects have a strong association with asymptomatic lacunar infarction. Circ J 73:530-3.

21. Jellinger KA, Lauda F, Attems J (2007) Sporadic cerebral amyloid angiopathy is not a frequent cause of spontaneous brain hemorrhage. Eur J Neurol 14:923-8.

22. Kirsch W, McAuley G, Holshouser B, et al (2009) Serial susceptibility weighted MRI measures brain iron and microbleeds in dementia. J Alzheimer's Dis 17:599-609.

23. Knudsen KA, Rosand J, Karluk D, Greenberg SM. (2001) Clinical diagnosis of cerebral amyloid angiopathy: validation of the Boston criteria. Neurology 56:537-539.

24. Koennecke HC (2006) Cerebral microbleeds on MRI: prevalence, associations, and potential clinical implications. Neurology 66:165-171.

25. Nicholl R, Balasubramanian V, Urguhart D, et al (2007) Postmortem brain MRI with selective tissue biopsy as an adjunct to autopsy following neonatal encephalopathy. Eur J Paediatr Neurol 11:167-74.

26. Pfefferbaum A, Sullivan E, Adalsteinssom E, et al (2004) Postmortem MR imaging of formalin-fixed human brain. Neuroimage 21:1585-95.

27. Pollock H, Hutchings M, Weller RO, Zhang ET (1997) Perivascular spaces in the basal ganglia of the human brain: their relationship to lacunes. J Anat 191:337-47.

28. Roher A, Kuo Y, Esh C, et al (2003) Cortical and leptomeningeal cerebrovascular amyloid and white matter pathology in Alzheimer's disease. Mol Med 9:112-22.

29. Rosand J, Muzikansky A, Kumar A, et al (2005) Spatial clustering of hemorrhages in probable cerebral amyloid angiopathy. Ann Neurol 58:459-462.

30. Schley D, Carare-Nnadi R, Please C, et al (2006) Mechanisms to explain the reverse perivascular transport of solutes out of the brain. J Theor Biol 21;238:962-74.

31. Schmierer K, Wheeler-Kingshott C, Boulby P, et al 2007 Diffusion tensor imaging of post mortem multiple sclerosis brain. Neuroimage 35:467-77.

32. Sehgal V, Delproposto Z, Haacke EM, et al. (2005) Clinical applications of neuroimaging with susceptibility-weighted imaging. J Magn Reson Imaging 22:439-450.

33. Soontornniyomkij V, Lynch M, Mermash S, et al (2009) Cerebral microinfarcts associated with severe cerebral beta-amyloid angiopathy. Brain Path, in press.

34. Sveinbjornsdottir S, Sigurdsson S, Aspelund T, et al (2008) Cerebral microbleeds in the population based AGES-Reykjavik study: prevalence and location. J Neurol Neurosurg Psychiatry 79:1002-6.

35. Tanaka A, Ueno Y, Nakayama Y, et al (1999) Small chronic microhemorrhages and ischemic lesion in association with spontaneous intracerebral hematomas. Stroke 30:1637-42.

36. Tatsumi S, Shinohara M, Yamamoto T (2008) Direct comparison of histology of microbleed with postmortem MR images: a case report. Cerebrovasc Dis 26:142-6.

37. Terai K, Walker D, McGeer E, McGeer P (1997) Neurons express proteins of the classical complement pathway in Alzheimer disease. Brain Res 769:385-90.

38. Tong KA, Ashwal S, Holshouser BA, et al (2003) Hemorrhagic shearing lesions in children and adolescents with posttraumatic diffuse axonal injury: improved detection and initial results. Radiology 227:332-339.

39. Tong KA, Ashwal S, Holshouser BA, et al (2004) Diffuse axonal injury in children: clinical correlation with hemorrhagic lesions. Ann Neurol. 56:36-50.

40. Viswanathan A, Chabriat H (2006) Cerebral microhemorrhage. Stroke 37:550-555.

41. Walker DA, Broderick DF, Kotsenas AL, Rubino FA (2004) Routine use of gradient-echo MRI to screen for cerebral amyloid angiopathy in elderly patients. AJR Am J Roentgenol 182:1547-1550.

42. Walker D, Dalsing-Hernandez J, Lue L (2008) Human postmortem brain-derived cerebrovascular smooth muscel cells express all genes of the classical complement pathway: A potential mechanism for vascular damage in cerebral amyloid angiopathy and Alzheimer's disease. Microvasc Res 75:411-19.

43. Wardlaw J, Dennis M, Warlow, Sandercock P (2001) Imaging appearance of the symptomatic perforating artery in patients with lacunar infarction: occlusion or other vascular pathology. Ann Neurol 50:208-15.

44. Yakushiji Y, Nishiyama M, Yakushiji S, et al (2008) Brain microbleeds and global cognitive function in adults without neurological disorder. Stroke 39:3323-8.

45. Yasojima K, Schwab C, McGeer E, McGeer P (1999) Up-regulated production and activation of the complement system in Alzheimer's disease brain. Am J Pathol 154:927-36.

CHAPTER 6

CONTINUING STUDY: IS DYNACTIN INVOLVED IN DYSFUNCTION AXONAL TRANSPORT OF COPPER IN ALZHEIMER'S DISEASE?

Matthew Schrag, Claudius Mueller, Matthew Zabel, Andrew Crofton, Christopher J. Chang, Wolff Kirsch

Introduction

While copper levels in the human brain are considerably lower than either iron or zinc, copper may play a central role in numerous neurodegenerative diseases. Alterations in copper metabolism can have numerous negative effects. For instance, removing the copper cofactor from super-oxide dismutase reduces its activity, rendering tissues more sensitive to oxidative stress – a mechanism central to amyotrophic lateral sclerosis (ALS) pathogenesis (Museth 2009, Hayward 2002); protein disulfide isomerase which is critical for proper protein folding in the endoplasmic reticulum requires a copper cofactor (Narindrasorasak 2003); and genetic abnormalities of copper chaperones (Menkes and Wilson's diseases) result in severe neurological dysfunction and early death (de Bie 2007). Copper is also bound by prion protein which is associated with Creutfeldt-Jakob disease, alpha-synuclein in Lewy bodies of Parkinsonian brain and by nearly every protein associated with Alzheimer's disease pathology (Wu 2010, Wang 2010, Macreadie 2008). Beta-secretase requires a copper cofactor, amyloid precursor protein binds and effluxes copper from neurons, and beta-amyloid plaques contain high concentrations of copper in their cores (Dingwall 2007, Lovell 1997).

Copper is also physiologically concentrated within synaptic vesicles and is released into the synaptic cleft in a burst with neurotransmitters. Although we do not completely understand its effects, this copper burst appears to be functionally important, inducing alterations in N-methyl D-aspartate (NMDA) receptors and in long-term potentiation (Leiva 2003, Schlief 2006). Because of our previous observation that copper in AD brain is depleted, we sought to determine whether copper in synaptic vesicles is also depleted in AD brain.

Preliminary Findings

From brain homogenate, an enriched fraction containing synaptic vesicles was isolated by ultracentrifugation as previously described and copper levels (normalized to protein concentration) were determined by graphite furnace atomic absorption spectroscopy also described previously (Ohsawa 1975, Schrag 2010). Copper levels were increased in isolated vesicles 5,000 fold over total brain copper levels (30,000 μg copper/g synaptic protein, vs 6 μg copper/g total brain protein) (Squitti 2006). Synaptic vesicles in cases with AD without significant CAA were found to be significantly depleted of copper compared to vesicles from controls and AD cases with severe CAA – n=4 in each group. Histological stains of unfixed brain sections with coppersensor 3 (CS3), a sensitive analogue of the CS1 probe used in previous studies, revealed a remarkable redistribution of copper in AD cases without CAA. The pattern was essentially unchanged between controls and AD / CAA cases, but in AD without CAA an intense axonal staining pattern was present. These findings may indicate that there is a defect in axonal transport or in incorporating copper into vesicles in these cases (Fig. 14).

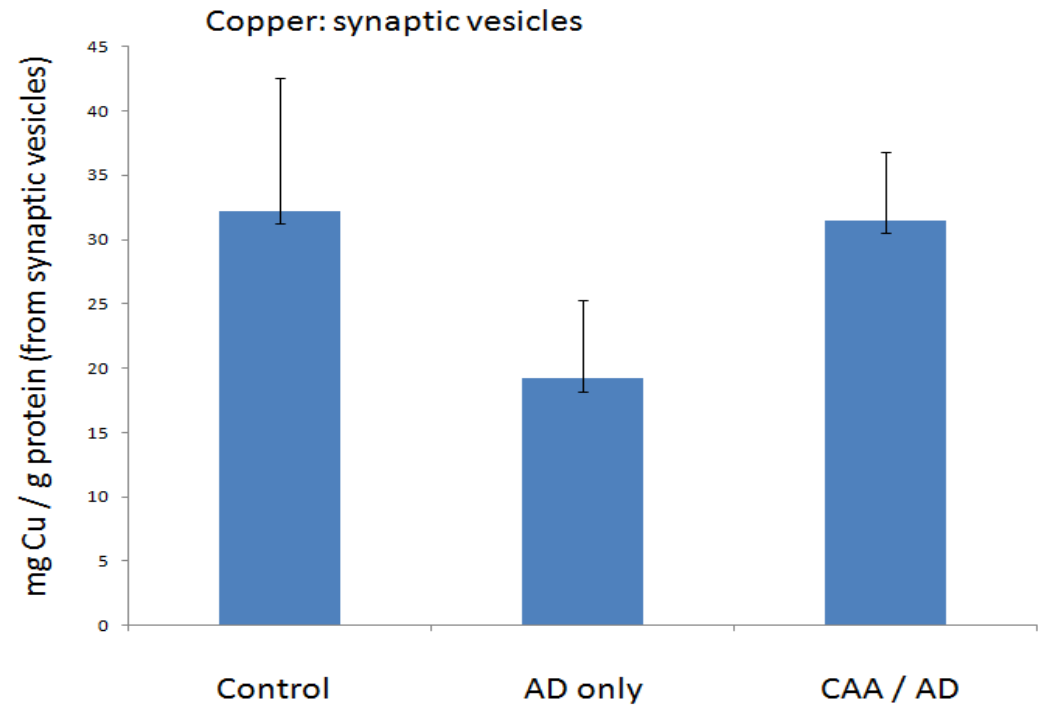
Copper: synaptic vesicles
mg Cu / g protein (from synaptic vesicles)
45
40
35
30
25
20
15
10
5
0
Control
AD only
CAA / AD

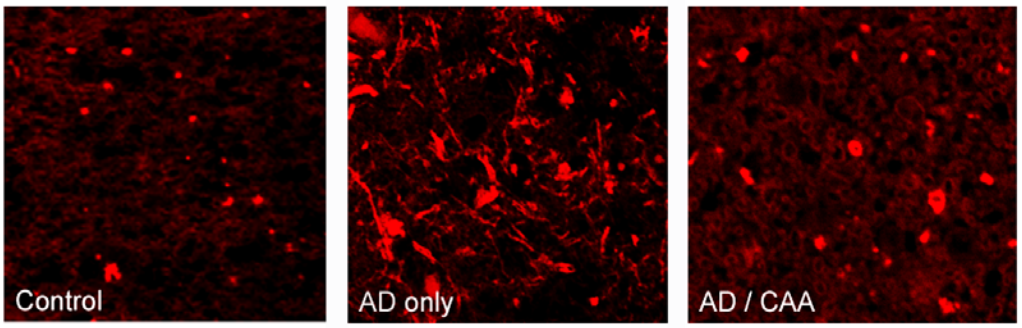
Control
AD only
AD / CAA

Figure 14: Copper levels in enriched synaptic vesicle preparation are significantly reduced in AD cases without significant CAA involvement (upper panel). CS3 staining of monovalent copper (lower panel) demonstrates accumulation of copper in the axons in brain from cases with AD pathology without significant CAA. Copper in synaptic vesicles is primarily divalent and therefore not visible in the histological images. These findings suggest there may be an abnormality in axonal trafficking of copper.

Next, we screened a proteomic database for serum protein changes occurring only in AD w/o CAA cases. In particular we focused on proteins and protein fragments related to axonal transport. Plasma was collected from four groups of patients – neurologic controls, patients with mild cognitive impairment, patients with AD without radiologic evidence microbleeding (AD only) and AD patients with multiple microbleeds (AD / CAA) – n=6 in each group. Samples were analyzed with an orbitrap LC/MS/MS technique as previously described and more than 1500 proteins were identified in the plasma samples (Mueller 2010). Dynactin sub-unit p62 was found to be significantly higher in plasma from AD patients without evidence of CAA (Fig. 15). Additionally, we assessed the levels of dynactin in the post-mortem brain by western blot. Dynactin was significantly reduced in the AD only group compared to both controls and AD/CAA, p=0.01.

Future Directions

The interaction between dynein and dynactin has previously been reported to decline with aging; moverover, reducing the expression of dynactin by siRNA in a cell culture system was found to increase both amyloid precursor protein (APP) levels and beta-cleavage of APP and also resulted in axonal accumulation of tau (Kimura 2007, 2009). Curiously, the p62 subunit of dynactin (the subunit found increased in plasma and decreased in brain from cases with AD without CAA) was found to binding ATP7b – a major copper chaperone (Lim 2006). Dynactin is a conceptual link between copper trafficking and axonal transport mechanisms. While the proteomic and post-mortem data support the hypothesis that lower p62 levels result in axonal trapping of copper and

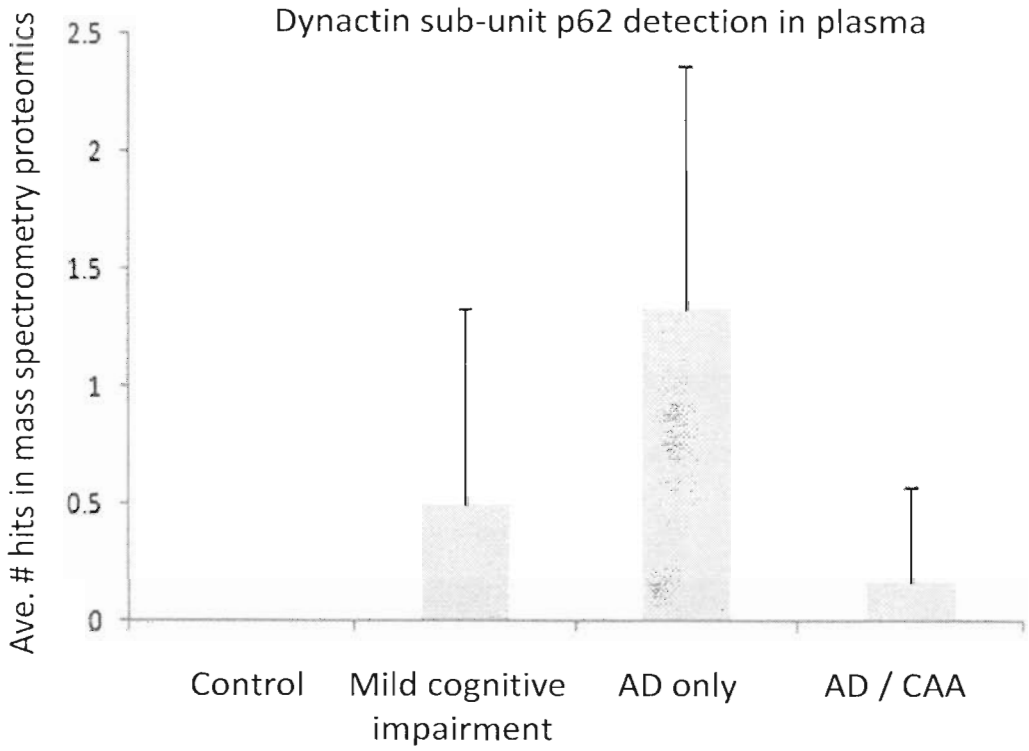
Dynactin sub-unit p62 detection in plasma
Ave. # hits in mass spectrometry proteomics
2.5
2
1.5
1
0.5
0
Control
Mild cognitive impairment
AD only
AD / CAA

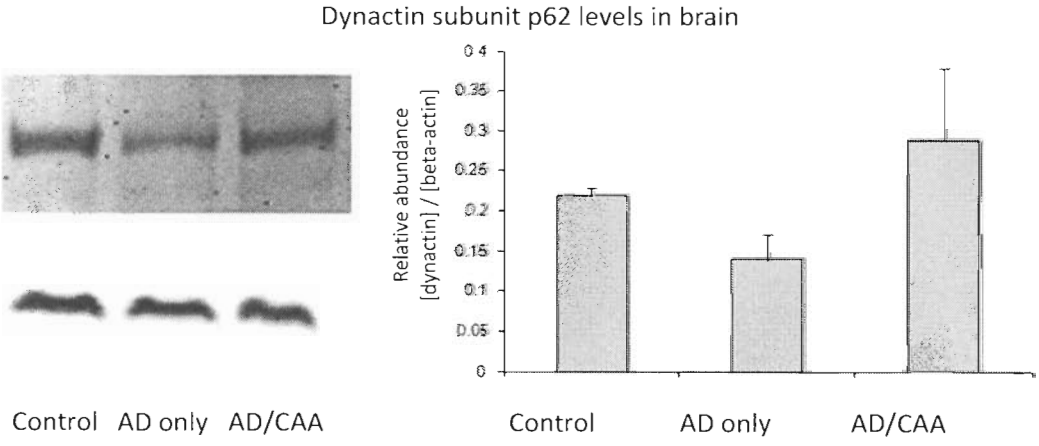
Dynactin subunit p62 levels in brain
Relative abundance [dynactin] / [beta-actin]
0.4
0.35
0.3
0.25
0.2
0.15
0.1
0.05
0
Control
AD only
AD/CAA
Control
AD only
AD/CAA

Figure 15: Plasma collected from neurologically normal patients was compared to plasma from those with mild cognitive impairment, AD without radiologic evidence of microbleeds and AD with multiple microbleeds (upper panel). The p62 subunit of dynactin was found to be significantly elevated in the AD only group and was undetectable in all of the control cases. Western blot analysis of p62 levels in the brain in comparable groups demonstrated the opposite pattern – p62 levels are significantly lowered in the AD only group compared to both controls and AD/CAA groups (lower panel).

reduced synaptic copper, these observations cannot establish a causal link between dynactin and copper trafficking. To accomplish this, we will knock down p62 expression in a neuronal cell culture system and determine whether the previous findings of decreased synaptic and increased axonal copper can be reproduced. If successful, these studies would establish the necessary causal link.

References

1. De Bie P, Muller P, Wijmenga C, Klomp L (2007) Molecular pathogenesis of Wilson and Menkes disease: correlation of mutations with molecular defects and disease phenotypes. J Med Genet. 44:673-88.

2. Dingwall C (2007) A copper-binding site in the cytoplasmic domain of BACE1 identifies a possible link to metal homeostasis and oxidative stress in Alzheimer's disease. Biochem Soc Trans 35:571-3.

3. Hayward L, Rodriguez J, Kim J, et al (2002) Decreased metallation and activity in subsets of mutant superoxide dismutases associated with familial amyotrophic later sclerosis. J Biol Chem 277:15923-31.

4. Kimura N, Imamura O, Ono F, Terao K (2007) Aging attenuates dynactin-dynein interaction: down-regulation of dynein causes accumulation of endogenous tau and amyloid precursor protein in human neuroblastoma cells. J Neurosci Res 85:1909-16.

5. Kimura N, Inoue M, Okabayashi S, et al (2009) Dynein dysfunction induces endocytic pathology accompanied by an increase in Rab GTPases: a potential mechanism underlying age-dependent endocytic dysfunction. J Biol Chem 284:31291-302.

6. Leiva J, Gaete P, Palestini M (2003) Copper interaction on the long-term potentiation. Arch Ital Biol 141:149-55.

7. Lim C, Cater M, Mercer J, La Fontaine S (2006) Copper-dependent interaction of dynactin subunit p62 with the N terminus of ATP7B but not ATP7A. J Biol Chem 281:14006-14.

8. Lovell M, Robertson J, Teesdale W, et al (1998) Copper, iron and zinc in Alzheimer's disease senile plaques. Journal of Neurological Science 158:47-52.

9. Macreadie I (2008) Copper transport and Alzheimer's disease. Eur Biophys J 37:295-300.

10. Mueller C, Zhou W, Vanmeter A, et al (2010) The heme degradation pathway is a promising serum biomarker source for the early detection of Alzheimer's disease. J Alz Dis 19:1081-91.

11. Museth A, Brorsson A, Lundqvist M, et al (2009) The ALS-associated mutation G93A in human copper-zinc superoxide dismutase selectively destailizes the remote metal binding region. Biochemistry 48:8817-29.

12. Narindrasorasak S, Yao P, Sarkar B (2003) Protein disulfide isomerase, a multifunctional protein chaperone, shows copper-binding activity. Biochem Biophys Res Commun 311:405-14.

13. Ohsawa K, Uchizono K (1975) New fractionation method of synaptic vesicles in the brain. Proc Japan Acad 51:202-8.

14. Schlief M, Gitlin J (2006) Copper homeostasis in the CNS: a novel link between the NMDA receptor and copper homeostasis in the hippocampus. Mol Neurobiol 33:81-90.

15. Schrag M, Dickson A, Jiffrey A, et al (2010) The effect of formalin fixation on the levels of brain transition metals in archived samples. Biometals *in press*.

16. Squitti R, Quattrochi C, Forno G, et al (2006) Ceruloplasmin (2D PAGE) pattern and copper content in serum of Alzheimer's disease patients. Biomark Insights 1:205-13.

17. Wang X, Moualla D, Wright J, Brown D (2010) Copper binding regulates intracellular alpha-synuclein, localization, aggregation and toxicity. J Neurochem 113:704-14.

18. Wu D, Zhang W, Luo Q, Luo H, et al (2010) Copper (II) promotes the formation of soluble neurotoxic PrP oligomers in acidic environment. J Cell Biochem in press.

CHAPTER 7

DISCUSSION AND CONCLUSIONS

Several studies conducted by our group demonstrated that iron was not increased in Alzheimer's disease brain by multiple modalities, contrary to a widely accepted belief in the field (Magaki 2007, Kirsch 2009). Additionally, key iron regulatory proteins including IRPs were shown to be unchanged in Alzheimer's disease and a systematic microchip analysis of the expression of iron metabolism-related genes failed to identify even a single gene altered by +/- 2 fold compared to age-matched normal brain (Magaki 2007 and unpublished observations). These findings are in stark contrast to most reports in the field which seem to indicate that iron levels and the associated homeostatic pathways are severely dysregulated in AD and forced us to re-evaluate the hypotheses behind our studies (Bush 2000, Rottkamp 2001).

These observations led us to several important and fundamental questions. First, because the notion that iron is increased in Alzheimer's disease is entrenched and central to a major hypothesis regarding the etiology of the disease and multiple clinical trials, it was important to resolve whether or not iron is truly dysregulated in Alzheimer's disease in a definitive way. Second, if iron is not generally dysregulated, it is reasonable to ask if perhaps the notion that it is dysregulated developed from a subset of patients in whom brain iron is increased. Therefore, identifying what subset of patients have altered metal levels and ultimately what mechanism(s) leads to alterations in transition metal handling

in the brains of Alzheimer's disease patients is the second major objective of these studies.

Through meta-analysis, we found that iron levels are not altered in Alzheimer's disease. We determined the tissue fixation depletes brain iron levels and this effect is greater in normal brain than in AD brain – this effect no doubt contributed in part to the misconception that brain iron is increased in AD as a substantial portion of that literature studied fixed tissues (Schrag 2010). Additionally, we found that all studies which quantitatively demonstrated increased iron in brain from AD patients were conducted at the same laboratory (Lovell 1997, Deibel 1996, Thompson 1988, Ehmann 1986, Wenstrup 1992, Cornett 1995). Seven independent laboratories found that iron was not increased in AD neocortex (Andrasi 2000, Corrigan 1991, Griffiths 1993, House 2007, Panayi 2002, Magaki 2007, Plantin 1987, Religa 2006, Stedman 1997, Ward and Mason 1987). Never-the-less, studies showing increased iron were cited more than 5 times as often as those showing no increase, and this effect was particularly strong among narrative review articles (ISI, Science Citation Index).

To answer the second question, we stratified Alzheimer's disease patients by the degree of vascular involvement in the neuropathology. Patients with severe CAA were place in one group, those with only parenchymal features were grouped in another and age-matched controls were the third group. When all AD patients were analyzed together, as expected no significant changes in iron levels were detected, but when CAA-predominant cases were analyzed separately they were found to have significantly more iron than both controls and AD patients with only parenchymal pathology. Additionally, heme degradation enzymes heme oxygenase 1 and biliverdin reductase B were increased

in the CAA group. These observations argue that pathologic iron deposition is a result of microbleeding associated with CAA and may account for the numerous qualitative reports of increased iron in AD.

We also felt it was necessary to identify potential mechanisms underlying the vascular fragility associated with CAA. We determined that both ferrous iron and monovalent copper prominently deposited on arterioles affected by amyloid deposition – these are both highly reactive oxidative species prone to participation in Fenton reactions which could undermine the stability of the vessels. Moreover, we identified foci of hypointensity in post-mortem MR imaging using susceptibility weight sequences of brain tissue from patients who were pathologically confirmed to suffer from severe CAA (Schrag 2010). We confirmed that these hypointensities represented microhemorrhagic events and were then able to observe in detail the pathology that is associated with microvascular bleeding. Consistent with previous observations, heme oxygenase-1 was found to be remarkably increased in the penumbral region about a microhemorrhage and cellular apoptosis was significantly increased in this region. Extravasated blood products were found to propagate along the local vascular elements propagating an inflammatory response regionally that may damage the microvasculature. One additional finding is particularly interesting, late complement component C6 (indicative of a lytic process) was heavily deposited on grey matter arterioles, although early complement (while present in parenchyma) could not be detected on vascular elements. This finding led us to believe that complement may be involved in beta-amyloid clearance from the parenchyma.

Finally, in the course of these studies, we became aware of a defect in copper transport and metabolism. In patients with severe parenchymal pathology without CAA, copper in synaptic vesicles was found to be significantly reduced compared to Alzheimer's disease patients with vascular involvement. Additionally, monovalent copper in this group of subjects was distributed differently – accumulation of copper in the axons and cell bodies was noted whereas monovalent copper was limited to a perinuclear distribution in both of the other cases. This led us to review proteomic data generated from serum collected from patients with Alzheimer's disease to attempt to identify evidence of abnormal protein fragments in peripheral blood that were associated with axonal transport. A subunit of dynactin (dynein activating complex), p62, was found in serum of patients with Alzheimer's disease without CAA. It was undetectable in all control cases and was only detected in one CAA case. We subsequently determined that p62 levels in brain are depleted in the AD-only group compared to both AD / CAA and control groups. It will be necessary to demonstrate that alterations in dynactin levels and copper in synaptic vesicles are linked. To evaluate this, we will determine whether silencing p62 expression *in vitro* in neuronal culture causes similar depletion of copper from synaptic vesicles and accumulation of copper in axon processes.

Cumulatively, these studies have resolved a number of longstanding questions in the field of Alzheimer's disease research. Most significantly, we have shown that the notion that iron levels are increased in Alzheimer's disease is a misconception – one that may have resulted in tens of millions of misdirected research dollars and has put patients at risk in clinical trials. Additionally, we worked on developing two biomarkers, one an MRI based finding that previously lacked adequate pathological confirmation and one a

new biochemical marker in plasma of altered copper metabolism and axonal transport. Finally, we have begun to show that AD without CAA and AD with CAA are biochemically quite different, and perhaps should not be approached therapeutically in the same ways. These findings have led to a new focus in our continuing work. In particular, we are working on dissecting copper metabolism and its relationship to AD. Nearly all of the major protein players in AD have copper binding sites and significant abnormalities of copper handling have already been identified. Clarifying the role of this metal in AD may reveal new targets for therapy. And finally, we will continue to work toward understanding the mechanism of vascular weakening in CAA. This work is promising because significant abnormalities in complement activation may treatable. A novel inhibitor of late complement was recently approved for clinical use in paroxysmal nocturnal hemoglobinuria. When we better understand the role of complement in the clearance of beta-amyloid from the brain and in the degeneration of the cerebral microvasculature, therapeutic application of this or other inhibitors of complement may be appropriate.

References

1. Andrasi E, Farkas E, Gawlik D, et al (2000) Brain iron and zinc contents of German patients with Alzheimer's disease. Journal of Alzheimer's Disease 2:17-26.

2. Bush A (2000) Metals and neuroscience. Curr Opin Chem Biol 4:184-91.

3. Corrigan F, Reynolds G, Ward N (1991) Reductions of zinc and selenium in brain in Alzheimer's disease. Trace Elements in Medicine 8:1-5.

4. Deibel M, Ehmann W, Markesbery W (1996) Copper, iron and zinc imbalances in severely degenerated brain regions in Alzheimer's disease: possible relation to oxidative stress. Journal of Neurological Science 143:137-42.

5. Ehmann W, Markesbery W, Alauddin M, et al (1986) Brain trace elements in Alzheimer's disease. Neurotoxicology 1:197-206.

6. Griffiths P, Crossman A (1993) Distribution of iron in the basal ganglia and neocortex in postmortem tissue in Parkinson's disease and Alzheimer's disease. Dementia 4:61-5.

7. House M, et al (2007) Correlation of proton transverse relaxation rates (R2) with iron concentrations in postmortem brain tissue from Alzheimer's disease patients. Magnetic Resonance in Medicine 57:172-180.

8. Kirsch W, McAuley G, Holshouser B, et al (2009) Serial susceptibility weighted MRI measures brain iron and microbleeds in dementia. J Alz Dis 17:599-609.

9. Lovell M, Robertson J, Teesdale W, et al (1998) Copper, iron and zinc in Alzheimer's disease senile plaques. Journal of Neurological Science 158:47-52.

10. Magaki S, Raghavan R, Mueller C, et al (2007) Iron, copper and iron regulatory protein 2 in Alzheimer's disease and related dementia. Neuroscience Letters 418:72-6.

11. Panayi A, Spyrou N, Part P (2001) Differences in trace element concentrations between Alzheimer and "normal" human brain tissue using instrumental neutron activation analysis. Journal of Radioanalytic and Nuclear Chemistry 249:437-41.

12. Plantin L, Lying-Tunell U, Kristensson K (1987) Trace elements in the human central nervous system studied with neutron activation analysis. Biological Trace Element Research 13:69-75.

13. Religa D, et al (2006) Elevated cortical zinc in Alzheimer's disease. Neurology 67:69-75.

14. Rottkamp C, Raina A, Zhu X, et al (2001) Redox-active iron mediates amyloid-beta toxicity. Free Radic Biol Med 30:447-50.

15. Schrag M, McAuley G, Pomakian J, et al (2010) Correlation of hypointesities in susceptibility-weighted images to tissue histology in dementia patients with cerebral amyloid angiopathy: a post-mortem MRI study. Acta Neuropathol 119:291-302.

16. Stedman J, Spyrou N (1997) Elemental analysis of the frontal lobe of "normal" brain tissue and that affected by Alzheimer's disease. Journal of Radioanalytical and Nuclear Chemistry 217:163-6.

17. Thompson C, Markesbery W, Ehmann W, et al (1988) Regional brain trace-element studies in Alzheimer's disease. Neurotoxicology 9:1-8.

18. Ward N, Mason J (1987) Neutron activation analysis techniques for identifying elemental status in Alzheimer's disease. Journal of Radioanalytical and Nuclear Chemistry 113:515-526.

19. Wenstrup D, Ehmann W, Markesbery W (1990) Trace element imbalances in isolated subcellular fractions of Alzheimer's disease brains. Brain Research 533:125-31.